

Diss. ETH No. 13733

# The Dynamical Theory of Non-isothermal Polymeric Materials

A dissertation submitted to the  
SWISS FEDERAL INSTITUTE OF TECHNOLOGY  
ZURICH

for the degree of  
Doctor of Natural Sciences

presented by  
MARCO DRESSLER  
dipl. Phys. Univ. des Saarlandes  
born January 8, 1970  
citizen of Germany

accepted on the recommendation of  
Prof. Dr. H. C. Öttinger, examiner  
Prof. Dr. U. W. Suter, co-examiner

2000

# Abstract

This thesis is concerned with the application of non-equilibrium thermodynamics and statistical mechanics of chain molecules in order to investigate the consequences of deformation and temperature on the rheology and structure of polymeric materials. The non-isothermal rheology of polymeric materials, although of considerable scientific and technological interest, is not yet satisfactorily understood, and no clear structure-property relationships have been established. In the past, the investigation of the non-isothermal rheology of polymeric materials has suffered from a lack of theoretical techniques of suitable applicability. The GENERIC framework, having made important progress during the last years, has finally brought the theoretical description of the non-isothermal rheology of polymeric materials within reach.

The present dissertation consists of three parts: First (Chaps. 2 and 3) we review thermodynamic potentials for polymeric materials to describe their thermodynamic properties in the quiescent state. The potentials are evaluated numerically and are compared with experimental data for hexadecane and linear PE (Chap. 2). Furthermore, we propose a recipe to check whether a given polymer is of purely entropic elasticity or not. The method is applied to linear PE and PIB and we see that PE is not of purely entropic elasticity, whereas PIB is (Chap. 3). The second part (Chap. 4) is devoted to the thermodynamics and mechanics of deforming polymeric materials. We adopt a modern formalism of non-equilibrium thermodynamics to derive a set of time evolution equations for the deforming material. Comparison with other thermodynamic approaches is made and constitutive equations for compressible, non-isothermal polymeric fluids are proposed. Isothermal, incompressible viscoelastic models of polymeric fluids are generalized to

non-isothermal, compressible conditions. An equivalent representation of these constitutive equations in terms of the conformation tensor is given with a clearer connection to the microstructure than the stress tensor. The third part (Chaps. 5 and 6) deals with the rheology and non-isothermal rheology of polymeric materials. The fundamental time evolution equations are solved for homogenous deformations and viscometric and rheoptical material properties are evaluated and discussed for non-isothermal, compressible processes. A microscopic interpretation of the phenomenological coefficients appearing in the models derived in Chap. 4 is given and it is suggested how they can be obtained from atomistic simulations (Chap. 5). For materials with energetic and entropic elasticity we discuss adiabatic, non-isothermal stress relaxation experiments and we compare our theoretical results with experimental findings. We propose an alternative fiber spinning process with simultaneous supercooling to the glass transition temperature. We see that small deformations are sufficient to produce highly oriented samples if the material is quenched during deformation (Chap. 6).

**Keywords.** Equilibrium and Non-equilibrium Thermodynamics, Thermodynamic Potentials (SG, FOV), GENERIC, Statistical Mechanics of Chain Molecules (RIS approximation), Microstructure, Transport Theory, Constitutive Equations (FENE-P, Giesekus, PTT, Feta), Rheology, Non-isothermal Rheology, n-alkanes, PE, PIB.

# Kurzfassung

Diese Arbeit befaßt sich mit der Anwendung der Nicht-gleichgewichtsthermodynamik und der statistischen Mechanik von Kettenmolekülen zur Untersuchung der durch Deformation und Temperatur induzierten rheologischen und strukturellen Veränderungen polymerer Materialien. Die nicht-isotherme Rheologie polymerer Materialien ist noch nicht befriedigend verstanden, trotz erheblicher wissenschaftlicher und technologischer Bedeutung, und keine klaren Beziehungen zwischen Struktur und Eigenschaften wurden eingeführt. Die Untersuchung der nicht-isothermen Rheologie wurde in der Vergangenheit durch das Fehlen geeigneter theoretischer Methoden stark eingeschränkt. Die Fortschritte, die im Formalismus von GENERIC im Laufe der vergangenen Jahre erzielt wurden, haben jedoch die theoretische Behandlung der nicht-isothermen Rheologie polymerer Stoffe in Reichweite gerückt.

Die vorliegende Dissertation besteht aus drei Teilen: Zuerst (Kap. 2 und 3) führen wir thermodynamische Potentiale für polymere Stoffe ein, um ihre thermodynamischen Eigenschaften im ruhenden Zustand zu beschreiben. Die Potentiale werden numerisch ausgewertet und mit experimentellen Daten für Hexadecan und PE verglichen (Kap. 2). Weiterhin schlagen wir eine Methode vor, um zu prüfen, ob ein gegebenes Polymer rein entropieelastisch ist oder nicht. Die Methode wird auf lineares PE und PIB angewendet und wir sehen, daß PE nicht rein entropieelastisch ist, während PIB es ist (Kap. 3). Der zweite Teil (Kap. 4) ist der Thermodynamik und der Mechanik sich verformender polymerer Stoffe gewidmet. Wir übernehmen einen modernen Formalismus der Nicht-gleichgewichtsthermodynamik, um einen Satz von Bewegungsgleichungen für das sich verformende Material herzuleiten. Ein Vergleich mit anderen thermodynamischen Zugängen wird angestellt

und konstitutive Gleichungen für kompressible, nicht-isotherme polymere Fluide werden vorgeschlagen. Isotherme, inkompressible Viskoelastizitätsmodelle für polymere Fluide werden auf nicht-isotherme, kompressible Bedingungen verallgemeinert. Eine äquivalente Darstellung dieser konstitutiven Gleichungen mittels des Konformationstensors, mit einer klareren Beziehung zur Mikrostruktur als der Spannungstensor, wird gegeben. Der dritte Teil (Kap. 5 und 6) handelt von der Rheologie und nicht-isothermen Rheologie polymerer Stoffe. Die grundlegenden Zeitentwicklungsgleichungen werden für homogene Deformationen gelöst, und viskosmetrische und rheooptische Materialeigenschaften werden ausgewertet und diskutiert. Eine mikroskopische Interpretation der phänomenologischen Koeffizienten, welche in den Modellen von Kap. 4 auftreten, wird gegeben und es wird vorgeschlagen, wie diese aus atomistischen Simulationen bestimmt werden können (Kap. 5). Für Materialien mit energetischer und entropischer Elastizität diskutieren wir adiabatische Spannungs-Relaxationsexperimente und vergleichen unsere theoretischen Ergebnisse mit experimentellen Befunden. Wir schlagen einen alternativen Faserspinnprozeß mit gleichzeitiger Abkühlung auf die Glastemperatur vor. Wir finden, daß kleine Deformationen ausreichen, um Materialproben höchster interner Orientierung herzustellen, falls das Material während der Deformation abgekühlt wird (Kap. 6).

**Stichworte.** Gleichgewichts- und Nicht-gleichgewichts Thermodynamik, Thermodynamische Potentiale (SG, FOV), GENERIC, Statistische Mechanik von Kettenmolekülen (RIS Approximation), Mikrostruktur, Transporttheorie, Konstitutive Gleichungen (FENE-P, Gisekus, PTT), Rheologie, Nicht-isotherme Rheologie, n-Alkane, PE, PIB.

# Contents

<b>1</b>	<b>Introduction</b>	<b>1</b>
<b>2</b>	<b>Thermodynamic Potentials for Polymeric Materials</b>	<b>7</b>
2.1	Introduction	8
2.2	General Relationships	9
2.3	Liquid Contribution	11
2.3.1	Spencer-Gilmore Potential	12
2.3.2	Modified Flory-Orwoll-Vrij Potential	13
2.4	Elastic Contribution	20
2.4.1	Thermodynamic Potential of a Fixed Polymer Network	20
2.4.2	Statistical Mechanics of Chain Molecules	21
2.5	Application to Normal Alkanes	27
2.5.1	Liquid Part of the Thermodynamic Potential	27
2.5.2	Conformational Part of the Thermodynamic Potential	30
2.6	Conclusions	35
<b>3</b>	<b>Molecular Theory of Energetic and Entropic Elasticity</b>	<b>37</b>
3.1	Introduction	38
3.2	Thermodynamics of Elastic Materials	39
3.2.1	General Relationships	39
3.2.2	Elasticity of a Network of Polymers	40
3.3	Rotational Isomeric State Approximation	43
3.3.1	General Relationships	43
3.3.2	Square of the Magnitude of the Chain Vector	44
3.4	Application to Linear Polymers	45
3.4.1	Polyethylene	45
3.4.2	Polyisobutylene	49
3.5	Conclusions	53
<b>4</b>	<b>Balance Equations for Flowing Polymeric Materials</b>	<b>57</b>
4.1	Introduction	58
4.2	Literature Review	60
4.2.1	The Time-Temperature Superposition Principle	61
4.2.2	Extension of the Time-Temperature Superposition Principle to Non-isothermal Flows	63
4.2.3	Theory of Simple Fluids with Fading Memory	65
4.2.4	The Theory of Purely Entropic Elasticity	67
4.2.5	Non-isothermal Constitutive Equations from Bead-Spring Models	69
4.2.6	Heat Conduction in Polymeric Fluids	72
4.3	Fundamental Balance Equations for Non-isothermal Polymeric Materials	74
4.3.1	Thermodynamics of Polymeric Materials at Quasi-Equilibrium	74
4.3.2	The Double Generator GENERIC Structure	75
4.3.3	Derivation of the Non-isothermal Flow Equations	77
4.4	Constitutive Equations for Non-isothermal Polymer Models	85
4.4.1	The Non-isothermal Maxwell and Oldroyd-B Models	86
4.4.2	The Non-isothermal Giesekus Model	91
4.4.3	The Non-isothermal FENE-P Model	92
4.4.4	The Non-isothermal Phan-Thien and Tanner Model	92
4.5	Conclusions	95
<b>5</b>	<b>Enhanced Constitutive Models for Polymer Melts and Microscopic Interpretation of the Phenomenological Coefficients</b>	<b>99</b>
5.1	Introduction	100
5.2	Conformation Tensor Formulation	101
5.3	Constitutive assumptions	103
5.4	Stress Tensor Formulation	105
5.5	Determination of Phenomenological Coefficients	110
5.5.1	Bead-Friction Coefficient, Relaxation Times, and Viscosity	110
5.5.2	Isotropic and Anisotropic Drag Coefficient	111

5.5.3	Degree of Non-affine Motion and Strength of Material Response . . . . .	113
5.6	Conclusions . . . . .	115
<b>6</b>	<b>Rheology of Non-isothermal and Compressible Viscoelastic Materials</b>	<b>117</b>
6.1	Introduction . . . . .	118
6.2	General Relationships . . . . .	120
6.2.1	Non-isothermal Rheology of Viscoelastic Materials	120
6.2.2	Material Properties . . . . .	122
6.3	Constitutive Assumptions . . . . .	123
6.3.1	Thermodynamic Potential . . . . .	123
6.3.2	Phenomenological Matrices . . . . .	126
6.4	Applications . . . . .	128
6.4.1	Non-isothermal Stress Relaxation . . . . .	129
6.4.2	Non-isothermal Fiber Spinning Process . . . . .	131
6.4.3	Non-isothermal Deformation with Compression . . . . .	138
6.4.4	The Problem of Critical Cooling . . . . .	144
6.5	Conclusions . . . . .	147
<b>7</b>	<b>Conclusions</b>	<b>149</b>
	<b>List of Abbreviations</b>	<b>153</b>
	<b>List of Figures</b>	<b>155</b>
	<b>Bibliography</b>	<b>157</b>
	<b>Index</b>	<b>171</b>

# Chapter 1

## Introduction

As the number of applications for complex materials continues to increase, from tennis rackets and artificial hip joints to transatmospheric vehicles, so does the desire for a better theoretical description of their behaviour during processing. Complex materials, such as advanced composites, liquid crystals, magnetorheological materials, and polymer blends are substances with an internal microstructure. They accordingly exhibit highly unusual properties with respect to crystalline materials or ceramics which can prove to be beneficial in a great number of applications. Since the properties of these materials constitute the limiting barrier to new technological applications, the interest in a theoretical understanding of the structure/property relationship and how this structure is altered during processing may be of some interest.

In the present dissertation we give a theoretical description of amorphous polymeric materials focussing on the connection between the configuration of the material's internal microstructure (chain configuration) and its macroscopic mechanical properties (mechanical stresses in the presence of deformation). This is done to demonstrate the practicality and utility of non-equilibrium thermodynamics in the description of complex materials. Certainly the structure/property relationship is not limited to the material's mechanical properties but comprises also its electrical and optical properties. However, here we focus on the mechanical properties of common polymeric materials such as linear PE, PIB or PS in their amorphous state. Linear polymers are suitable candidates for a project in basic theoretical research for several reasons. First of all

a great amount of experimental work is carried out and has been done in the past so that theoretical results can be compared with experimental data. Furthermore, these polymers possess a well defined internal microstructure represented by their chemical constitution and they show complicated nonlinear mechanical behaviour which is common to many complex materials.

The description of polymers mentioned in the preceding paragraph is the main emphasis of the present thesis. To be sure, much work has been done since the 1940s concerning media with internal microstructure from a continuum point of view. Irreversible thermodynamics has been applied to these materials in this setting through the works of several researchers who put in a mathematical form the governing equations for the constitutive behaviour of complex media. Furthermore, in the 1960s statistical mechanics of chain molecules emerged as an efficient and very successful tool to connect chemical structure, *i. e.* constitution and configuration, with the configurational and conformational statistics of chain molecules. Since then these tools have been further refined and have evolved into the central work of Macromolecular Physical Chemistry. Despite all this progress, the proper modeling of transport processes is very difficult and requires a lot of experience. As a result, it seems that today fewer researchers use any thermodynamic information in their modeling. Furthermore, in physics, engineering, and rheology the material's detailed chemical structure is not taken into account in the theoretical description of complex materials and often coarse grained chain models are invoked to describe the material properties related to the internal microstructure. Implications thus arising are reflected in the failure of the numerical solution of the corresponding equations of motion or in the prediction of aphysical results. The use of a *priori* coarse grained mechanical models has implications on the modeling of material properties related to the internal microstructure, such as energetic and entropic elasticity.

In the present thesis a modern approach to non-equilibrium thermodynamics is adopted to derive a full set of thermodynamically and mechanically consistent time evolution equations (Eqs. (4.42a)-(4.42d), p. 79) for non-isothermal and compressible polymeric materials. The GENERIC formalism [1] adopted herein is closely related to the single generator Hamiltonian formalism of non-equilibrium thermodynamics [2]. This is the set of time evolution equations adopted in the present dissertation to study flow phenomena of polymeric materials. To apply

the evolution equations to specific materials equilibrium thermodynamics of chain fluids and statistical mechanics of chain molecules have been adopted. This allows us to treat the rheology, rheoptics, and non-isothermal rheology of amorphous polymeric materials. The single chapters are organized as follows.

After this introduction (Chap. 1) thermodynamic potentials for polymeric materials are presented and evaluated (Chap. 2). A possible choice of physical variables to describe the thermodynamics of polymers are the mass density, the internal energy density (or temperature), and a second rank conformation tensor describing the average shape and extension of the molecules. The thermodynamic theories, in terms of a second rank conformation tensor, emerge as the simplest ones able to provide models representing the polymer rheology under a broad variety of flow conditions. For the liquid contribution to the thermodynamic potential we define two Massieu functions leading to a SG [3, 4] and a modified FOV [5, 6, 7, 8, 9] equation of state, respectively. For the elastic part to the potential we adopt the Massieu function of the Hookean spring and we perform detailed atomistic calculations using the RIS approximation [10, 11, 12, 13]. Numerical examples appropriate to linear PE and to hexadecane are given and comparison with experimental data for the liquid state is made. Then it is shown how to compute the characteristic elastic constant for real polymer chains adopting the RIS approximation (Chap. 3). The energetics and entropics for the chain conformations are extracted from the characteristic elastic constant and the consequences for the Theory of Purely Entropic Elasticity and for polymer processing are discussed. This allows to check if the material is of purely entropic elasticity or not. Numerical examples for PE and PIB are given. PE is not of purely entropic elasticity whereas PIB is. The result for the latter is consistent with experimental findings in stress relaxation experiments [14]. The mesoscopic friction coefficient and the relaxation time spectrum for polymer melts (*i. e.* their fading memory) can be understood on the Rouse model and the reptation model [15, 16, 17, 18] and are discussed briefly at the end of Chap. 3. The temperature and density dependence of these quantities is described by the equation of Ferry [19, 20] and the WLF equation for undercooled systems [21]. To have a guess for the magnitude of the material's frictional properties at a fixed temperature and pressure molecular dynamics data from MD/MC simulations of atomistic, polydisperse PE melts [22, 23] can be taken. With Chaps. 2 and 3 we dispose of a full thermodynamic description of the quiescent material in the unoriented and in the slightly

preoriented state. To compute further material properties such as viscosities or normal stress coefficients and to discuss fluid dynamics of these materials a set of macroscopic time evolution equations for the deforming/flowing material has to be derived. Therefore non-equilibrium thermodynamics has to be invoked: this is the topic of Chap. 4 where we have shown that modern frameworks of non-equilibrium thermodynamics can be adopted to describe the macroscopic flow behaviour of non-isothermal and compressible polymeric materials.

In Chap. 4 the thermodynamics and mechanics of deforming non-isothermal polymeric materials are examined within the auspices of a new methodology wherein the laws of physics and principles of mechanics which are applicable to these thermodynamic systems are imbedded in a definite mathematical structure of a general, abstract equation [1, 24]. Such a concept allows to derive a full set of macroscopic time evolution equations for the fundamental variables to the description of deforming polymeric materials: the density, the internal energy density, the conformation tensor, and the momentum density. All non-resolved degrees of freedom are represented by the internal energy density. This quantity can be expressed in terms of the other macroscopic thermodynamic variables through an equation of state (*cf.* Chap. 2). (This so called quasi equilibrium hypothesis is further explained in the next paragraph.) In addition to that our approach allows new insight to be obtained concerning some aspects of non-isothermal flows of polymeric fluids, and permits a consistent expression and interpretation of other thermodynamic theories for these systems which have been developed over the past forty years. These theories comprise the time temperature superposition principle [19, 25, 20, 21, 26, 27] and its extensions to non-isothermal flows [28, 29, 30, 31, 32], the Theory of Simple Fluids with Fading Memory [33, 34, 35], Rational Thermodynamics [36, 37, 38, 39, 40, 41], and the Theory of Purely Entropic Elasticity [42, 43, 44, 45, 46]. A major portion of the analysis is devoted to demonstrating the above statements, and in so doing some common misconceptions occurring in a significant fraction of the literature regarding this subject are exposed. The definite mathematical structure of the new methodology permits the thermodynamically consistent generalization of isothermal, incompressible models of polymeric materials to non-isothermal, compressible conditions. Doing thus reproduces, corrects, and extends non-isothermal models which have been developed over the years [47, 30, 48, 49, 50, 51, 52, 53, 54], and also allows for simpler (but equivalent) representations of these models in terms of al-

ternate variables with a clearer connection to the microstructure of the material than the stress tensor and heat flux vector fields. Furthermore, a generalization of the GENERIC structure is proposed that accommodates interactions between phenomena of differing parities, which impose antisymmetry upon the corresponding elements of the dissipative operator matrix.

Before discussing the content of the remaining Chaps. 5 and 6 we wish to explain the quasi equilibrium assumption made in connection with the discussion in the preceding paragraph: we assume that for the time and length scales of observation, the internal energy of the system has had time to become equilibrated among the non-resolved degrees of freedom, and that the velocity distribution of the particles around the average has had the time to achieve a Maxwellian shape characterized by the temperature. In this case, it is useful to distinguish between the energy associated with the non-equilibrated degrees of freedom present in the continuum formulation and the energy corresponding to the non-resolved degrees of freedom represented by the internal energy. The local change of internal energy density per unit change in entropy density defines the thermodynamic temperature. Entropy is viewed as a state variable of the system which, together with the other state variables, is enough to describe the physical state of the system.

In Chaps. 5 and 6 we discuss some particular solutions of the PDE's derived in Chap. 4 using thermodynamic data collected in Chaps. 2-3. A Runge Kutta scheme has been applied to compute the rheological and rheo-optical properties for a large number of viscoelastic constitutive equations. This allows a unified treatment of polymer rheology [26, 55, 56] by means of constitutive equations of the differential type and it allows to discuss properties of the processed material which are related to the deformation induced changes in the internal microstructure. Such properties can be measured in rheo-optics [57, 58, 59]. In Chap. 5 an alternative representation of the recently proposed enhanced viscoelastic fluid models (the so called FETA models [60]) in terms of the conformation tensor is proposed. We show the equivalence of this representation with the originally proposed formulation in terms of the extra stress tensor. Furthermore, we give a microscopic interpretation of the phenomenological coefficients appearing in these models and we make suggestions how they may be obtained from atomistic simulations. Chap. 6 is devoted to non-isothermal rheology of polymeric materials [61, 62, 57, 63]. We present a numerical study of non-isothermal fiber

spinning processes taking into account compressibility and energetic elasticity of the processed material. For the thermodynamic potential we adopt a combination of a FOV free energy and the thermodynamic potential of a Hookean dumbbell. We use thermodynamic data and RIS models appropriate to PE (*cf.* Chaps. 2, 3) as an input for our numerical calculations. The basic equations of motion arise from a modern framework of non-equilibrium thermodynamics derived in Chap. 4 and are solved for homogenous deformation, temperature, and density. We discuss the morphology and the physical and thermodynamic properties of the processed sample. Accounts on non-isothermal stress relaxation experiments and the problem of critical cooling are given and a summary is made at the end (Chap. 7).



## Chapter 2

# Thermodynamic Potentials for Polymeric Materials

### Abstract

Thermodynamic potentials for polymer melts are presented. For the liquid contribution to the thermodynamic potential we define two Massieu functions leading to a SG and a FOV equation of state, respectively. The elastic part of the potential is determined through the internal microstructure of the fluid. For this part to the potential we adopt the Massieu function of the Hookean dumbbell and we perform detailed atomistic simulations using the Rotational Isomeric State approximation. Numerical examples appropriate to linear PE and to hexadecane are given and comparison with experimental data for the liquid state is made.

## 2.1 Introduction

In the past decade much effort has been devoted to the investigation of various aspects of non-isothermal polymeric liquids, like the thermodynamics and kinetic theory of these materials under non-equilibrium conditions [2, 1, 24, 64] and the numerical methods required to treat the time evolution equations, see *e. g.*, [65]. Furthermore, simulation techniques for atomistic polymers have been further refined to understand the thermodynamics of unstrained and strained (preoriented) polymer melts [22]. In what follows we discuss the thermodynamic properties of linear polyethylene (PE) and hexadecane above their melting temperatures taking into account the detailed chemical structure. Thereby we allow for non-isothermal behaviour and take into account the compressibility of the material. We give analytical expressions for the thermodynamic potential of the polymer from which the thermodynamic properties ( $\rho pT$ -behaviour and heat capacity) of the quiescent material will be determined.

Theoretical studies of the statistical mechanics and the thermodynamic properties of high polymers have a long history, beginning with the pioneering works of Prigogine and coworkers [66, 67] and Flory and coworkers [5, 6, 7]. The problem is quite complicated, since analytical expressions for the thermodynamic potential of these materials are not well established and one has to consider the liquid contribution as well as the elastic contribution of the internal microstructure to the thermodynamic potential.

It is well known that the theoretical discussion of thermodynamic properties of polymeric liquids is difficult even in the incompressible case, since the temperature changes affect the pressure of the material. The influence of non-isothermal conditions is further enhanced by the considerable free volume of polymeric fluids which calls in question the approximation of incompressibility. Besides the effect on density variations considered, for instance in [64], it is also desirable to include the detailed chemical structure into the study of polymeric liquids. The appropriate tools are well understood and have been applied successfully to a huge number of polymers [10, 11, 12, 13]. This is important since the energetics of the bond conformations manifests measurable influence on the elastic properties of the polymer [68, 69, 70] which may become important in extreme deformation and temperature histories

as encountered in polymer industry. Another problem generally overlooked is the accurate description of the effect of temperature variations on the internal microstructure of the material [47, 49].

In the present work we include all these ingredients in the thermodynamic potential of  $n$ -alkanes. To capture the properties of the material's internal microstructure we adopt the Rotational Isomeric State (RIS) approximation [10, 11, 12]. This approach is broadly applicable to chains of any length, to copolymers of any specified composition and to asymmetric chains of any stereochemical configuration. The application of these methods to amorphous polymers in the bulk has been a topic of some controversy but experimental evidence has shown that single polymer chains behave like random coils under  $\Theta$ -conditions in the amorphous phase [71, 72, 73, 74, 75].

In Sec. 2.2 we give the basic variables of a polymeric liquid and we review the general thermodynamic relationships for materials with internal microstructure. In Sec. 2.3 we give two thermodynamic potentials accounting for the liquid contribution to the thermodynamic potential. From these thermodynamic potentials we calculate the equations of state, the coefficients of the pressure and the density, and the heat capacity. Sec. 2.4 deals with the contribution of the internal microstructure to the thermodynamic potential and the basics of the RIS approximation. Applications to linear PE and hexadecane are given and comparison with experimental data is made in Sec. 2.5.

## 2.2 General Relationships

Since we are interested in practical applications of non-equilibrium thermodynamics (calculation of viscosities, normal stress coefficients, strain birefringence, non-isothermal stress-relaxation experiments, and phase transitions under flow) we want to specify analytical expressions for the material's thermodynamic potential to understand the quasi-equilibrium thermodynamic properties of the melt. We wish to take the Massieu function (the Legendre transformation of the entropy density [24, 76]) as the thermodynamic potential since it depends on measurable quantities: the density,  $\rho$ , the temperature,  $T$ , and the contravariant conformation tensor,  $\mathbf{c}$ . The conformation tensor is the second moment of the end-to-end vector of the chain and describes the average exten-

sion and orientation of the polymer chain at a reference temperature. For a simple (*i. e.* one component) polymeric fluid the thermodynamic potential can be split into two contributions [2, 1, 24, 77]

$$\omega(\rho, T, \mathbf{c}) = \omega_0(\rho, T) + \omega_1(\rho, T, \mathbf{c}), \quad (2.1)$$

where  $\omega_0(\rho, T)$  is the liquid contribution due to intermolecular interactions and  $\omega_1(\rho, T, \mathbf{c})$  is the elastic contribution due to the internal microstructure. The pressure is defined as

$$p = T \left( \omega - \rho \left. \frac{\partial \omega}{\partial \rho} \right|_{T, \mathbf{c}} \right), \quad (2.2)$$

which represents the thermal equation of state of the chain fluid. From the equation of state the temperature coefficient of the pressure can be calculated

$$\gamma = \left. \frac{\partial p}{\partial T} \right|_{\rho, \mathbf{c}}. \quad (2.3)$$

Inversion of the equation of state (2.2) with respect to the mass density yields the thermal expansion coefficient and the isothermal compressibility

$$\beta = -\frac{1}{\rho} \left. \frac{\partial \rho}{\partial T} \right|_{p, \mathbf{c}}, \quad (2.4)$$

$$\kappa = \frac{1}{\rho} \left. \frac{\partial \rho}{\partial p} \right|_{T, \mathbf{c}}. \quad (2.5)$$

Note that in the density variable formulation the pressure is not a problem variable. The conjugate variable to  $\rho$  is  $\mu \equiv \partial \omega / \partial \rho|_{T, \mathbf{c}}$  and not  $p$ . Consequently the expressions of Eqs. (2.4) and (2.5) do not involve the proper thermodynamic derivatives. But these quantities are the measurable coefficients of the density and therefore we wish to use them in the future. A well known thermodynamic relationship states that only two of the material properties are independent

$$\gamma = \frac{\beta}{\kappa}. \quad (2.6)$$

The heat capacity (at constant mass density) is defined as

$$c = c_\rho = \frac{T}{\rho} \left( 2 \left. \frac{\partial \omega}{\partial T} \right|_{\rho, \mathbf{c}} + T \left. \frac{\partial^2 \omega}{\partial T^2} \right|_{\rho, \mathbf{c}} \right). \quad (2.7)$$

The quantity  $c_p$  (heat capacity at constant pressure), cannot be obtained from the thermodynamic potential,  $\omega$ , because the pressure,  $p$ , is not a variable in the density variable formulation. This quantity has to be calculated from the heat capacity,  $c$ , and the coefficients of the mass density

$$c_p = c - \frac{T \beta^2}{\rho \kappa}. \quad (2.8)$$

In general the heat capacity is a complicated function of the mass density. For the density coefficient of the heat capacity we have

$$\left. \frac{\partial c}{\partial \rho} \right|_{T,c} = -\frac{T}{\rho^2} \left. \frac{\partial \gamma}{\partial T} \right|_{\rho,c}, \quad (2.9)$$

and for the pressure coefficient of  $c_p$

$$\left. \frac{\partial c_p}{\partial p} \right|_{T,c} = -\frac{T}{\rho} \left( \beta^2 + \left. \frac{\partial \beta}{\partial T} \right|_{p,c} \right). \quad (2.10)$$

In what follows we want to specify analytical expressions for the liquid contribution to the thermodynamic potential (Sec. 2.3) and for its elastic contribution (Sec. 2.4). Furthermore, analytical expressions for the temperature and the pressure coefficients will be given. With the analytical expressions at hand we will specify the characteristic properties of  $n$ -alkanes and we make a comparison with experimental data (Sec. 2.5).

## 2.3 Liquid Contribution

In this section we present two Massieu functions for the liquid contribution to the thermodynamic potential,  $\omega_0$ . For both functions we derive the constitutive equation for the pressure. Furthermore, we calculate the thermodynamic coefficients of these Massieu functions and the heat capacity. The Massieu function presented in the first subsection leads to the equation of state according to Spencer and Gilmore. This thermodynamic potential is easy to handle from a mathematical point of view. The second Massieu functions leads to a modified Flory-Orwoll-Vrij equation which gives a better fit to the equilibrium  $\rho p T$  behaviour. This will become evident in Sec. 2.5 when we give numerical examples appropriate to linear PE and hexadecane.

### 2.3.1 Spencer-Gilmore Potential

We take the following Massieu function for the liquid contribution to the thermodynamic potential

$$\omega_0(\rho, T) = \rho \alpha_0 k_B \left\{ 1 + \ln \left[ \left( \frac{1}{\rho \alpha_0} - \frac{1}{\rho_0 \alpha_0} \right) \check{c} T^{\frac{3}{2}} \right] \right\} - \frac{\pi}{T}, \quad (2.11)$$

which is the thermodynamic potential of a van-der-Waals fluid. In the above equation  $\alpha_0$  is a phenomenological parameter of units  $\text{mass}^{-1}$ ,  $k_B$  is Boltzmann's constant,  $\rho_0$ ,  $\pi$ ,  $\check{c}$  are coefficients depending on the material (*cf.* Tab. 2.1, p. 14).  $\alpha_0$  can be taken as Avogadro's Number divided by the molecular weight of the structural unit or rather the molecular weight of interacting units in the fluid,  $\alpha_0 = N_A/M_W$ . Inserting Eq. (2.11) into Eq. (2.2) for the pressure we obtain

$$(p + \pi)(\rho_0 - \rho) = \alpha_0 \rho_0 \rho k_B T, \quad (2.12)$$

which is the Spencer-Gilmore equation [3, 4].

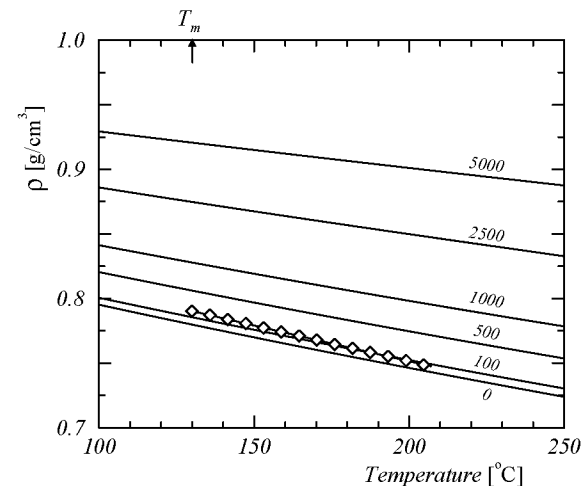


**Figure 2.1:** The mass density of linear PE as a function of temperature for different pressures calculated according to Eq. (2.12). The numbers denote the pressure in bar, the diamonds correspond to experimental values. The arrow denotes the melting point of approximately 130°C.

From Eq. (2.12) we can calculate the thermal expansion coefficient, the isothermal compressibility, and the temperature coefficient of the pressure according to Eqs. (2.4), (2.5), (2.6)

$$\beta^{-1} = \frac{1}{\rho_0} \left[ \rho_0 T + \frac{1}{\alpha_0 k_B T} (p + \pi)^2 \right], \quad (2.13)$$

$$\kappa^{-1} = \frac{1}{\rho_0} \left[ \rho_0 (p + \pi) + \frac{1}{\alpha_0 k_B T} (p + \pi)^2 \right], \quad (2.14)$$

$$\gamma = \frac{p}{T} + \frac{\pi}{T} = \frac{\alpha_0 \rho_0 \rho k_B}{\rho_0 - \rho}. \quad (2.15)$$

The heat capacity is the constant  $c = 3/2\alpha_0 k_B$ . Furthermore, we have  $c_p - c = \alpha_0 k_B$ . The coefficients of the heat capacities vanish identically which is consistent with Eqs. (2.9), (2.10). In Figs. 2.1 we have plotted the density of PE as a function of temperature with the pressure as a parameter. The symbols denote experimental data [7]. Eqs. (2.13)-(2.15) may be used to obtain a guess for the magnitude of  $\beta$ ,  $\kappa$ ,  $\gamma$ . A more detailed discussion is given in Sec. 2.5, p. 27.

### 2.3.2 Modified Flory-Orwoll-Vrij Potential

To obtain more sophisticated equations of state for chain fluids it is convenient to introduce reduced quantities for the mass density, the pressure, and the temperature of the polymeric liquid

$$\tilde{\rho} = \frac{\rho}{\rho^*}, \quad \tilde{p} = \frac{p}{p^*}, \quad \tilde{T} = \frac{T}{T^*}, \quad (2.16)$$

where  $\rho^*$ ,  $p^*$ , and  $T^*$  are, respectively, the characteristic density, pressure and temperature. These quantities can be determined from a microscopic cell model [5, 8, 66] where all mers of the melt interact via a Lennard-Jones Potential. Numerical values for the characteristic properties of hexadecane and PE are collected in Tab. 2.1, p. 14. In general only two of these quantities are independent,  $p^* = \alpha_0 \rho^* \tilde{c} k_B T^*$ , where the quantity  $\tilde{c}$  is assumed to be independent of temperature and volume over the range of application of the thermodynamic potential to be set down. This factor is supposed to take into account the restrictions on the precise location of a given segment by its neighbors in the same chain [5].  $\alpha_0$  is a constant taking into account the molecular characteristics of the interacting fluid particles. The characteristic temperature is

$T^* = \tilde{s}\tilde{\eta}/\tilde{c}/k_B$ , where  $\tilde{\eta}$  is a characteristic mer-mer interaction energy,  $\tilde{s}$  denotes the number of contacts per mer ( $\approx 3-6$ ), and  $3\tilde{c}$  is the number of degrees of freedom per mer [8, p. 812].

From the thermal and the caloric equations of state (2.18), (2.28) we construct the thermodynamic potential

$$\omega_0(\tilde{\rho}, \tilde{T}) = \frac{\tilde{\rho} p^*}{T^*} \left\{ 1 + \ln \left( \Gamma_0 \frac{\tilde{T}^{\Gamma} \tilde{T}^{\Delta}}{\alpha_0 \rho^*} \right) + 3 \ln \left( \tilde{\rho}^{-\frac{1}{3}} - \delta \right) + A \frac{\tilde{\rho}^2}{\tilde{T}} - \frac{B}{2} \frac{\tilde{\rho}^4}{\tilde{T}} \right\}, \quad (2.17)$$

where  $A$ ,  $B$ ,  $\Delta$ ,  $\Gamma$ , and  $\delta$  are coefficients,  $\Gamma_0$  is a geometrical factor, and  $\alpha_0$  is a phenomenological coefficient accounting for the strength of the liquid contribution to the total Massieu function (2.1).  $A$  and  $B$  are parameters in the Lennard-Jones potential and are determined by the geometry of the cell lattice.  $\delta$  is a geometrical factor which is determined by the cell geometry (e. g.  $\delta = 1$  for a simple cubic geometry,  $\delta = 1/2^{\frac{1}{2}}$  for a *hcp* geometry [8]). The parameters  $A$ ,  $B$ ,  $\delta$  have the values 1.2045, 1.001, and 0.9532, respectively [9].

**Table 2.1:** Characteristic thermodynamic properties for hexadecane and for PE from Refs. [9, 78] (1 bar = 0.1 MPa =  $10^5$  kg/m/s<sup>2</sup>).

	$p^*$ (bar)	$\rho^*$ (g cm <sup>-3</sup> )	$T^*$ (K)
C <sub>16</sub> H <sub>34</sub>	5046.0	0.9142	4344.6
PE	5452.0	0.9544	5484.7
	$M_W$ (g mole <sup>-1</sup> )	$\pi$ (bar)	$\rho_0$ (g cm <sup>-3</sup> )
PE	28.0	3470.0	1.0526

Inserting Eq. (2.17) in the definition of the pressure (2.2) we obtain the following constitutive equation

$$\tilde{p} = \frac{\tilde{\rho} \tilde{T}}{1 - \delta \tilde{\rho}^{\frac{1}{3}}} - \tilde{\rho}^2 (2A \tilde{\rho} - 2B \tilde{\rho}^3). \quad (2.18)$$

For  $A = B = 0$  and  $\delta = 1$  this equation of state reduces to the classical FOV equation [5, 6, 7, 8, 9].

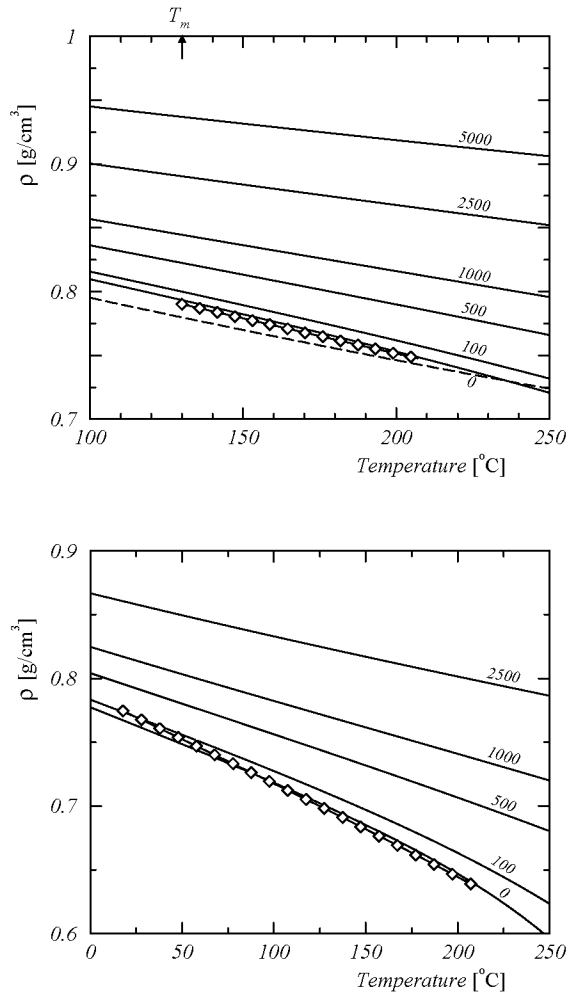


**Figure 2.2:** The same as Fig. 2.1 according to the modified FOV equation (2.18) for a) PE and b) hexadecane. The long dashed line in a) corresponds to the Spencer-Gilmore equation at zero pressure, symbols are experimental data at atmospheric pressure.

In terms of the reduced variables the coefficients of the density and the pressure are

$$\beta = - \frac{\tilde{p}\tilde{T}}{\tilde{\rho}\tilde{T}} \left. \frac{\partial \tilde{\rho}}{\partial \tilde{T}} \right|_{\tilde{p}}, \quad (2.19)$$

$$\kappa = \frac{\tilde{p}}{\tilde{\rho}\tilde{p}} \left. \frac{\partial \tilde{\rho}}{\partial \tilde{p}} \right|_{\tilde{T}}, \quad (2.20)$$

$$\gamma = \frac{\tilde{p}\tilde{T}}{\tilde{\rho}\tilde{T}} \left. \frac{\partial \tilde{p}}{\partial \tilde{T}} \right|_{\tilde{\rho}}. \quad (2.21)$$

Substituting the constitutive equation for the pressure (2.18) into the above equations we obtain the thermal expansion, the isothermal compressibility, and the temperature coefficient of the pressure

$$(\beta T)^{-1} = \frac{\delta \tilde{\rho}^{\frac{1}{3}}}{3(1 - \delta \tilde{\rho}^{\frac{1}{3}})} - 1 + \frac{2\tilde{p} + \tilde{\rho}^2(-2A\tilde{\rho} + 6B\tilde{\rho}^3)}{\tilde{p} + \tilde{\rho}^2(2A\tilde{\rho} - 2B\tilde{\rho}^3)}, \quad (2.22)$$

$$(\kappa p)^{-1} = \left[ \frac{\delta \tilde{\rho}^{\frac{1}{3}}}{3(1 - \delta \tilde{\rho}^{\frac{1}{3}})} - 1 \right] \left[ 1 + \frac{\tilde{\rho}^2}{\tilde{p}}(2A\tilde{\rho} - 2B\tilde{\rho}^3) \right] + 2 + \frac{\tilde{\rho}^2}{\tilde{p}}(-2A\tilde{\rho} + 6B\tilde{\rho}^3), \quad (2.23)$$

$$\gamma \frac{T}{p} = 1 + \frac{\tilde{\rho}^2}{\tilde{p}}(2A\tilde{\rho} - 2B\tilde{\rho}^3). \quad (2.24)$$

In the appropriate limit these expressions reduce to the known coefficients of the FOV equation [5]. In the limit of zero pressure we have

$$(\beta T)^{-1} = \frac{\delta \tilde{\rho}^{\frac{1}{3}}}{3(1 - \delta \tilde{\rho}^{\frac{1}{3}})} - 1 + \frac{-2A\tilde{\rho} + 6B\tilde{\rho}^3}{2A\tilde{\rho} - 2B\tilde{\rho}^3}, \quad (2.25)$$

$$\kappa^{-1} = \left[ \frac{\delta \tilde{\rho}^{\frac{1}{3}}}{3(1 - \delta \tilde{\rho}^{\frac{1}{3}})} - 1 \right] \tilde{\rho}^2 p^*(2A\tilde{\rho} - 2B\tilde{\rho}^3) + \tilde{\rho}^2 p^*(-2A\tilde{\rho} - 6B\tilde{\rho}^3), \quad (2.26)$$

$$\gamma = \frac{p^* \tilde{\rho}^2}{T}(2A\tilde{\rho} - 2B\tilde{\rho}^3). \quad (2.27)$$

In Figs. 2.3-2.5 we display the thermodynamic coefficients (2.22)-(2.24) for PE and hexadecane as a function of temperature with the pressure as a parameter.

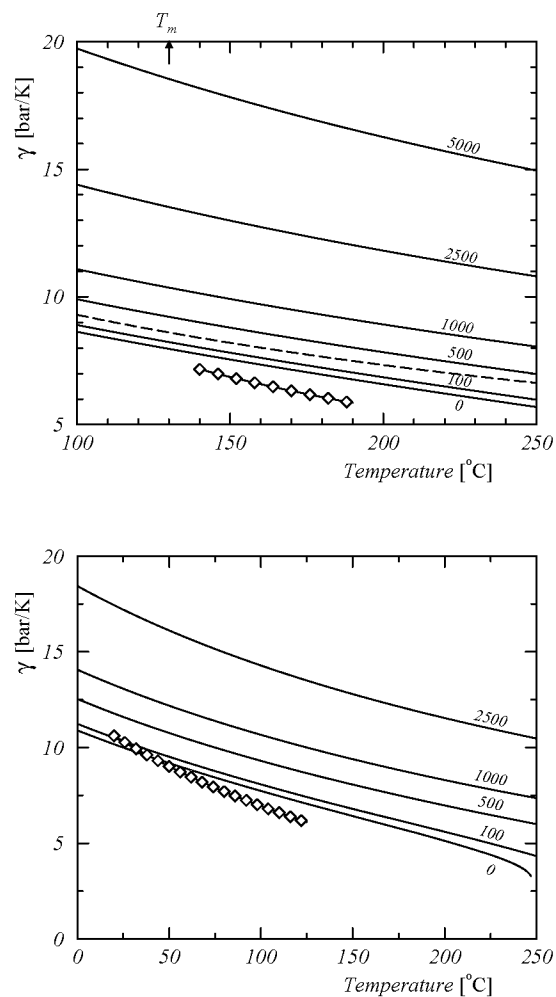


**Figure 2.3:** The temperature coefficient of the pressure according to the modified FOV equation (2.24), p. 16 for a) PE and b) hexadecane and different pressures (denoted in bar with each curve). The long dashed line in a) corresponds to the Spencer-Gilmore equation for  $p = 0$ , the symbols denote experimental data at atmospheric pressure.

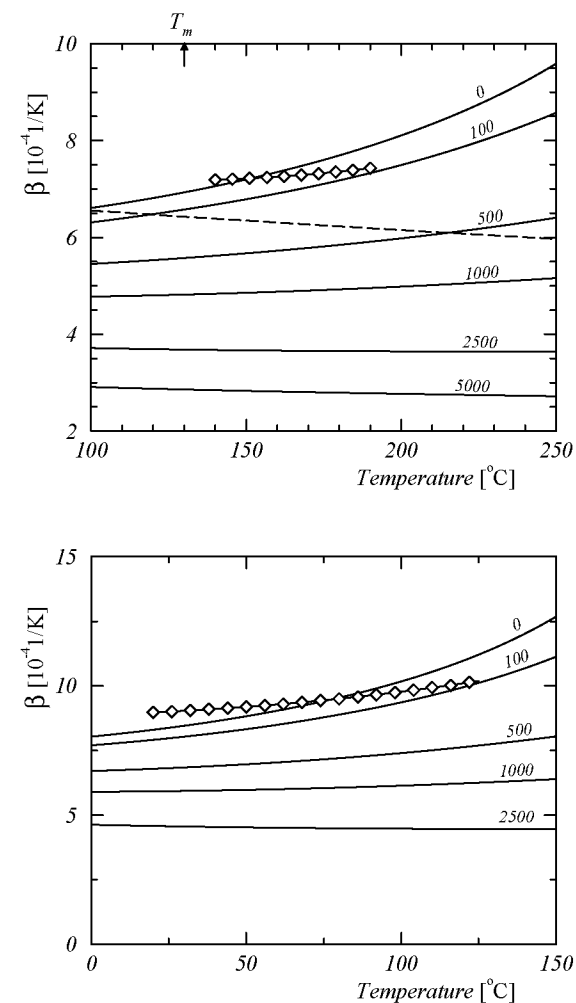


**Figure 2.4:** The same as Fig. 2.3 for the thermal expansion coefficient according to Eq. (2.22), p. 16 for a) PE and b) hexadecane. The long dashed line in a) is the Spencer-Gilmore equation.

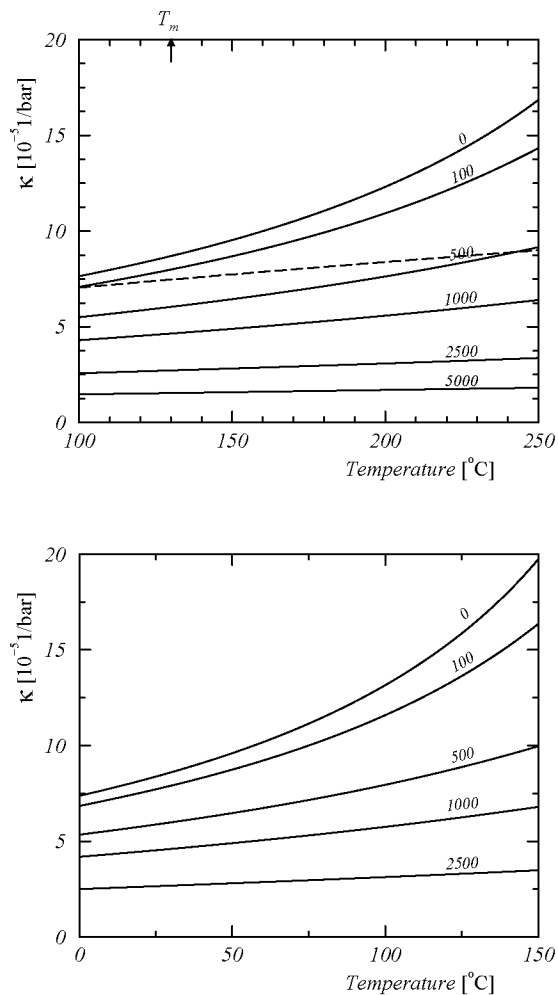


**Figure 2.5:** The same as Fig. 2.3 for the isothermal compressibility according Eq. (2.23), p. 16 for a) PE and b) hexadecane. The long dashed line in a) corresponds to the Spencer-Gilmore equation.

Inserting (2.17) into the equation for the heat capacity (2.7) yields

$$c = \alpha_0 k_B (2\tilde{c}\Gamma^2 \tilde{T} + \tilde{c}\Delta\Gamma), \quad (2.28)$$

which is linear in temperature. According to this equation  $c$  does not depend on density. From Eq. (2.24) it follows that  $\partial\gamma/\partial T|_\rho = 0$ . Fig. 2.9 (p. 29) shows the heat capacity for PE as a function of temperature. In the lower part of the figure we plotted the conformational part of the heat capacity arising from material elasticity (*cf.* Sec. 2.4). A detailed discussion of the thermodynamic properties of  $n$ -alkanes (Figs. 2.2-2.5 and 2.9) is postponed to Sec. 2.5. In the subsequent Sec. 2.4 we want to introduce the Massieu function of a network of Hookean dumbbells and we show how it can be related to the chemical structure of the polymer under consideration.

## 2.4 Elastic Contribution

### 2.4.1 Thermodynamic Potential of a Fixed Polymer Network

To give a description of non-isothermal and compressible chain fluids we wish to adopt the thermodynamic potential of the Hookean dumbbell with infinite chain extensibility. In this case the elastic contribution to the Massieu function is given by the elastic energy of the polymer plus the Boltzmann entropy of an assembly of many chains [2, 24, 77]

$$\omega_1(\rho, T, \mathbf{c}) = -\frac{1}{2T}\rho\alpha_1 K(T)\text{tr}\mathbf{c} + \frac{1}{2}\rho\alpha_1 k_B \ln(\det \mathbf{c}). \quad (2.29)$$

The parameter  $\alpha_1$  in the above equation is a measure of the degree of elasticity per unit mass of the polymeric fluid, which gives a quantitative measure of the strength of elastic forces per unit mass in the material. As an example, for a polymer melt,  $\alpha_1$  is given by the number of crosslinks or entanglement points per unit volume divided by the mass density. It is taken herein as a material constant; *i. e.*, it is not a function of temperature. According to Kuhn and Gr $\ddot{u}$ n [79] the spring constant is defined as

$$K(T) = \frac{3}{2} \frac{k_B T}{\text{tr}\langle \mathbf{R}\mathbf{R} \rangle_0}, \quad (2.30)$$

where  $\mathbf{R}$  is the end-to-end vector of the polymer chain or the distance between crosslinks or entanglement points and  $\langle \mathbf{R}\mathbf{R} \rangle_0$  is the second moment of the the end-to-end vector evaluated at equilibrium. Substituting Eq. (2.29) into Eq. (2.2) we see that the pressure arising from  $\omega_1$  vanishes. This represents the main assumption of the present work which may be removed by taking into account the finite extensibility of the chains. Preliminary studies in this direction could be undertaken, e. g., in the framework of non-equilibrium molecular dynamics (NEMD). The conformational part of the heat capacity (*cf.* Fig. 2.9) is given as

$$c_{\text{conf}} = -\frac{1}{2} T \alpha \text{trc} \frac{\partial^2 K(T)}{\partial T^2} . \quad (2.31)$$

To apply the above Massieu function to polymeric liquids it is essential to find the functional form of the spring constant for the special polymer under consideration. This means that the temperature dependencies of the statistical averages of the vector  $\mathbf{R}$  have to be determined. In former works on non-equilibrium thermodynamics of polymeric liquids  $\text{tr}\langle \mathbf{R}\mathbf{R} \rangle$  has been assumed to be a constant or phenomenological forms of the spring constant have been assumed [47, 49]. Here we want to use detailed atomistic representations of the polymer and to calculate the moments of  $\mathbf{R}$  as a function of temperature. To this end we resort to the RIS approximation [10, 11, 12].

## 2.4.2 Statistical Mechanics of Chain Molecules

In the RIS approximation each molecule is treated as occurring in one or another of several discrete rotational states. The states are chosen to coincide with potential minima of the conformational energy as a function of the rotation angle about the skeletal bonds, the lengths of the bonds and the bond angles being considered as constant. A given configuration of the molecule is then specified by a set of torsional angles  $\{\phi\}$ . Then for each bond  $i$  of the chain a statistical weight matrix

$$\mathbf{U}_i = [ u_{\zeta\eta} ]_i , \quad 1 < i < n , \quad (2.32)$$

can be defined with states ( $\zeta$ ) for bond  $i - 1$  indexing the rows and those ( $\eta$ ) for bond  $i$  the columns ( $\zeta, \eta = \alpha, \beta, \dots, \nu$ ). The energies  $E_{\zeta\eta}$  corresponding to the statistical weights  $u_{\zeta\eta}$  are defined through the

Boltzmann factors

$$u_{\zeta\eta;i} = \exp \left( -\frac{E_{\zeta\eta;i}}{RT} \right) , \quad (2.33)$$

where  $E_{\zeta\eta;i}$  is the contribution to the total energy of the configuration,  $E(\{\phi\})$ , associated with the assignment of bond  $i$  to state  $\eta$ , bond  $i - 1$  being in state  $\zeta$ .

The configurational partition function for a chain with  $n$  bonds is then given as

$$Z = \mathbf{U}_1 \mathbf{U}_2^{(n-2)} \mathbf{U}_n , \quad (2.34)$$

where the  $\mathbf{U}_i$ ,  $1 < i < n$ , are square matrices of order  $\nu \times \nu$ ;  $\mathbf{U}_1$ ,  $\mathbf{U}_n$  are row, column vectors of order  $\nu$

$$\mathbf{U}_1 = ( 1 \ 0 \ \dots \ 0 ) , \quad \mathbf{U}_n = ( 1 \ 1 \ \dots \ 1 )^T , \quad (2.35)$$

and we have introduced the notation proposed by Flory to denote the serial product [11]

$$\mathbf{U}_2^{(n-2)} = \mathbf{U}_2 \mathbf{U}_3 \dots \mathbf{U}_{n-2} . \quad (2.36)$$

Consider a configuration dependent molecular property  $f = f(\{\phi\})$  (e. g. the chain displacement vector  $\mathbf{R}$  connecting its ends, or various products that may be formed from  $\mathbf{R}$ ) which can be expressed as a sum of contributions each attributable to an individual skeletal bond of the chain. For a specified configuration  $\{\phi\}$  of the chain the property  $f = f(\{\phi\})$  can be generated by serial multiplication of generator matrices  $\mathbf{F}_i$  of order  $s$  (*cf.* next subsection). For the purpose of generating the average over all configurations of the chain, we formulate the generator matrix [11]

$$\mathcal{F}_i = (\mathbf{U}_i \otimes \mathbf{E}_s) \|\mathbf{F}_i\| , \quad 1 < i < n , \quad (2.37)$$

where  $\mathbf{E}_s$  is the identity matrix of order  $s$ ,  $\|\mathbf{F}_i\|$  is the diagonal array of the generator matrices  $\mathbf{F}_i(\alpha), \dots, \mathbf{F}_i(\nu)$ , and  $\otimes$  denotes the direct product<sup>1</sup>. The terminal matrices are given by

$$\mathcal{F}_{[1]} = \mathbf{U}_1 \otimes \mathbf{F}_{[1]} , \quad \mathcal{F}_{[n]} = \mathbf{U}_n \otimes \mathbf{F}_{[n]} . \quad (2.38)$$

<sup>1</sup>The direct product,  $\mathbf{A} \otimes \mathbf{B}$ , of matrices  $\mathbf{A}$  and  $\mathbf{B}$  of orders  $\alpha \times \alpha'$  and  $\beta \times \beta'$ , respectively, is the matrix of order  $(\alpha\alpha') \times (\beta\beta')$  obtained by replacing  $A_{ij}$  by  $A_{ij}\mathbf{B}$  for each  $i, j$ .



The average  $\langle f \rangle_0$  of the quantity  $f$  is then given as

$$\langle f \rangle_0 = \frac{\mathcal{F}_{[1} \mathcal{F}_2^{(n-2)} \mathcal{F}_n]}{Z}. \quad (2.39)$$

Once the statistical weight matrices  $\mathbf{U}_i$  and the generator matrix  $\mathbf{F}_i$  for the configuration dependent property (e. g. the chain displacement vector) are known the averages can be calculated according to the above equation (2.39). In what follows we focus on the evaluation of the first and second moment of the chain end-to-end vector. First we present the generator matrices for the chain displacement vector (2.43) and the second order tensor of the end-to-end vector (2.47). In Sec. 2.5 we apply the RIS models to linear  $n$ -alkanes and in this framework we write down the matrix of statistical weights.

### Chain Displacement Vector

Properties of the chain molecule that depend on configuration include the dimensions of the spatial configuration as measured by the chain displacement vector  $\mathbf{R}$  connecting its ends, or various products that may be formed from  $\mathbf{R}$ . Evaluation of these properties requires summation over contributions from the individual bonds or groups comprising the chain. These contributions being vectors or tensors identified with the respective skeletal bonds numbered 1 to  $n$ , are conveniently expressed in local reference frames. A cartesian coordinate frame is therefore defined for each skeletal bond [10]. For a fixed configuration,  $\{\phi\}$ , the chain vector is then given as

$$\mathbf{R} \equiv \mathbf{R}_{0n} = \sum_{i=1}^n \mathbf{T}_1^{(i-1)} \mathbf{l}_i, \quad (2.40)$$

where  $\mathbf{l}_i$  is the bond vector of bond  $i$  and  $\mathbf{T}_i$  is the matrix of transformation between reference frame  $i+1$  and  $i$  and  $\mathbf{T}_1^{(j-1)}$  is the serial product of transformation matrices Eq. (2.36). The transformation matrix depends on the bond angle  $\theta_i$  and the torsional angle  $\phi_i$  of bond  $i$

$$\mathbf{T}_i = \begin{bmatrix} \cos \theta_i & \sin \theta_i & 0 \\ \sin \theta_i \cos \phi_i & -\cos \theta_i \cos \phi_i & \sin \phi_i \\ \sin \theta_i \sin \phi_i & -\cos \theta_i \sin \phi_i & \cos \phi_i \end{bmatrix}. \quad (2.41)$$

The above sum Eq. (2.40) is more conveniently written as

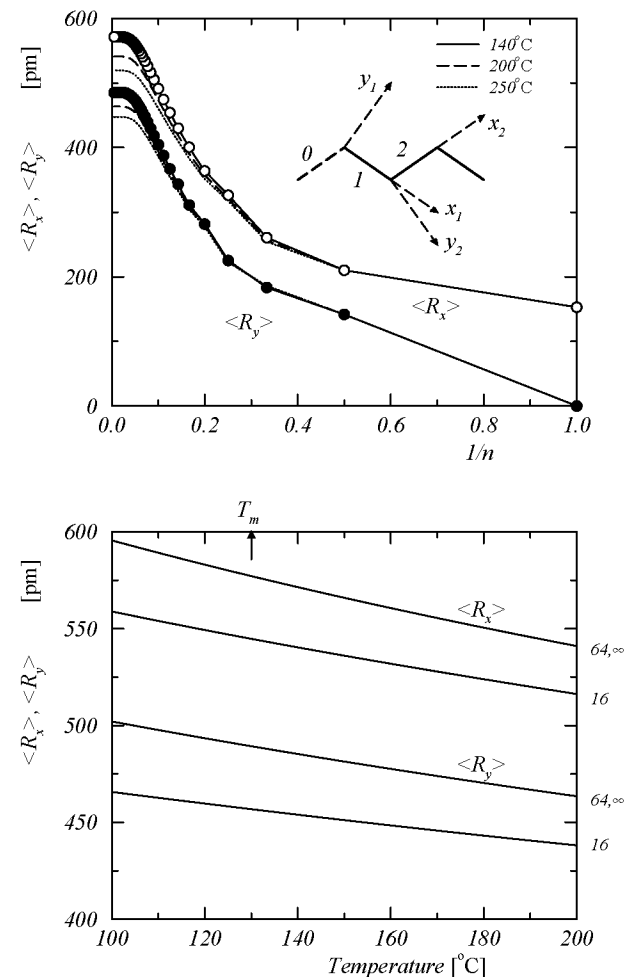


**Figure 2.6:** The mean end-to-end vector for  $n$ -alkanes calculated from the RIS approximation. The coordinate system is defined through the first bond of the chain with a virtual zeroth bond trans to the second bond [12, p. 111, Fig. 6.1]. a) Dependence on the number of bonds for different temperatures. b) Dependence on temperature for different chain lengths indicated with each curve.

$$\mathbf{R} = \mathbf{A}_{[1} \mathbf{A}_2^{(n-2)} \mathbf{A}_n], \quad (2.42)$$

where

$$\mathbf{A}_i = \begin{bmatrix} \mathbf{T} & \mathbf{1} \\ \mathbf{0} & \mathbf{1} \end{bmatrix}_i, \quad 1 < i < n, \quad (2.43)$$

is the generator matrix for the end-to-end vector and  $\mathbf{A}_{[1}$  is the first row of  $\mathbf{A}_1$  and,  $\mathbf{A}_n]$  is the the final column of  $\mathbf{A}_n$

$$\mathbf{A}_{[1} = [\mathbf{T} \quad \mathbf{1}]_1, \quad \mathbf{A}_n] = \begin{bmatrix} \mathbf{1} \\ \mathbf{1} \end{bmatrix}_n. \quad (2.44)$$

Such generator matrices may be formulated for all configuration dependent properties of a chain molecule. The quantity of interest is given in analogy to Eq. (2.42) [11]. Fig. 2.6 displays the persistence vector for  $n$ -alkanes (*cf.* Sec. 2.5.2, p. 30 for a more detailed explanation).

### Quantities of Higher Order

The dyadic product  $\mathbf{R}\mathbf{R}^T$  is the matrix of the symmetric second order tensor formed from the components of  $\mathbf{R}$ . That is

$$\mathbf{R}\mathbf{R}^T = \begin{bmatrix} R_x^2 & R_x R_y & R_x R_z \\ R_y R_x & R_y^2 & R_y R_z \\ R_z R_x & R_z R_y & R_z^2 \end{bmatrix}. \quad (2.45)$$

The direct product of  $\mathbf{R}$  with itself gives the  $9 \times 1$  vector comprising the same elements taken in reading order, row by row, and arranged as a column; *i. e.*,

$$\begin{aligned} \mathbf{R} \otimes \mathbf{R} = & \\ & (R_x^2 \ R_x R_y \ R_x R_z \ R_y R_x \ R_y^2 \ R_y R_z \ R_z R_x \ R_z R_y \ R_z^2)^T \equiv \\ & \text{col}(\mathbf{R}\mathbf{R}^T). \end{aligned} \quad (2.46)$$

It follows from the generating scheme for  $\mathbf{R}$  together with the theorem of direct products<sup>2</sup> that

$$\mathbf{R} \otimes \mathbf{R} = (\mathbf{A} \otimes \mathbf{A})_{[1} (\mathbf{A} \otimes \mathbf{A})_2^{(n-2)} (\mathbf{A} \otimes \mathbf{A})_n]. \quad (2.47)$$

Tensors of higher order can be developed analogously [10, 11, 12]. In Fig. 2.7 we display the second moment of the vector  $\boldsymbol{\rho} = \mathbf{R} - \langle \mathbf{R} \rangle$  for  $n$ -alkanes (*cf.* Sec. 2.5.2 for details).

<sup>2</sup>According to this theorem  $(\mathbf{A}\mathbf{C}) \otimes (\mathbf{B}\mathbf{D}) = (\mathbf{A} \otimes \mathbf{B})(\mathbf{C} \otimes \mathbf{D})$

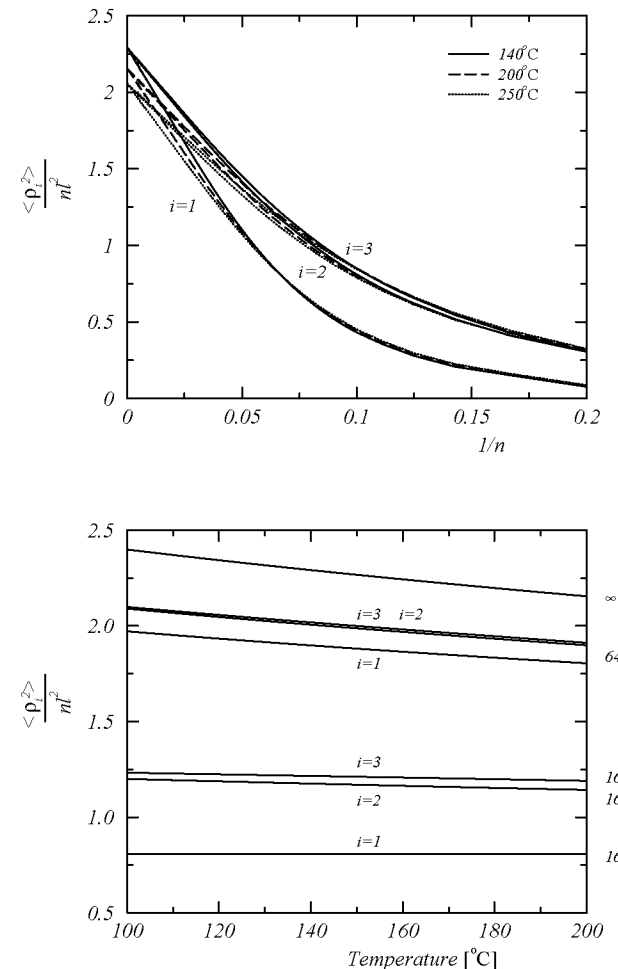


**Figure 2.7:** The second moment of the end-to-end vector for PE calculated from the RIS approximation. Diagonalization of  $\langle \boldsymbol{\rho}\boldsymbol{\rho}^T \rangle$  has been achieved by a rotation ( $\tan 2\chi = 2\langle uv \rangle / (\langle u^2 \rangle - \langle v^2 \rangle)$ ) about the  $z_1$ -axis (*cf. inset of Fig. 2.6a, p. 24*) [80, p. 5368, Eq. (7)]. a) Dependence on the number of bonds,  $n$ , for three different temperatures. b) Dependence on temperature for different chain lengths,  $n$ .

## 2.5 Application to Normal Alkanes

The above Massieu functions (2.11), (2.17), and (2.29) have been applied to linear  $n$ -alkanes and linear PE and comparison with experimental data has been made.

### 2.5.1 Liquid Part of the Thermodynamic Potential

The molecular weight of the structural unit of PE is  $28 \text{ g mol}^{-1}$ . The numerical parameters for the thermodynamic potential Eq. (2.11) are collected in Tab. 2.1, p. 14. The thermodynamic properties of a PE melt have been calculated up to  $250^\circ\text{C}$  and comparison with experimental data at atmospheric pressure has been made. The mass density of PE is a decreasing function of temperature. For higher pressures the temperature variations of the density become less pronounced (*cf.* Fig. 2.1, p. 12). The qualitative behaviour of  $\gamma$  as predicted by the Massieu function (2.11) is reproduced quite well, whereas we have poor agreement of  $\beta$  with the experimental values. The experimental data of the thermodynamic properties have been taken from [7].

The thermodynamic potential (2.17) has been applied to PE and to hexadecane. The agreement with experimental data is good. The parameters  $A$ ,  $B$ ,  $\delta$  in the modified FOV equation have the same values (*cf.* p. 14) for all polymers studied in [9]. The coefficients  $\Delta$ ,  $\Gamma$  are taken to give a fit to the measured heat capacity. The characteristic pressure, mass density, and temperature are collected in Tab. 2.1. Fig. 2.2, p. 15 shows the temperature dependence of the mass density for PE and hexadecane. The pressure has been taken as a parameter and its value in bar is indicated with each curve. The temperature coefficient of the pressure as calculated from Eq. (2.24) is depicted in Fig. 2.3, p. 17 for both materials. For PE this quantity is overestimated over the entire temperature range at zero pressure. In comparison with the SG equation (dashed line) we have a more accurate representation. The thermal expansion coefficient Eq. (2.22) is portrayed in Fig. 2.4, p. 18. The FOV equation gives a good impression of the qualitative behaviour of this quantity. Fig. 2.5 displays the temperature dependence of the isothermal compressibility for the two materials at several pressures according to Eq. (2.23). This quantity is determined through the other two coefficients via the Maxwell relation (2.6). Fig. 2.8 shows the

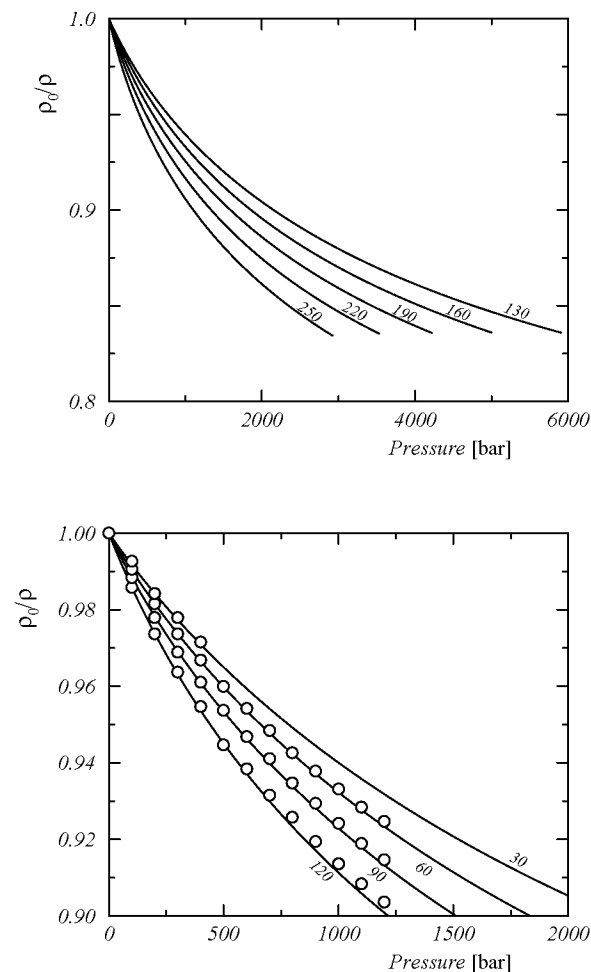


**Figure 2.8:** The isotherms for a) PE and b) hexadecane according to the modified FOV equation. The numbers indicate the temperature in centigrade. Circles are experimental data from Ref. [7].

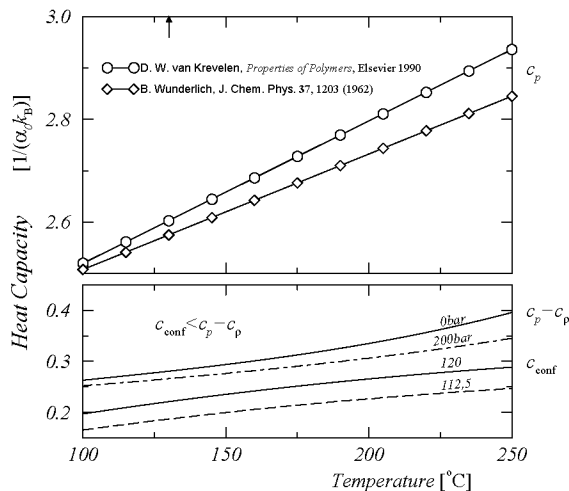


**Figure 2.9:** The heat capacity for linear PE. The upper graph shows experimental curves. The lower graph shows the external heat capacity  $c_p - c_p$  according to the modified FOV equation for  $p = 0\text{bar}$  and  $p = 200\text{bar}$  and the conformational part of the heat capacity according to Eq. (2.31) for two RIS models ( $\Phi^\pm = 120^\circ$  and  $\Phi^\pm = 112.5^\circ$ ).

isotherms for PE and hexadecane for several temperatures. The values of the temperature are indicated at each curve. In the second figure we have also reported experimental values for hexadecane [7]. The modified FOV equation (2.18) is more accurate than the original FOV equation of state [5]. Fig. 2.9 shows experimental and theoretical heat capacities for linear PE. In the upper diagram we report experimental data of  $c_p$  according to [78, 81]. The lower curve shows the external heat capacity,  $c_p - c$ , calculated from Eq. (2.8) for the FOV equation for two different pressures. Furthermore, we have calculated the conformational part of the heat capacity according to Eq. (2.31) for two different RIS models (cf. next subsection). We have used torsional angles for the  $g^\pm$ -states of  $\pm 120^\circ$  and  $\pm 112.5^\circ$  respectively. In the temperature range considered  $c_{\text{conf}}$  is smaller than  $c_p - c$  at moderate low pressures. In former works [82] the RIS approximation has been adopted to calculate the conformational part of the heat capacity. This involves the definition of a characteristic temperature (similar to the Debye temperature) to fit the experimental data.

## 2.5.2 Conformational Part of the Thermodynamic Potential

In the RIS approximation the PE molecule is represented as a linearly connected sequence of groups, the identities of the single atoms being ignored. The methylene groups are regarded as the entities which engage mutual interactions [10]. In this work we adopt the three state RIS model for PE proposed in [10, 83, 80]. With three rotational states, *trans*, *gauche*<sup>+</sup> and *gauche*<sup>-</sup> assigned to each bond, the statistical weight matrix for an internal bond  $i$  in the chain of  $n$  bonds takes the general form

$$\mathbf{U}_i = \begin{pmatrix} 1 & \sigma & \sigma \\ 1 & \psi\sigma & \nu\sigma \\ 1 & \nu\sigma & \psi\sigma \end{pmatrix}, \quad 1 < i < n, \quad (2.48)$$

where  $\sigma$  accounts for first order (three-bond) interactions and  $\psi, \nu$  account for second order (four-bond) interactions. In the above matrix the rotational states are indexed in the order  $t, g^+, g^-$ . The statistical weights are given as

$$\sigma = \exp\left(\frac{-E_\sigma}{RT}\right), \quad (2.49)$$

where  $R$  is the molar gas constant and  $T$  the temperature. The statistical weight for a  $g^\pm g^\mp$  pair in excess of the energy  $2E_\sigma$  is

$$\nu = \exp\left(\frac{-E_\nu}{RT}\right), \quad (2.50)$$

The statistical weight  $\psi$  is defined in analogy to the above equations for  $\sigma$  and  $\nu$ ; in the RIS model used in this work it is set equal to 1. For a chain with independent hindered rotations we have  $\nu = 1$ , the freely rotating chain is recovered from the chain with interdependent hindered rotations taking  $\nu = \sigma = 1$  [80]. In our RIS calculations the length of the C – C bond and the supplement of the CCC skeletal bond angle were assigned the values  $l = 1.53 \text{ \AA}$  and  $\theta = 68^\circ$ , respectively. For the torsion angles we have adopted the set of symmetrically located states at  $\varphi = 0^\circ, \pm 120^\circ$ . For the energies we have chosen  $E_\sigma = 500 \text{ cal/mole}$ ,  $E_\nu = 2000 \text{ cal/mole}$ . With these assumptions it is possible to calculate all conformational averages of the chain.

With the generator matrix Eq. (2.43) we have calculated the mean end-to-end vector  $\langle \mathbf{R} \rangle \equiv \mathbf{a}$  in the reference frame defined in [84].

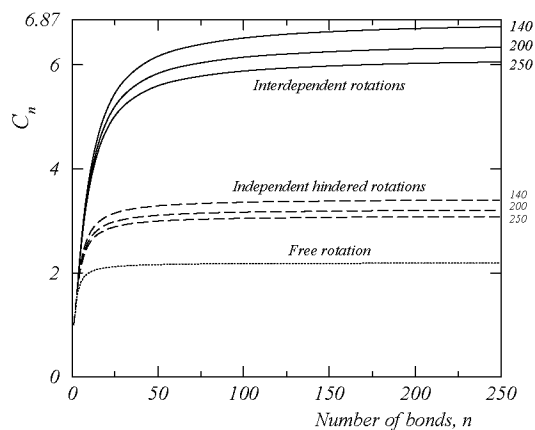


**Figure 2.10:** The characteristic ratio for linear  $n$ -alkanes for various chain models for three different temperatures (indicated in centigrade with each curve). The upper boundary of the figure is the asymptote for the chain with interdependent hindered rotations at  $140^\circ\text{C}$ . The chain with free rotations does not perform conformational changes upon temperature variations.

Since the chain is symmetric, the expectation value of the  $z$ -component of  $\langle \mathbf{R} \rangle$  vanishes identically. The  $x$ - and  $y$ -component increase with the chain length and approach limiting values of 575 pm and 486 pm, respectively. Fig. 2.6, p. 24 shows the mean square end-to-end vector as function of chain length for three different temperatures and as a function of temperature for short and long chains. Furthermore, we have calculated the second moment of the vector  $\boldsymbol{\rho} = \mathbf{R} - \mathbf{a}$  representing the displacement of  $\mathbf{R}$  for a given configuration from its average over all configurations [80]. This quantity can be identified with the conformation tensor, *i. e.*  $\mathbf{c} \equiv \langle \boldsymbol{\rho} \boldsymbol{\rho}^T \rangle_0$ . Fig. 2.7, p. 26 shows the conformation tensor as a function of chain length for chains with  $n > 5$  for different temperatures and the same quantity as a function of temperature for short chains and infinitely long chains. Diagonalization of  $\boldsymbol{\rho} \boldsymbol{\rho}^T$  has been achieved by appropriate rotation of the coordinate system [80]. A remark on the diagonalization of the second moment tensor and the definition of the coordinate system are given at the end of this section.

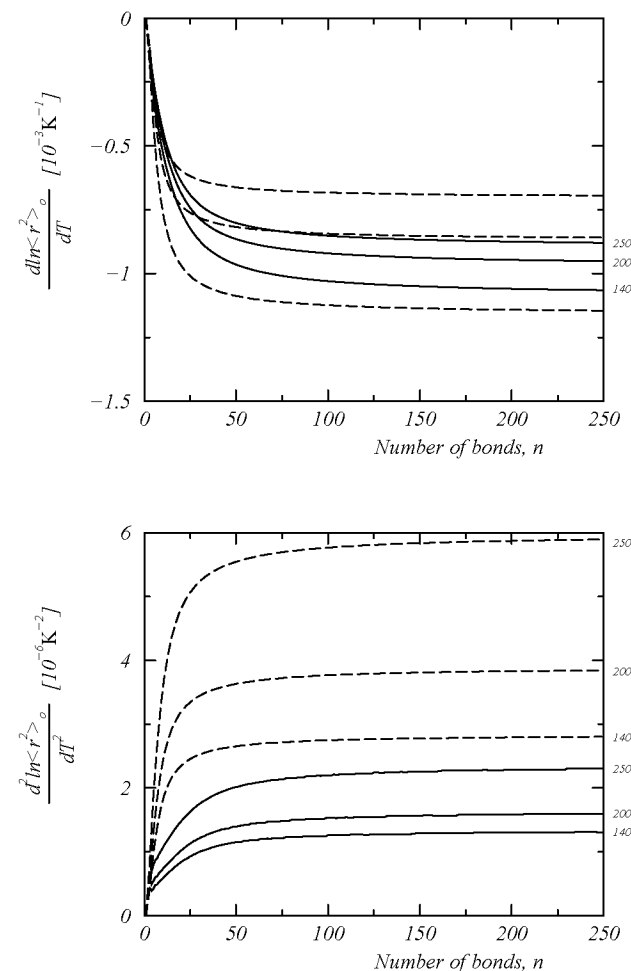


**Figure 2.11:** The temperature coefficient a) and its derivative b) of the unperturbed mean square end-to-end distance for a polyethylene chain for three different temperatures. Solid lines are for a chain with interdependent rotations, dashed lines for the curve with independent hindered rotations. Values of  $T$  are indicated with each curve.

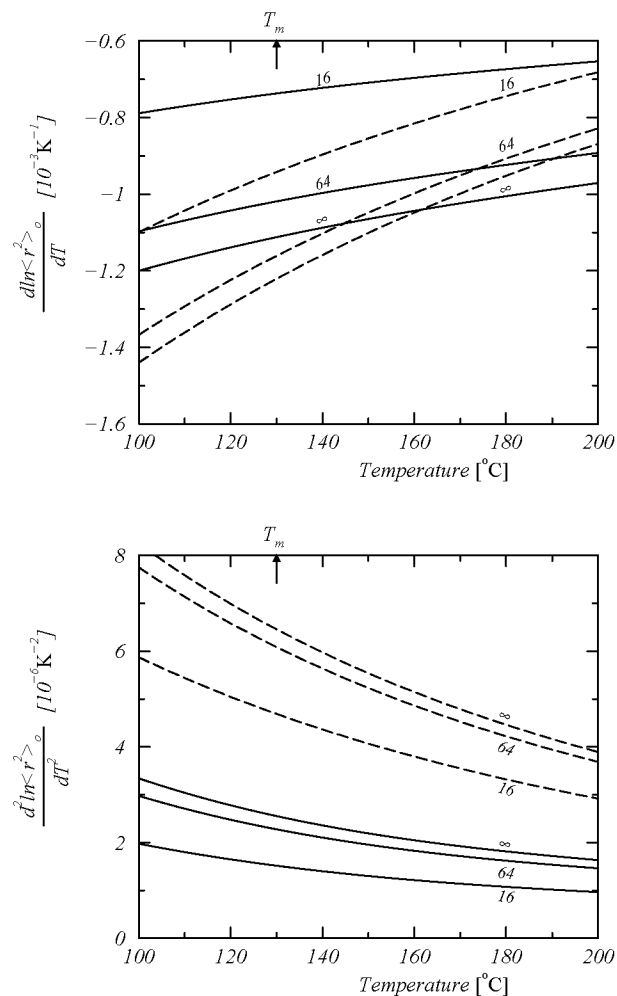


**Figure 2.12:** The same as Fig. 2.11 for different  $n$ -alkanes as a function of temperature. Values of  $n$  are indicated with each curve.

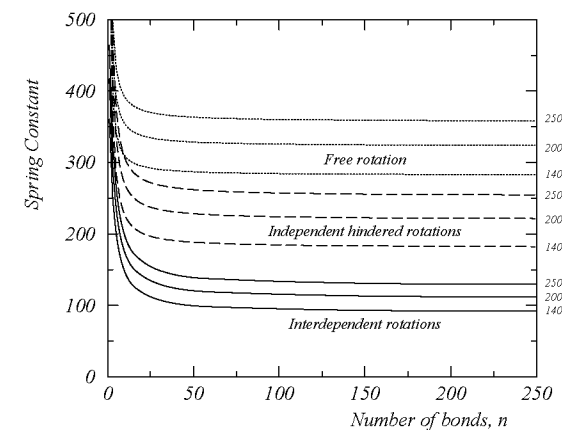


**Figure 2.13:** The same as Fig. 2.10 for the spring constant.

We see that in the temperature range considered  $\mathbf{c}$  is only a weak function of temperature. For infinitely long chains the principal axes of the conformation tensor are identical which means that the random coil has the shape of a perfect sphere. Fig. 2.10, p. 31 shows the characteristic ratio  $C_n = \langle R^2 \rangle_0 / (nl^2)$  for three different chain models and temperatures above the melting point (the generator matrix of  $R^2$  is given on p. 44, Eq. (3.13)). The characteristic ratio is a decreasing function of temperature for the chain with interdependent hindered rotations. This is also found for the chain with independent hindered rotations whereas the characteristic ratio of the freely rotating chain is independent of temperature. For these chain models the quantity  $C_n$  can be calculated analytically from Eq. (2.39) [10, p. 16, Eq. (20) and p. 27, Eqs. (53), (54)]. In the limit of infinitely long chains we have  $C_\infty = (1 + \alpha') / (1 - \alpha')$  for the freely rotating chain and  $C_\infty = (1 + \alpha') / (1 - \alpha') \cdot (1 + \eta') / (1 - \eta')$  for the chain with independent hindered rotations, where  $\alpha' = \cos \theta$  and  $\eta' = \langle \cos \phi \rangle = (1 - \sigma) / (1 + 2\sigma)$  [10, p. 59, Eq. (9)]. To obtain the characteristic ratio of the chain with interdependent hindered rotations Eq. (2.39) has been evaluated numerically. The upper bound of the Fig. 2.10,  $C_\infty = 6.87$ , is the characteristic ratio of a linear PE chain at 140°C. The limiting value of the characteristic ratio is reached already for chain lengths of a few hundred units. Note that the mean square

magnitude of the chain vector,  $\langle R^2 \rangle_0$ , is much smaller than the contour length of the chain,  $R_{\max} = nl \sin \theta / 2$ . Figs. 2.11 and 2.12 (pp. 32, 33) show the temperature coefficient of the characteristic ratio and its derivative as a function of chain length and temperature. At 140°C we have  $d \ln \langle R^2 \rangle_0 / dT = -1.1 \cdot 10^{-3} \cdot 1/K$  for PE. This value is in agreement with the experiments in crosslinked PE [68]. We made calculations for the chains with interdependent hindered rotations (solid lines) and chains with independent hindered rotations (long-dashed line). The dependence on the chain lengths mirrors essentially the features of Fig. 2.10. The temperature coefficient of PE is an increasing function of temperature. Only the RIS approximation which takes into account second order interactions in the polymer chain manages to reproduce the experimental findings for the characteristic ratio and the temperature coefficient. Fig. 2.13, p. 34 shows the spring constant for the three polymer models for several temperatures. We have normalized the spring constant with  $nl^2$  ( $K = 3/2k_B T / C_n$ ). The dotted lines are for the freely rotating chain having a linear spring constant,  $K(T)$ . The dashed lines and the solid lines are for the chain with independent hindered rotations and the chain with interdependent rotations, respectively. Note the different temperature behaviour of the freely rotating chain and the chain with interdependent hindered rotations for  $n = 250$ .

A note on the calculation of the conformational properties of the chain should be added for completeness. All configurational averages have been evaluated in a reference frame defined as follows [84]: The  $x$ -axis is taken along the first bond; the  $y$ -axis is in the plane of bonds 1 and 2 with its direction chosen at an acute angle with bond 2; the  $z$ -axis, perpendicular to the plane, completes a right handed Cartesian system. Diagonalization of the second moment tensor is achieved by a rotation about the  $z$ -axis of the coordinate system [80, p. 5368, Eq. (8)].

## 2.6 Conclusions

We have discussed the thermodynamic properties of simple polymeric liquids above the melting point for arbitrary pressures. Furthermore, we have compared our results with experimental data for linear PE and hexadecane. For the liquid contribution we have given two thermodynamic potentials which may be applied to a special polymer by

definition of characteristic properties. However, the liquid behaviour of the chain fluid is very difficult to capture theoretically, since we have no order in the *liquid* structure. To capture the thermodynamic behaviour of the internal microstructure we took the thermodynamic potential of the Hookean dumbbell and we adapted methods of equilibrium statistical mechanics in order to apply it to real polymer melts. Since the single polymer chains possess a well defined internal *microstructure* their thermodynamic behaviour is accessible via methods of statistical mechanics. The application of these results to other polymer melts is straightforward.

Further investigations in the direction laid down in the present chapter should focus on the evaluation of higher moments of the chain end-to-end vector of  $n$ -alkanes. Another interesting point is the calculation of optical properties as a function of temperature from the RIS scheme. In the following Chap. 3 we give a further look at the RIS models to treat the problem of energetic and entropic elasticity of polymers. The studies of Chap. 3 should continue in a distinct direction, namely the investigation of other polymers and macromolecules. Therefore we reconsider some of the aspects introduced in the present Chap. 2 in Chap.3. We complete the description of the quiescent material studying its relaxation time spectrum, *i. e.* its fading memory, in the conclusions of Chap. 3, p. 53. Then we adopt non-equilibrium thermodynamics to derive macroscopic balance equations for deforming polymers (Chap. 4).

## Chapter 3

# Molecular Theory of Energetic and Entropic Elasticity

### Abstract

We show how to compute the characteristic elastic constant for real polymer chains adopting the Rotational Isomeric State approximation. The energetics and entropics for the chain conformations are extracted from the elastic constant, and the consequences for the Theory of Purely Entropic Elasticity and for polymer processing are discussed. This allows us to check if the material is of purely entropic elasticity or not. Numerical examples for PE and PIB are given. PE does not obey the Theory of Purely Entropic Elasticity, whereas PIB does. The result for the latter is consistent with experimental findings in stress relaxation experiments.

### 3.1 Introduction

In the past decade much effort has been devoted to the development of powerful formalisms for non-equilibrium thermodynamics to treat complex materials such as amorphous polymers with entropic and energetic elasticity and to describe their physical properties under compressible and non-isothermal conditions [2, 1, 24]. The Rotational Isomeric State (RIS) approximation has gained considerable success in relating the chemical structure of amorphous polymers to their physical behaviour since the very beginning of its development and its application to polymer elasticity [10, 11, 12, 13]. This approximation is especially adequate to compute the characteristic elastic constant of linear polymers since the energetics and the entropics of the conformations are treated on the same footing. The application of these methods to amorphous polymers in the bulk has been a topic of some controversy but experimental evidence has shown that single polymer chains behave like random coils under  $\Theta$ -conditions in the amorphous phase [71, 72, 73, 74, 75]. In what follows we show how non-equilibrium thermodynamics and statistical mechanics can be combined to evaluate the energetic and entropic elasticity of flexible polymers.

Theoretical considerations on the elasticity of polymers have a long history beginning with the fundamental work of Kuhn and Gr $\ddot{u}$  n [79]. Later, the pioneering works of Flory and co-workers showed how the elastic properties of polymers can be related to their chemical structure [68, 83]. In what follows we adopt a constitutive equation for the elastic part of the free energy of a polymer network and we discuss the entropic as well as the energetic contributions to the free energy. To capture the elastic properties of the special polymer under consideration we adopt the RIS approximation to compute the temperature dependence of the mean square end-to-end distance of the chain vector and the characteristic elastic constant of the material.

Consequently we dispose of a criterion which allows us to evaluate whether or not the Theory of Purely Entropic Elasticity [42, 43, 44, 46, 45] is appropriate to the description of the macroscopic flow behaviour of complex fluids. This is of special importance in polymer processing since the Theory of Purely Entropic Elasticity seems to fail dramatically if the temperature of the polymer melt is near the glass transition temperature [14]. But even in the deformation of polymer



networks above their melting point the energetics of the bond conformations of the polymer chains yielded measurable effects [68] which may become relevant in extreme deformation and temperature histories as encountered in polymer processing. Therefore it is of prior importance to compute the nonlinear elastic constant of the material in order to apply the system equations of non-equilibrium thermodynamics [2, 24] to special polymers taking into account energetic and entropic elasticity.

In Sec. 3.2 we present general relationships of the thermodynamics of elastic materials and their application to polymer networks. We determine the entropic and the energetic contribution to the elastic free energy and the heat capacity of the network. In Sec. 3.3 we review the basics of the RIS scheme and the generator matrix method to calculate configuration dependent properties of polymer chains such as the mean square end-to-end distance. Sec. 3.4 deals with the presentation of the results of our calculations to obtain the characteristic elastic constant for polyethylene and polyisobutylene. In the final Sec. 3.5 we present the conclusions and we discuss the experimental and theoretical consequences.

## 3.2 Thermodynamics of Elastic Materials

### 3.2.1 General Relationships

The Helmholtz free energy of a material with internal microstructure is a function of the mass density of the fluid,  $\rho$ , the temperature,  $T$ , and the contravariant conformation tensor,  $\mathbf{c}$ . The conformation tensor is the second moment of the end-to-end vector of the chain and describes the average extension and orientation of the polymer chain at a reference temperature

$$a_1 \equiv a_1(\rho, T, \mathbf{c}) . \quad (3.1)$$

Note that here we are employing the so called density variable formulation (*i. e.* we are working in terms of volumetric quantities) which has been proven useful in the Hamiltonian framework of non-equilibrium thermodynamics [2] and in the GENERIC framework [1, 24]. In this description the free energy has units of force/length<sup>2</sup>. The entropy den-

sity and the internal energy per unit volume are given as

$$s_1 = - \left. \frac{\partial a_1}{\partial T} \right|_{\rho, \mathbf{c}} , \quad (3.2)$$

$$\epsilon_1 = a_1 - T \left. \frac{\partial a_1}{\partial T} \right|_{\rho, \mathbf{c}} . \quad (3.3)$$

The heat capacity (at constant mass density) is defined as

$$c_{\text{conf}} = - \left. \frac{T}{\rho} \frac{\partial^2 a_1}{\partial T^2} \right|_{\rho, \mathbf{c}} , \quad (3.4)$$

since, in general, the potential  $a$  is a nonlinear function of temperature. In what follows we adopt the free energy of a network of polymer chains and we calculate the network's entropy, its free energy and its heat capacity related to material elasticity (Sec. 3.2.2), according to the above Eqs. (3.2)-(3.4). After that we will adapt the RIS scheme to study some specific polymers (Sec. 3.3).

### 3.2.2 Elasticity of a Network of Polymers

The free energy of a network of polymer chains is [2, 24, 77]

$$a_1(\rho, T, \mathbf{c}) = \frac{1}{2} \rho \alpha_1 K(T) \text{tr} \mathbf{c} - \frac{1}{2} \rho \alpha_1 k_B T \ln(\det \mathbf{c}) , \quad (3.5)$$

where  $\text{tr} \mathbf{c}$  and  $\det \mathbf{c}$  denote the trace and the determinant of the conformation tensor, respectively. The first term represents the free energy of a Hookean spring and the second arises from a statistical consideration of an assembly of many chains. The parameter  $\alpha_1$  in the above equation is a measure of the degree of elasticity per unit mass of the polymeric fluid, which gives a quantitative measure of the strength of elastic forces per unit mass in the material. As an example, for a polymer melt,  $\alpha_1$  is given by the number of crosslinks or entanglement points per unit volume divided by the mass density. It is taken herein as a material constant; *i. e.*, it is not a function of temperature. For the elastic constant of a flexible macromolecule we take the definition of Kuhn and Grün [79]

$$K(T) = \frac{3}{2} \frac{k_B T}{\text{tr} \langle \mathbf{R}\mathbf{R} \rangle_0} , \quad (3.6)$$

where  $\mathbf{R}$  is the end-to-end vector of the polymer chain or the distance between crosslinks or entanglement points and  $\langle \mathbf{R}\mathbf{R} \rangle_0$  is the second moment of the the end-to-end vector evaluated at equilibrium. This quantity is a nonlinear function since the end-to-end vector changes with temperature. It has the units of energy/length<sup>2</sup>. From the free energy (3.5) of the network we can calculate the energetic and the entropic elasticity according to Eq. (3.2), (3.3)

$$s_1(\rho, T, \mathbf{c}) = -\frac{1}{2}\rho\alpha_1\frac{\partial K(T)}{\partial T}\text{tr}\mathbf{c} + \frac{1}{2}\rho\alpha_1k_B\ln(\det\mathbf{c}), \quad (3.7)$$

$$\epsilon_1(\rho, T, \mathbf{c}) = \frac{1}{2}\rho\alpha_1\left[K(T) - T\frac{\partial K(T)}{\partial T}\right]\text{tr}\mathbf{c}, \quad (3.8)$$

As an illustration, Fig. 3.1 shows the deviation of the elastic constant,  $K(T)$ , from its linear behaviour for  $n$ -alkanes. The simulation procedure and further discussions are postponed to Secs. 3.3 and 3.4.

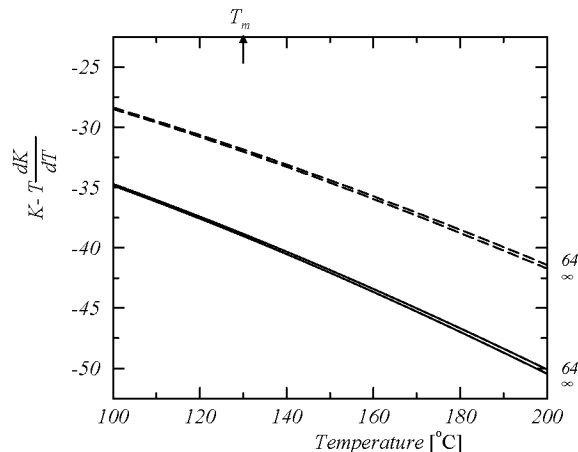


**Figure 3.1:** Deviation of the elastic constant from linear behaviour for  $n$ -alkanes with interdependent hindered rotations (solid lines) and independent hindered rotations (dashed lines). This quantity is a measure for the energetic elasticity of the chain according to Eq. (3.8). The value of  $n$  is indicated with each curve. We have assumed bond rotation angles of  $\phi = 0^\circ, 120^\circ$ .

Applying Eq. (3.4) to the potential (3.5) we obtain

$$c_{\text{conf}} = -\frac{1}{2}T\alpha_1\text{trc}\frac{\partial^2 K(T)}{\partial T^2}, \quad (3.9)$$

for the conformational part of the heat capacity in terms of the nonlinear spring constant. This quantity increases linearly with  $\text{tr}\mathbf{c}$  and consequently it may become important in highly oriented systems. In Fig. 3.2 we show the temperature dependence of the conformational heat capacity (3.9) for  $n$ -alkanes (*cf.* Secs. 3.3 and 3.4.1 for details).

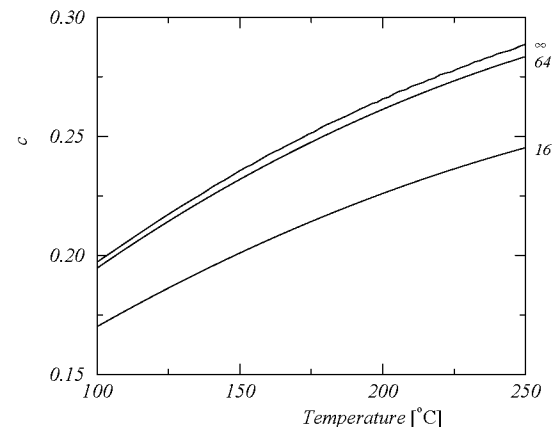


**Figure 3.2:** The absolute value of the conformational part of the heat capacity according to Eq. (3.9) for three  $n$ -alkanes. The value of  $n$  is indicated with each curve. We have assumed bond rotation angles of  $\phi = 0^\circ, 120^\circ$ .

To apply the above Helmholtz free energy to polymeric liquids it is essential to find the functional form of the spring constant for the special polymer under consideration. This means that the temperature dependence of the quantity  $\text{tr}\langle \mathbf{R}\mathbf{R} \rangle_0$  has to be determined. In former works on non-isothermal rheology  $\text{tr}\langle \mathbf{R}\mathbf{R} \rangle_0$  has been assumed to be a constant [47] or phenomenological forms of the spring constant have been adopted [49]. Here we want to use detailed atomistic representations of the polymer and to calculate the mean square of the magnitude

of the chain vector as a function of temperature. To this end we resort to the RIS approximation of Physical Chemistry [10, 11, 12] which allows us to calculate configuration dependent properties of molecules.

### 3.3 Rotational Isomeric State Approximation

#### 3.3.1 General Relationships

In the RIS [10, 11, 12] approximation each molecule is treated as occurring in one or another of several discrete rotational states. The states are chosen to coincide with potential minima of the conformational energy as a function of the rotation angle about the skeletal bonds, the lengths of the bonds and the bond angles being considered as constant. A given configuration of the molecule is then specified by a set of torsional angles  $\{\phi\}$ . Then for each bond  $i$  of the chain a statistical weight matrix

$$\mathbf{U}_i = [ u_{\zeta\eta} ]_i, \quad 1 < i < n, \quad (3.10)$$

can be defined with states ( $\zeta$ ) for bond  $i - 1$  indexing the rows and those ( $\eta$ ) for bond  $i$  the columns ( $\zeta, \eta = \alpha, \beta, \dots, \nu$ ). The energies  $E_{\zeta\eta}$  corresponding to the statistical weights  $u_{\zeta\eta}$  are defined through the Boltzmann factors  $u_{\zeta\eta;i} = \exp(-E_{\zeta\eta;i}/RT)$ , where  $E_{\zeta\eta;i}$  is the contribution to the total energy of the configuration,  $E(\{\phi\})$ , associated with the assignment of bond  $i$  to state  $\eta$ , bond  $i - 1$  being in state  $\zeta$ . Note that in the RIS approximation a coarse grained description of the polymer chain is adopted and therefore the conformational energies,  $E_{\zeta\eta;i}$ , should be taken as temperature dependent functions. However, for simplicity we wish to work with constant conformational energies herein. We shall say more about a possible temperature dependence of the conformational energies in Sec. 3.4.2, p. 53.

The configurational partition function and the generator matrices for higher moments of the end-to-end vector,  $\mathbf{R}$ , have been presented in Sec. 2.4.2, p. 21. In the following Sec. 3.3.2 we introduce the generator matrix for the mean squared end-to-end vector of the polymer chain.

#### 3.3.2 Square of the Magnitude of the Chain Vector

The square magnitude of  $R^2$  is given by

$$R^2 = \sum_{h=1}^n l_h^2 + 2 \sum_{h < j} \mathbf{l}_h^T \mathbf{T}_h \mathbf{T}_{h+1} \cdots \mathbf{T}_{j-1} \mathbf{l}_j, \quad (3.11)$$

where  $\mathbf{l}_h^T$  is the transposed of bond (column) vector  $\mathbf{l}_h$ , and  $l_h$  is its magnitude. Each term of the double sum is the scalar product of a pair of bond vectors.  $\mathbf{T}_i$  denotes the matrix of transformation between the reference frame of bond  $i + 1$  and bond  $i$  [10]. It is a function of the bond angle  $\theta_i$  and the torsional angle  $\phi_i$

$$\mathbf{T}_i = \begin{bmatrix} \cos \theta_i & \sin \theta_i & 0 \\ \sin \theta_i \cos \phi_i & -\cos \theta_i \cos \phi_i & \sin \phi_i \\ \sin \theta_i \sin \phi_i & -\cos \theta_i \sin \phi_i & \cos \phi_i \end{bmatrix}. \quad (3.12)$$

The generator matrix of the square end-to-end distance is

$$\mathbf{G}_i = \begin{bmatrix} 1 & 2\mathbf{l}^T \mathbf{T} & l^2 \\ \mathbf{0} & \mathbf{T} & \mathbf{1} \\ 0 & \mathbf{0} & 1 \end{bmatrix}_i, \quad 1 < i < n, \quad (3.13)$$

and it follows that

$$R^2 = \mathbf{G}_{[1} \mathbf{G}_2^{(n-2)} \mathbf{G}_n], \quad (3.14)$$

where  $\mathbf{G}_{[1}$  and  $\mathbf{G}_n]$  are, respectively, the first row of  $\mathbf{G}_1$  and the final column of  $\mathbf{G}_n$

$$\mathbf{G}_{[1} = [ 1 \quad 2\mathbf{l}^T \mathbf{T} \quad l^2 ]_1, \quad \mathbf{G}_n] = \begin{bmatrix} l^2 \\ 1 \\ 1 \end{bmatrix}_n. \quad (3.15)$$

Such generator matrices may be formulated for all configuration dependent properties of a chain molecule, e. g. the radius of gyration, molecular dipole moments or optical anisotropies. The quantity of interest is given in analogy to Eq. (3.14).

Figs. 3.3 and 3.6 show the characteristic ratio  $C_n = \langle R^2 \rangle / n l^2$  for  $n$ -alkanes and for PIB as a function of temperature. The chain properties have been calculated with the appropriate statistical weight matrices (3.16), p. 45 and (3.19), p. 49 and the general relationship (2.39), p. 23 with  $\mathbf{F} = \mathbf{G}$  from Eq. (3.13). A detailed discussion follows in Sec. 3.4.

## 3.4 Application to Linear Polymers

### 3.4.1 Polyethylene

In the RIS approximation the polyethylene (PE, repeat unit  $-\text{CH}_2-$ ) molecule is represented as a linearly connected sequence of groups, the identities of the single atoms being ignored. The methylene groups are regarded as the entities which engage mutual interactions [10]. In this work we adopt the three state RIS model for PE proposed in [83]. With three rotational states *trans*, *gauche*<sup>+</sup> and *gauche*<sup>-</sup> assigned to each bond, the statistical weight matrix for an internal bond  $i$  in the chain of  $n$  bonds takes the general form

$$\mathbf{U}_i = \begin{pmatrix} 1 & \sigma & \sigma \\ 1 & \psi\sigma & v\sigma \\ 1 & v\sigma & \psi\sigma \end{pmatrix}, \quad 1 < i < n, \quad (3.16)$$

where  $\sigma$  accounts for first order (three-bond) interactions and  $\psi$ ,  $v$  account for second order (four-bond) interactions [10]. In the above matrix the rotational states are indexed in the order  $t$ ,  $g^+$ ,  $g^-$ . The statistical weights are given as

$$\sigma = \exp\left(\frac{-E_\sigma}{RT}\right), \quad (3.17)$$

where  $R$  is the molar gas constant and  $T$  the temperature. The statistical weight for a  $g^\pm g^\mp$  pair in excess of the energy  $2E_\sigma$  is

$$v = \exp\left(\frac{-E_v}{RT}\right). \quad (3.18)$$

The statistical weight  $\psi$  is defined in analogy to the above equations for  $\sigma$  and  $v$ ; in the RIS model adopted in this work it is set equal to 1. For a chain with independent hindered rotations we have  $v = 1$ , the freely rotating chain is recovered taking  $v = \sigma = 1$  [80]. The mean square end-to-end vector of these chain models can be represented analytically [10] and has been taken as a check for the treatment of the chain with interdependent hindered rotations.

In our RIS calculations the length of the C – C bond and the supplement of the CCC skeletal bond angle were assigned the values  $l = 1.53 \text{ \AA}$  and  $\theta = 68^\circ$ , respectively. For the torsion angles we have adopted the set of symmetrically located states at  $\phi = 0^\circ, \pm 120^\circ$ . In some

instances we used  $\phi = 0^\circ, \pm 112.5^\circ$  to study the dependence on the torsional angles. For the energies we have chosen  $E_\sigma = 500 \text{ cal/mole}$ ,  $E_v = 2000 \text{ cal/mole}$ . With these assumptions it is possible to calculate all conformational averages of chain properties according to [10, 83, 80].

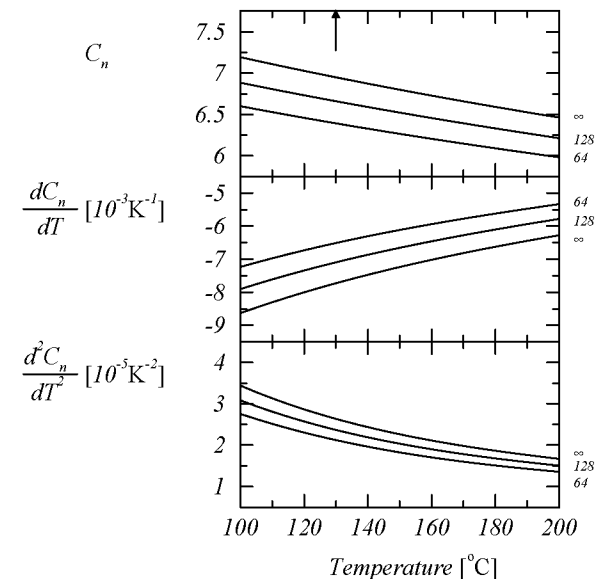


**Figure 3.3:** The characteristic ratio and its temperature coefficients for a polymethylene chain as a function of temperature for three different  $n$ -alkanes. We have assumed bond rotation angles of  $\phi = 0^\circ, 120^\circ$ . The value of  $n$  is indicated with each curve. The arrow indicates the melting point of linear PE of  $130^\circ\text{C}$ .

Fig. 3.3 shows the temperature dependence of the characteristic ratio and its first and second temperature coefficient as a function of temperature for short chains, chains of intermediate length, and infinitely long chains between  $100^\circ\text{C}$  and  $200^\circ\text{C}$ . The arrow denotes the melting point of linear polyethylene of  $130^\circ\text{C}$ . At  $140^\circ\text{C}$  we have  $C_\infty = 6.87$  for the characteristic ratio and  $d \ln \langle R^2 \rangle_0 / dT = -1.1 \cdot 10^{-3} \cdot 1/\text{K}$  for the temperature coefficient of PE. These values are in agreement with the experiments in dilute solution to obtain the characteristic ratio and

in crosslinked PE to obtain the temperature coefficient [68]. Only the sophisticated RIS approximation which takes into account second order interactions in the polymer chain manages to reproduce the experimental findings for the characteristic ratio and the temperature coefficient. The RIS approximations in [85] ignore second order interactions and therefore fail to reproduce both quantities. Furthermore, we have calculated the elastic constant and its first and second temperature coefficient from the characteristic ratio. We have normalized the elastic constant with  $nl^2$  ( $K \equiv 3/2k_B T/C_n$ ).

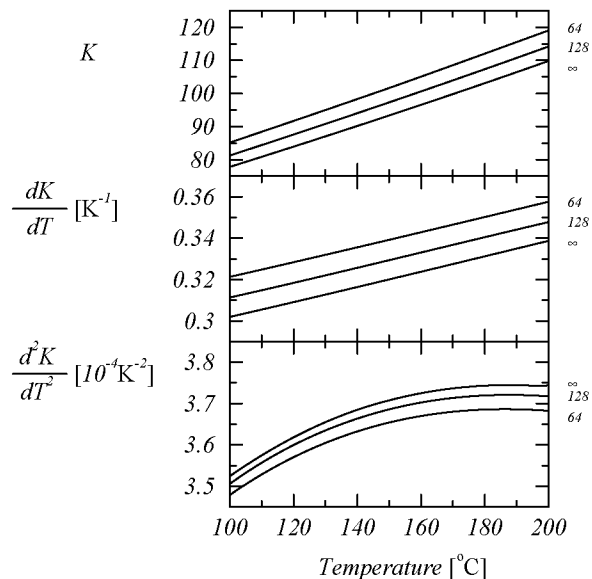


**Figure 3.4:** The same as Fig. 3.3 for the elastic constant and its first and second temperature coefficient.

Fig. 3.4 shows the elastic constant and its temperature coefficients as a function of temperature for several chain lengths. The characteristic elastic constant,  $K(T)$ , is a measure for the total free energy of the polymer network according to Eq. (3.5). (Keep in mind that in the undeformed network  $\text{tr} \mathbf{c} = 3$  and  $\det \mathbf{c} = 1$ .)

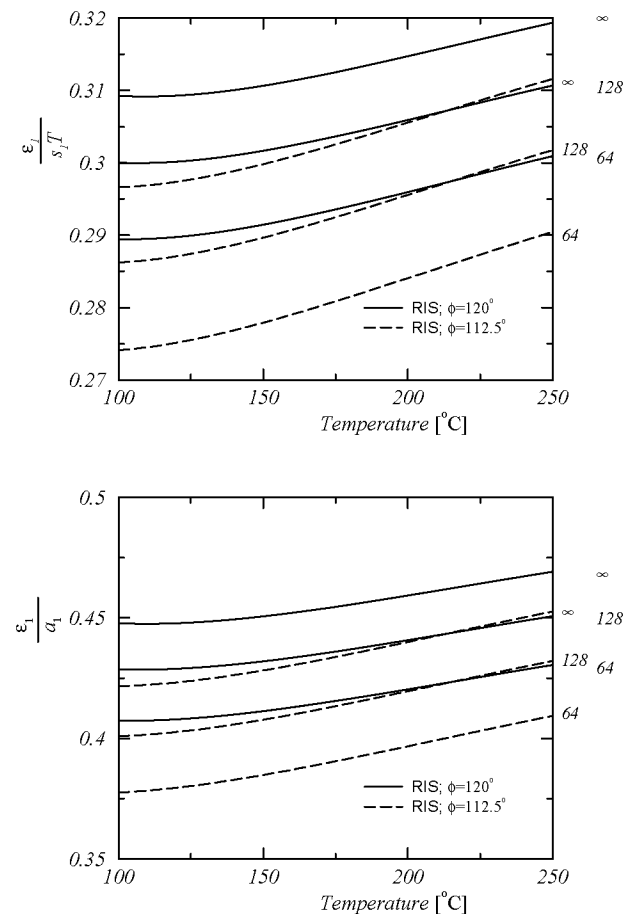


**Figure 3.5:** Ratio of energetic to entropic energy (a) and energetic versus total elastic energy (b) for the chain with interdependent hindered rotations for three different  $n$ -alkanes. The value of  $n$  is reported with each curve. We have assumed bond rotation angles  $\phi = 0^\circ, 120^\circ$  (solid lines) and  $\phi = 0^\circ, 112.5^\circ$  (dashed lines).

The first derivative of the elastic constant with respect to temperature,  $\partial K/\partial T$ , is a measure for the entropics of the bond conformations according to Eq. (3.7). The second derivative of the elastic constant,  $\partial^2 K/\partial^2 T$ , is proportional to the heat capacity of the network, Eq. (3.9), which we have depicted in Fig. 3.2, p. 42 as a function of temperature. Fig. 3.1, p. 41 considers the deviation of the spring constant from its linear behaviour and mirrors the energetics of the bond conformations according to Eq. (3.8). We have also performed calculations for chains with independent hindered rotations (dashed lines in Fig. 3.2) to show that the energetic elasticity of the chains with interdependent hindered rotations (solid lines) is more pronounced. The quantities  $K(T)$  and  $\partial K/\partial T$  are measures for the total elastic energy and the entropic energy of the polymer network, respectively. At this point it is interesting to study the strength of the energetic elasticity of the network with respect to its entropic elasticity and with respect to its total free energy. Fig. 3.5a displays the ratio of energetic to entropic elasticity for several  $n$ -alkanes and Fig. 3.5b the ratio of the energetics to the total energy of the chain. Our calculations for two sets of torsional angles show that more pronounced rotations around the skeletal bonds enhance the energetics of the bond conformations.

### 3.4.2 Polyisobutylene

For polyisobutylene (PIB, repeat unit  $-\text{CH}_2\text{C}(\text{CH}_3)_2\text{CH}_2-$ ) we have adopted the RIS model of Suter *et al.* [86]. The PIB chain has a repeat unit of two bonds with four rotational states  $trans_+$ ,  $trans_-$ ,  $gauche^+$ , and  $gauche^-$ . After renormalization the statistical weight matrices for an internal bond  $i$  in the PIB chain are

$$\mathbf{U}_{\mathbf{a}i} = \begin{pmatrix} 0 & 0 & 1 & \xi \\ 0 & 0 & \xi & 1 \\ 1 & \xi & 0 & 0 \\ \xi & 1 & 0 & 0 \end{pmatrix}, \quad \mathbf{U}_{\mathbf{b}i} = \begin{pmatrix} 1 & 0 & 1 & 0 \\ 0 & 1 & 0 & 1 \\ 1 & 0 & 1 & 0 \\ 0 & 1 & 0 & 1 \end{pmatrix}. \quad (3.19)$$

In the above matrices the rotational states are indexed in the order  $t_+$ ,  $t_-$ ,  $g^+$ ,  $g^-$ . The statistical weight is given as

$$\xi = \exp\left(\frac{-E_\xi}{RT}\right). \quad (3.20)$$

In our RIS calculations the length of the C – C bond was  $l = 1.53 \text{ \AA}$ , the valence angles were  $123^\circ$  and  $109^\circ$ , and the torsion angles  $\pm 165^\circ$  and  $\pm 50^\circ$  for the *trans*- and *gauche*-states, respectively. For the energy we took  $E_\xi = 3000 \text{ cal/mole}$ .

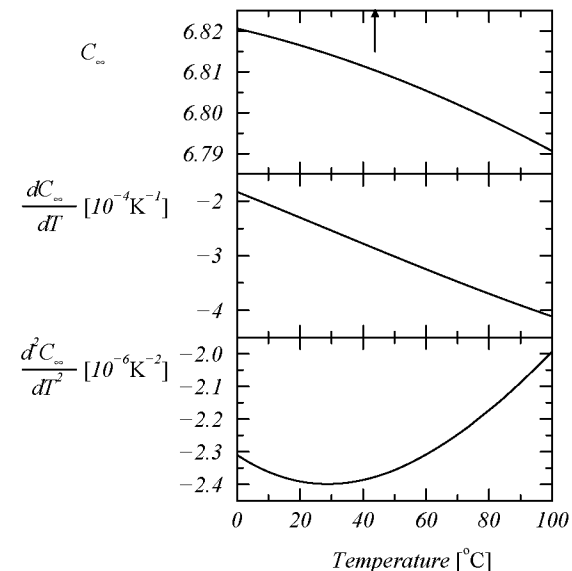


**Figure 3.6:** The characteristic ratio and its temperature coefficients for the PIB chain as a function of temperature. The RIS parameters are reported in the text. The arrow indicates the melting point of linear PIB of  $44^\circ \text{C}$ .

Fig. 3.6 shows the characteristic ratio and its temperature coefficients for the PIB chain between  $0^\circ \text{C}$  and  $100^\circ \text{C}$  calculated from the statistical weight matrices (3.19). At  $27^\circ \text{C}$  we have  $C_\infty = 6.81$  for the characteristic ratio and  $d \ln \langle R^2 \rangle_0 / dT = -0.036 \cdot 10^{-3} \cdot 1/\text{K}$  for the temperature coefficient for PIB [68]. The number of *gauche* conformations in the chain increases with increasing temperature since  $C_\infty$  is a decreasing function of temperature. Note that PIB is a glass forming liquid and as it approaches its glass transition temperature in supercooling it remains amorphous. The temperature coefficient of PIB is 30

times smaller than the same quantity for PE. Consequently the energetic potential of PIB is found to be much smaller than the energetic potential (*cf.* Fig. 3.8, p. 52) and the material obeys the Theory of Purely Entropic Elasticity.

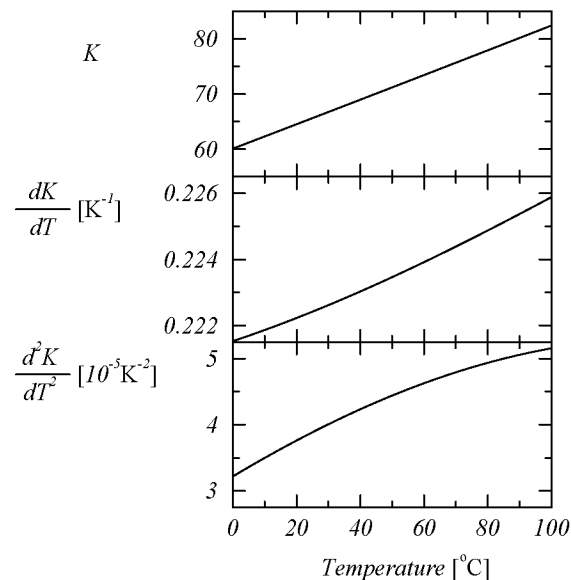


**Figure 3.7:** The same as Fig. 3.6 for the elastic constant and its first and second temperature coefficient.

Fig. 3.7 shows the elastic constant and its first and second temperature coefficient as a function of temperature. For both polymers, PE and PIB, we recover essentially the same temperature behaviour of the elastic spring constant and its temperature coefficients. Fig. 3.8 displays the ratio of energetic to entropic elasticity (a) and the ratio of the energetic to the total elasticity (b) for PIB. We see that the energetics of the bond conformations is considerably smaller for PIB than for PE which makes it more appropriate for a description as a material with purely entropic elasticity. In non-isothermal stress relaxation experiments [14] PIB was found to be of purely entropic elasticity. This is consistent with our RIS calculations and the results of Fig. 3.8.

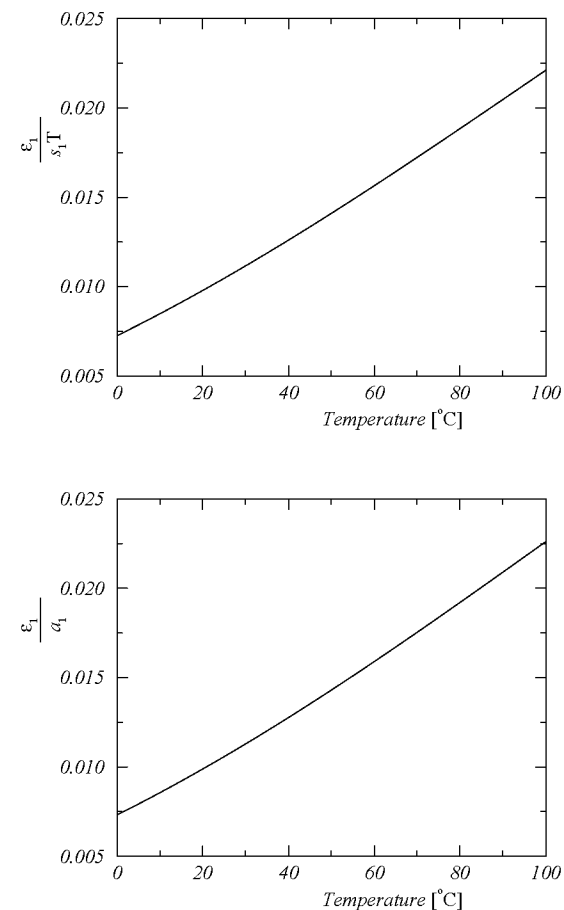


**Figure 3.8:** Ratio of energetic to entropic energy (a) and energetic versus total elastic energy (b) for PIB.

For PE and PIB the ratio  $\epsilon_1/s_1/T$  was found to increase with increasing temperature (cf. Fig. 3.5, p. 48 and Fig. 3.8, p. 52). This is due to the fact that the number of gauche conformations in the chain increases with increasing temperature which enhances the energetics of the bond conformations. Taking the conformational energies,  $E_{\zeta\eta;i}$ , as temperature dependent functions one may observe an opposite trend of the ratio  $\epsilon_1/s_1/T$ . Intuitively, this may be more reasonable because the entropy of the chain increases with increasing temperature. It would be interesting to check the trend of the ratio  $\epsilon_1/s_1/T$  for chains with a positive temperature coefficient.

We want to give the characteristic ratio and its temperature coefficient for some common polymers: For the characteristic ratio we have  $C_\infty = 6.3$  at 343 K, 9.1 at 300 K, and 10.23 at 300 K for polydimethylsiloxane (PDMS), poly(vinyl acetate) (PVA) and atactic polystyrene (PS), respectively [13, and references therein]. Note that the value for atactic PS depends on the RIS model adapted. The corresponding temperature coefficients are  $d\ln\langle R^2 \rangle_0/dT = +0.67 \cdot 10^{-3} \cdot 1/K$ ,  $+0.52 \cdot 10^{-3} \cdot 1/K$ , and  $-0.9 \cdot 10^{-3} \cdot 1/K$ .

### 3.5 Conclusions

We wish to summarize briefly the results that we obtain by combining thermodynamics and statistical mechanics to evaluate the entropic and the energetic elasticity of polymer networks. We started from a constitutive assumption for the Helmholtz free energy of polymer networks consisting of a free energy contribution of a Hookean spring and a contribution due to the assembly of many chains. From this free energy we extracted the energetic and the entropic elasticity of the network. Adopting the RIS scheme we have calculated the temperature dependence of the characteristic ratio and its first and second temperature coefficient. The characteristic ratio is related to the elastic constant of the polymer. We performed calculations for PE and PIB and we showed that the Theory of Purely Entropic Elasticity used in engineering applications has to be considered with scepticism. Its validity depends strongly on the material under consideration. It is not appropriate to the description of  $n$ -alkanes since the energetics of the bond conformations is between 25% and 45% of the total elastic energy. This value

varies with chain length, temperature, and the RIS states adopted in the model under consideration. For PIB the Theory of Purely Entropic Elasticity seems to be more appropriate since we obtain values between 0.7% and 2.5% for the ratio of the energetics to the total energy of the bond conformations. This result for PIB is consistent with findings in non-isothermal stress relaxation experiments.

To have a complete description of quiescent polymeric materials we have to know their relaxation time spectrum. Therefore we give a short introduction concerning the fading memory of polymeric materials. In the past much effort has been undertaken to understand the rich spectrum of relaxation times inherent to polymeric materials. The first attempts in this direction pointed at the development and experimental investigation of phenomenological relationships to quantify the temperature and density variation of viscosities, relaxation times, and shift factors [19, 87, 20, 88, 21, 89]. In Sec. 6.3.2, p. 126 such phenomenological relationships will be adopted to compute viscosities and thermodynamic properties of a deforming material under non-isothermal conditions. An important milestone in the understanding of the relaxation time spectrum of polymers was the development of phenomenological bead-spring models like the Rouse model and the reptation model. The usual approach followed in these models is to divide the polymer into sections consisting of the single Flory atoms (*i. e.* the  $\text{CH}_2$  groups in the PE chain). If the Flory atoms are linked together by springs representing the covalent bonds of the chain backbone we have what is commonly called a bead-spring model. With this model the problem of the molecular motion is equivalent to the problem of a collection of interacting Brownian particles. Adopting molecular dynamics simulation of the detailed atomistically represented chains or coarse grained polymer chains the relaxation time spectrum of polymers can be determined from computer simulations. The numerical results are subsequently mapped onto bead-spring models as the Rouse model or the reptation model to analyse the scaling laws for the relaxation times and in order to determine friction coefficients, diffusion constants, and viscosities [23]. The problem of calculating relaxation times of atomistic polymer chains employing computer simulations is quite complicated since the relaxation times of polymers increase rapidly with chain length. In molecular dynamics simulations of the atomistically represented polymer runs on the order of 90 ns are the upper limit of what can be achieved with such techniques actually. Such simulations have



been carried out for a system of 650 chains with  $N = 100$  carbon atoms per chain. The system can be considered as free of entanglements, the region of entanglements setting in at  $N = 150$  carbon atoms, approximately [23, and references therein]. The situation becomes even more difficult if temperature variations and supercooling are considered, since the relaxation time is a strong function of the material's temperature. In fact the relaxation times can increase over several orders of magnitude in undercooled systems. Voigt and Kröger [90] have calculated the chain length dependence of the zero shear viscosity using NEMD simulations. Simulation details can be found in [90]. In this type of simulations the material is modeled as a system of particles interacting via a Lennard-Jones potential  $V_{LJ} = 4\epsilon[(\sigma/r)^{12} - (\sigma/r)^6]$ , where  $\epsilon$  and  $\sigma$  are the characteristic energy and length of the potential, respectively. Furthermore, a FENE-P potential mimics the elastic forces between adjacent particles  $F = Kr/(1 - (r/b)^2)$ , where  $K$  is a characteristic spring constant and  $b$  is the maximum allowed spring length. The distance between neighboring particles in a chain can be identified with the persistence length of the real polymer or the Lennard-Jones length in the MD simulation. Then the system is subjected to an external shear deformation and the rheological and thermodynamic properties can be extracted from the computer experiment. Voigt and Kröger found a linear increase of the zero shear viscosity for the short chain regime and a  $N^{3.3}$  power law dependence for chains with  $\tilde{N} > 100$  with this simulation technique. The result for the short chain regime is in agreement with the Rouse model predicting a linear increase of the zero shear viscosity with increasing chain length. A physical explanation for the Rouse behaviour in the short chain regime is the absence of screening effects in the dense amorphous state. Furthermore, the Rouse model neglects hydrodynamic interactions. This last effect is taken into account in the Zimm model which predicts an increase of the zero shear viscosity scaling with an exponent of  $\nu = 1/2$  [17, p. 113, Eq. (4.149)]. However, the Zimm model is for dilute solutions only.

## Chapter 4

# Balance Equations for Flowing Polymeric Materials

### Abstract

The thermodynamics and mechanics of non-isothermal polymeric fluids are examined within the auspices of a new methodology wherein the laws of physics and principles of mechanics which are applicable to these thermodynamic systems are imbedded in a definite mathematical structure of a general, abstract equation. This permits the thermodynamically consistent generalization of isothermal, incompressible models of polymeric fluids to non-isothermal, compressible conditions. Doing thus reproduces, corrects, and extends non-isothermal models which have been developed over the years, and also allows for simpler (but equivalent) representations of these models in terms of alternate variables with a clearer connection to the microstructure of the material than the stress tensor and heat flux vector fields. A generalization of the GENERIC structure is proposed that accommodates interactions between phenomena of differing parities, which impose antisymmetry upon the corresponding elements of the dissipative operator matrix.

## 4.1 Introduction

If we scan the literature of the past forty years or so which is concerned with non-isothermal polymeric fluids (about two hundred articles and book chapters scattered randomly), two points seem to be universally accepted: 1.) the issue is extremely important; 2.) scant work has been done on this topic. In practically all of the papers that are concerned with this subject, you can find these two points pointed out explicitly in the introduction of the article. Although point 1.) remains valid, after reading and digesting these papers it is evident that point 2.) is no longer a valid one, because much work has now been done on this topic. This statement certainly holds true for theoretical work, although there is still a glaring need for sound experimental data (woefully true for practically any subject). Several groups of researchers have put forth theories for the thermodynamics and mechanics of these non-isothermal materials over the previous four decades, and although each has earned success to one degree or another, each suffers from limitations of universality and/or practicality which can only be overcome by unifying all of the discrepant parts into a coherent entity. Hence point 2.) above should now be replaced with something like: 2.) scant effort has been expended to produce a universal and practical theory from the sum of its parts. Without doing so, little has been gained, and indeed, most modern textbooks of rheology and fluid mechanics of polymeric fluids do not treat the subject of non-isothermal flows, nor do they even acknowledge its existence.

Taking for granted the validity of point 1.), several groups of researchers have realized the pertinence of the updated point 2.), and have attempted to address it. Braun [91] and Peters [92] have presented very general theories of the thermodynamics of non-isothermal polymeric fluids which cover a wide range of phenomena one might observe experimentally. Furthermore, over the past ten years, a few unifying attempts have been made using a new style of thermodynamic theory of complex fluids that endeavors to condense all relevant thermodynamical and mechanical principles into a single, practical, mathematical structural equation for the material's dynamical evolution, valid under non-isothermal conditions. Whether this mathematical structure is the extended Gibbs relation of Extended Irreversible Thermodynamics [93], the dynamical evolution equations of dissipative potential theory [77], the global rate expression of single generator Bracket Theory [94, 95, 2],

or the two generator GENERIC operator equation [96, 1], the underlying theme is essentially the same. Hence we must take the opportunity to unify and to amplify not only the previous theories for non-isothermal polymer fluids, but also the unifying formalisms. Neither of these is conceptually difficult given the proper starting point.

In prior publications [97, 98], the unification of the single generator Bracket Theory and the GENERIC equation was achieved, demonstrating the relative merits of each approach, hence allowing the most useful elements of each formalism to be implemented in a given situation. The double generator structure, involving the associated degeneracy conditions, emerged from that analysis as a new opportunity for further progress in non-equilibrium thermodynamics. That these two formalisms proved to be so closely related derives from the fact that they both emerged as the practical outgrowth of the impractical dissipative potential theory [77]. Hence most of the unifying of the structural theories has heretofore been accomplished and rendered to the literature. (Furthermore, the unification of all of these formalisms with the Matrix Model [99, 100, 101] of isothermal fluids has also been accomplished [102].) We shall make use of these results in Chap. 4, and also realize that the GENERIC approach is conceptually compatible with one of the main tenets of Extended Irreversible Thermodynamics, once the generators in the former are taken as not necessarily equilibrium quantities, as in [2, Sec. 10.1]. Hence certain results from the latter [103, 93], such as non-equilibrium corrections to the pressure, temperature, *etc.*, can be introduced, if desired, into the former, gaining additional structure thereby, without the need for an expansion of the equilibrium Gibbs relation to include non-equilibrium fluxes as independent variables. Grmela *et al.* [104] have explored the interrelationships between the GENERIC structure and Extended Irreversible Thermodynamics. This investigation has demonstrated that the proper state variables for hydrodynamical investigations are not the extra stress tensor field and heat flux vector field as originally used in Extended Irreversible Thermodynamics, but rather fields related to the internal structure of the material [104], as in [105, 2]. Wapperom and Hulsen [64] adopted a multiple conformation tensor approach to give a description of non-isothermal polymeric liquids. Furthermore, they derived a temperature equation from the balance equations of mass, internal energy, and polymer conformation. The description presented in Chap. 4 is closely related to the one adopted by Wapperom and Hulsen.

The objective of Chap. 4 is to give a modern, practical, treatment of the thermodynamical and mechanical theory of non-isothermal polymeric fluids. Hence we intend to take advantage of the newly emerged methodology to recast the prior work within a more universal and more practical framework. Several advantages ensue. First, the definite mathematical structure of the new methodology imposes mechanical consistency upon the dynamical evolution equations for the field variables used to describe the physical state of the non-isothermal material. Ergo, common errors can be avoided that occur when writing out a set of evolution equations using a typical modeling procedure of successive application of various disjointed mathematical principles and physical laws. Examples of these common errors will be discussed below. Second, the underlying mathematical structure of the dynamical evolution equations can lead to important new results regarding the system's stability [106, 107] and structural compatibility of closure approximations [108]. Most importantly, the full thermodynamic consistency of the system dynamical evolution equations can be guaranteed; a significant point since it has been demonstrated that violation of thermodynamic consistency can lead to aphysical system behavior [2]. The set of equations obtained herein is more specific to the problem at hand than that of [104], being expressed in terms of fewer degrees of freedom with regard to the choice of field variables. The set of equations derived in [104] is a special case of the more general set derived earlier in [105] and Sec. 10.1 of [2] in terms of exactly the same set of variables. Hence the number of degrees of freedom in the present work is equivalent to that of [91, 94, 95, 92].

## 4.2 Literature Review

The complex behavior of polymeric materials under non-isothermal conditions has caused many problems for the engineers and physicists who were faced with the task of quantifying their material properties and rheological characteristics. With the rapid expansion of the high polymer industry in the 1940s and 1950s, much effort was devoted to the study and characterization of these new materials, creating an impetus which survives and flourishes today. Over the past fifty years, a steady accumulation of knowledge has led to a gradual development of theoretical means to describe the varied and complex behavior of

these materials under processing conditions. In this section, we give an overview of some of the important theoretical advances which have occurred in this area, each building upon the successes of the previous one. At the end of the survey, we shall recognize that there is still much room for important new advances, and, indeed, that such are critical if one ever wishes to have a complete description of the flow phenomena of these materials under non-isothermal conditions.

In the remaining sections of Chap. 4, we shall make a critical examination of these prior theoretical efforts via a formal development in terms of the GENERIC structure discussed in Sec. 4.1. Although all of the work discussed below had merit in its time, progress has revealed that its limitations had to be removed for further theoretical refinement of the physical system description. We shall find that the internal consistency of the new structural approach described above allows further refinement, and, in some cases, corrects, clarifies, and extends past contributions to this subject.

### 4.2.1 The Time-Temperature Superposition Principle

Our thermodynamic story begins at the point where the temperature became an important variable in the description of the material properties of polymeric fluids. It was well understood early on after the large-scale development of high molecular weight polymers that solutions or melts of these materials, after removal of an applied load, would undergo a long time viscoelastic relaxation back to the undeformed state which could be quantified with a spectrum of relaxation modes, each with a characteristic relaxation time [26]. The expanding polymer industry demanded quantitative information about the material properties of these fluids under processing conditions, and these are all related in one way or another to the relaxation spectrum. It was thus of immediate import to take measurements of the relaxation rates of polymeric fluids over extensive ranges of deformations. The rub was that the typical experimental apparatus had a limited range of deformations which could be applied to the sample, whereas a typical processing operation did not. Hence for a given polymeric fluid, only a portion of the relaxation spectrum could be investigated experimentally.

Based upon a multitude of experimental evidence of creep and recovery in polymeric fluids, Leaderman [19] first enunciated the time-temperature superposition principle: “The effect of variation of temperature is thus seen to cause a shift of the sigmoidal creep curve along the axis of logarithmic time.” This insightful statement, though not suggesting any hint of universality, lead to the tremendously useful empiricism of experimentally determining a shift factor,  $a_T$ , which could be used to superimpose mechanical property data taken at different temperatures. Although not of universal validity, this principle did apply to a number of polymeric fluids of practical import in the polymer industry. It rests on the assumption that the molecular processes which govern each relaxation mode of a given polymer are accelerated (retarded) equally by an increase (decrease) of temperature [25]. These fluids were described as “thermo-rheologically simple” [25]. Hence an experimental determination of  $a_T$  would then subsequently allow an experimenter to extend effectively the deformation range of his apparatus by raising or lowering the temperature. Furthermore, data taken at one specific temperature could be used to infer those at another. The situation became even more pleasant with the discovery of reasonably accurate empiricisms for predicting the shift factor [20, 21, 26], which were valid approximately from the glass transition temperature,  $T_g$ , to  $T_g + 100$  K. Of course, this empirical theory cannot claim universal validity, but it is remarkable that it does work effectively for a large number of polymeric fluids over a wide range of temperatures. Markovitz [27] has given a critical account of this empiricism, which so effectively defined the usefulness and limitations of the theory that no further significant comments on the subject have appeared in the literature.

In applying the time-temperature superposition principle, it is implicitly assumed that the fluid under investigation is always at a constant temperature, spatially and temporally. Hence the temperature is not a problem variable, but merely an experimentally controlled parameter. Nevertheless, it did serve notice that the material properties of polymeric fluids are influenced greatly by variations of temperature in a more complicated fashion than the usual Arrhenius temperature dependence of the Newtonian shear viscosity. Furthermore, it provides a reasonably sound basis to which subsequent fully non-isothermal theories of polymeric fluids should conform, in the appropriate limits.

### 4.2.2 Extension of the Time-Temperature Superposition Principle to Non-isothermal Flows

For the design of polymer processing operations, it is not enough to know only the material properties of the fluid as functions of temperature (and other requisite variables, such as the deformation rate, of course). All of these variables can display spatial and temporal inhomogeneities, which are induced by inlet/outlet and boundary/initial conditions of the process itself. In important processing operations like blow molding, film blowing, fiber spinning, wire coating, injection molding, extrusion, and calendaring, temperature gradients can be as high as 100 K/mm perpendicular to the material streamlines due to viscous heating [63]. Post-processing quench procedures also lead to rapid temperature variations, but now parallel as well as perpendicular to the material streamlines. Consequently, the time-temperature superposition principle alone, even if it were universally valid, would be inadequate for describing the spatially as well as temporally varying material properties of the processed polymeric liquid. It is thus necessary to have available a fully non-isothermal set of evolution equations for the variables which describe completely the state of the fluid in space and time. Typical variables used to quantify the fluid are the stress tensor field, the velocity vector field, and the scalar temperature field; however, for processing operations involving crystallization or residual orientation it is necessary to use structural variables which quantify the conformational state of the fluid microstructure – a point to be emphasized below. The development of this set of evolution equations, and indeed, even the determination of the proper set of field variables, represents the foremost problem in this field.

The first mathematical endeavors to obtain a fully non-isothermal flow theory attempted to extend the idea of time-temperature superposition to flows with spatial and temporal inhomogeneities. Morland and Lee [28] examined the linear viscoelasticity of thermo-rheologically simple fluids by defining a “reduced” or “pseudo” time for the system which depended on both the spatial,  $\mathbf{r}$ , and real time,  $t$ , variables. Effectively, under the appropriate definition, a given viscoelastic law or material function in reduced time,  $\xi$ , is related to its constant temperature one evaluated in real time through the shift factor:

$$\xi(\mathbf{r}, t) \equiv ta_T(T(\mathbf{r})). \quad (4.1)$$

Two realizations are necessary to carry this off: 1.) even though the material is spatially inhomogeneous, the time-temperature superposition principle holds for each fluid particle independently; 2.) there is no explicit dependence of the shift factor on the temperature history of the fluid particle. The usefulness of this theory is very limited, however, and not only by the assumption of thermo-rheological simplicity. In the words of the authors: “Unfortunately the equilibrium and compatibility conditions are changed in form, and the usual character of the elasticity equations is lost. Expressing the viscoelastic law in terms of the real time variable gives either differential operators with non-isothermal coefficients, or integral operators whose kernels have functional arguments; in both cases there appears to be no general method of solution of the corresponding stress analysis equations.”

Using fundamental ideas from the approach of Coleman for materials with fading memory (to be discussed below), Crochet and Naghdi wrote a series of articles [29, 30, 31, 32] extending the Morland and Lee hypothesis by relaxing realization 2.) of the preceding paragraph: the reduced time is effectively taken as a function of the thermal history of the fluid particle. Again, the modified time scale is taken as central to the application of the idea of thermo-rheological simplicity to the analysis, with the restriction that the requisite strain functional is given by an isothermal functional of the stress history of a given fluid particle. This restriction in principle allowed typical constitutive functionals for isothermal fluids to be introduced into the theoretical description, but the only concrete applications of the theory were performed in the limit of linear viscoelasticity [29, 30, 32]. The practical utility of the methodology was limited by computational tractability, and effectively by the specification of the constitutive functionals.

The theory was also limited by the presumption of thermo-rheological simplicity of the material, which is far from being a universal property of these fluids. Furthermore, the temperature history of the fluid particle was assumed to be such that the temperature variation is small in the recent past, although it may be arbitrarily large from the initial condition. This is an interesting point, since Matsumoto and Bogue [62] have shown experimentally that for rapid temperature changes the time-temperature superposition principle fails dramatically. They suggest that the shift factor should be taken as a function of the present temperature and the rate of temperature variation, which clearly leads us back to the present theory, but in a form with the above-

mentioned assumption removed. Rather than proceed in this direction, given the other limitations of the theory described above, it is more important to press on in the development of a more universal set of equations for quantifying non-isothermal processes.

### 4.2.3 Theory of Simple Fluids with Fading Memory

In the early 1960s, Coleman and his co-workers developed several theories for different, restricted classes of “simple fluids”, the most well-known of these being the Theory of Simple Fluids with Fading Memory [33, 34, 35]. The fundamental tenet of this theory is that the stress tensor and heat flux vector at a given material point depend not only on the instantaneous values of the deformation gradient and temperature, but also on all past values of these quantities in a fashion which decays moving backward in time. The stress tensor field and the heat flux vector field of the simple fluid then depend on functionals of the deformation gradient and temperature, which are assumed to obey certain continuity and smoothness conditions, allowing subsequent mathematical analysis. Thermodynamics is then used to restrict the allowable functionality of the constitutive relationships between stress/heat flux and deformation/temperature gradient by assuming the validity of postulated macroscopic balance equations. The forms of these balance equations also serve to help define the meaning of “simple fluids.”

The most sacrosanct macroscopic balance equation in this theory is the postulated form of the global entropy balance,

$$\frac{d}{dt} \int_V \rho \eta dV + \int_S \frac{1}{T} \mathbf{q} \cdot \mathbf{n} dS - \int_V \rho \frac{Q}{T} dV = \int_V \rho \sigma_s dV. \quad (4.2)$$

In this expression,  $\rho$  is the mass density,  $\eta$  is the specific entropy,  $\mathbf{q}$  is the heat flux vector field,  $\mathbf{n}$  an outwardly-directed unit vector,  $Q$  the specific radiation energy per unit time,  $T$  the absolute temperature, and  $\sigma_s$  the local entropy source term. The appearance of  $Q$  in this expression has long been questioned; *e. g.*, Lavenda [41] writes: “If it ( $Q$ ) is a heat supply then it has to pass over the surface ( $S$ ) and so it should be included in the heat flux term. On the contrary, if it is a volume source term, then it should be accounted for in the entropy source term.” Equation (4.2) then provides a local expression for the

entropy production rate,

$$\sigma_s = \frac{D\eta}{Dt} + \frac{1}{\rho} \nabla \cdot \left( \frac{\mathbf{q}}{T} \right) - \frac{Q}{T} \geq 0, \quad (4.3)$$

where  $D/Dt$  denotes the material derivative. This balance equation is then considered along with the local balance equations of energy and momentum,

$$\frac{Du}{Dt} = -\frac{1}{\rho} \nabla \cdot \mathbf{q} + Q + \frac{1}{\rho} \mathbf{T} : \nabla \mathbf{v}, \quad (4.4)$$

$$\frac{D\mathbf{v}}{Dt} = \frac{1}{\rho} \nabla \cdot \mathbf{T} + \mathbf{b}, \quad (4.5)$$

where  $u$  is the specific internal energy,  $\mathbf{T}$  the total stress tensor field,  $\mathbf{v}$  the velocity vector field, and  $\mathbf{b}$  a body force vector field. Elimination of the radiation field between Eqs. (4.3) and (4.4) yields the Clausius-Duhem inequality which is the focal point of the theory:

$$\sigma_s = \frac{D\eta}{Dt} - \frac{1}{T} \frac{Du}{Dt} + \frac{1}{\rho T} \mathbf{T} : \nabla \mathbf{v} - \frac{\mathbf{q} \cdot \nabla T}{\rho T^2} \geq 0. \quad (4.6)$$

Note that the radiation term has dropped out of the final inequality, and that the balance equations have effectively limited simple fluids to those whose entropy flux is due solely to the process of a Fourier-type of heat conduction [41]. Inequality (4.6) then serves to restrict the allowable choice of functionals for the constitutive relationships in the theory.

Ultimately, Coleman’s theory suffered from the same criticisms as its famous prodigy, Rational Thermodynamics, which are well documented [36, 37, 38, 39, 40, 41]. However, it possessed peculiarities of its own which limited its universality and practicality. As with the Crochet and Naghdi theory above, it proved to be computationally intractable, due to the presence of complex functionals, except in the simplest situations. Consequently, it provided no real quantifiable physical behavior far beyond the limits of linear viscoelasticity. Another problem with the theory arises from its restriction to simple fluids with fading memory; this is far from universal behavior for all fluids. In particular, Rivlin [36] points to the exclusion of Newtonian fluids from this category. Indeed, not only Newtonian fluids, but all Jeffreys’ type viscoelastic fluid models containing an explicit solvent viscosity seem to be implicitly excluded as well, since in the limit of small relaxation time the Newtonian fluid is

recovered. This would be particularly unfortunate since much evidence suggests that the viscous heat generated under processing conditions can greatly affect, if not overwhelm, the elastic characteristics of the flowing material [55, 54, 109, 51, 110, 111]. Materials with an inherent microstructural anisotropy, such as liquid crystals, are also excluded from the class of simple fluids, as, of course, are other complex fluids of practical interest, such as polymer blends and mixtures. Hence the designation “simple fluids” seems quite apt, and the applicability of the theory is quite limited by contemporary standards.

#### 4.2.4 The Theory of Purely Entropic Elasticity

Another school of thought concerning non-isothermal flows of polymeric liquids arose during the early 1970s, that of Purely Entropic Elasticity. The main tenet of this school is taken directly from the very successful Theory of Rubber Elasticity, where the entire elastic response of the solid material is determined by the entropy function. This idea of a purely entropic elastic response was first applied to viscoelastic materials by Tobolsky and Andrews [42], but was not developed into a fully non-isothermal flow theory until thirty years later by Astarita and Sarti [43, 44, 45, 46].

The theory is a local field formalism, where the local expression of the first law of thermodynamics is taken as the starting point [43], expressed as Eq. (4.4). The local form of the second law of thermodynamics is then derived as Eq. (4.6). At this point, two assumptions are made which define the material with purely entropic elasticity and limit the universality of the theory. The first assumption is that the material is incompressible, and the second is that the specific internal energy is a unique function of temperature only,  $u = u(T)$  [43]. Defining the specific heat capacity as  $c \equiv du/dT$ , Eq. (4.4) can be written in the form of a temperature balance,

$$\rho c \frac{DT}{Dt} = \mathbf{T} : \nabla \mathbf{v} - \nabla \cdot \mathbf{q} + \rho Q. \quad (4.7)$$

This is the form of the temperature equation which is used in practically all of the engineering analyses of non-isothermal flows of which we are aware (as well as all commercially available software for these problems), but it has limitations [43]: “The implications of this ... are

very important in the engineering analysis of such polymer processing operations as extrusion and injection molding, where frictional heating is a crucial phenomenon. Polymer melts are known to be nonlinear viscoelastic materials, and unless the assumption ( $u = u(T)$ ) is made, their frictional heating behavior would not be described by (Eq. 4.7).” Although Astarita and Sarti [46] make a case for the experimental validity of  $u = u(T)$  for some polymeric fluids, this assumption and the other one concerning fluid incompressibility should be avoided in a universal theory, as they can seriously affect the dynamical behavior exhibited by the evolution equations of the system. More experiments are needed to test the validity of this assumption, as only a few polymeric fluids have been examined, and even one of these shows deviations from the expected behavior based on the assumption of purely entropic elasticity [14]. In Chap. 3 we have proposed a recipe to check whether a given polymer obeys the Theory of Purely Entropic Elasticity or not.

A further point is made by Astarita and Sarti [45] concerning internal state variables and memory functionals (such as those appearing in Coleman’s work) in dynamical theories of polymeric fluids. They describe how computationally intractable memory functionals can, in principle and in practice, be replaced by a set of internal structural variables, of which only the instantaneous values need be known. Hence computational tractability can be achieved at very little expense. This structural variable *ansatz* is the method followed and advocated in this article, and described thoroughly below.

On only several occasions has a more general expression for the temperature equation appeared in the literature. Ironically, Astarita and Sarti [44] wrote down an extended temperature equation for Coleman’s theory, but never made use of it under the auspice of purely entropic elasticity. Stickforth [112] and Braun and Friedrich [113, 91] presented similar forms of the temperature equation, which were related to that of Astarita and Sarti [44], for entropic *and* energetic elasticity. Braun’s form of the temperature equation is [91]

$$\rho c \frac{DT}{Dt} = -\nabla \cdot \mathbf{q} + \boldsymbol{\sigma} : \mathbf{A} - \rho \left. \frac{Du}{Dt} \right|_T, \quad (4.8)$$

where  $\mathbf{A}$  is the symmetric part of the velocity gradient tensor field and  $\boldsymbol{\sigma}$  is the extra stress tensor field. This expression is exact for an incompressible material, but it is not particularly useful unless the last term

on the right-hand side is determined analytically. (Keep in mind that for an incompressible material  $\boldsymbol{\sigma} : \mathbf{A} = \mathbf{T} : \nabla \mathbf{v}$ , provided that the extra stress tensor field is symmetric.) Braun subsequently specialized this expression for materials with linear relationships between the extra stress tensor field and a deformation tensor, but did not explicitly consider relaxational phenomena in his temperature equation, as in Eq. (4.9) below. Peters [92] obtained a generalization of this temperature equation for a fluid with multiple relaxation modes and non-affine deformation. If we neglect these complexities, his equation is

$$\rho c \frac{DT}{Dt} = -\nabla \cdot \mathbf{q} + \boldsymbol{\sigma}^v : \mathbf{A} + \boldsymbol{\sigma}^e : \mathbf{Z} + \rho T \frac{\partial \boldsymbol{\sigma}^e / \rho}{\partial T} : (\mathbf{A} - \mathbf{Z}), \quad (4.9)$$

where  $\boldsymbol{\sigma}^v$  is the viscous contribution to the extra stress tensor field,  $\boldsymbol{\sigma}^e$  the elastic contribution, and  $\mathbf{Z}$  is a relaxation matrix which is used to fit various rheological models. Although this temperature equation is more general than Eq. (4.7), we are only aware of one instance where it was used in an engineering analysis of non-isothermal polymer flows [114]. The last term on the right-hand side of Eq. (4.9) is not analytically known without a microstructural interpretation, resulting in a set of coupled partial differential equations which is difficult to solve computationally. (Peters does introduce a microstructural interpretation in his development, but this requires questionable closure approximations in order to reduce averages over the orientational distribution function to arbitrary functions of the second moment [92]).

#### 4.2.5 Non-isothermal Constitutive Equations from Bead–Spring Models

All of the preceding theoretical efforts were essentially continuum approaches, describing the gross, macroscopic dynamics of gross, macroscopic processes. In 1972, Marrucci [47] wrote down the first detailed kinetic treatment of non-isothermal polymer flows based upon the Hookean dumbbell model of dilute polymer solutions. Here, the free energy density is taken as purely entropic, with the assumed form

$$a = nK(T)\text{tr}[\langle \mathbf{R}\mathbf{R} \rangle - \langle \mathbf{R}\mathbf{R} \rangle_0], \quad (4.10)$$

where  $n$  is the number density of dumbbells,  $K(T)$  is the temperature dependent elastic spring factor,  $\langle \mathbf{R}\mathbf{R} \rangle$  is the second moment of the distribution function for dumbbell extension and orientation, and  $\langle \mathbf{R}\mathbf{R} \rangle_0$

is the same evaluated at equilibrium. The spring factor is assumed to have a linear dependence on temperature,

$$K(T) = k_B T \mu, \quad (4.11)$$

where  $\mu$  is assumed to be the constant

$$\mu = \frac{3}{2\text{tr}\langle \mathbf{R}\mathbf{R} \rangle_0}; \quad (4.12)$$

i. e., it is assumed to be independent of temperature.

By taking the second moment of the diffusion equation for the distribution function, Marrucci ultimately obtained a constitutive equation for the extra stress tensor field, which reads

$$\sigma_{\alpha\beta} + \frac{\zeta}{4K(T)} \left[ \sigma_{\alpha\beta}^{(c)} - \sigma_{\alpha\beta} \frac{D \ln T}{Dt} \right] = \frac{\zeta n k_B T}{2K(T)} A_{\alpha\beta}, \quad (4.13)$$

where  $\zeta$  is the friction coefficient of the dumbbell beads and  $\boldsymbol{\sigma}^{(c)}$  is the upper-convected derivative of the extra stress tensor field, defined as

$$\sigma_{\alpha\beta}^{(c)} \equiv \frac{D\sigma_{\alpha\beta}}{Dt} - \sigma_{\alpha\gamma} \nabla_\gamma v_\beta - \sigma_{\beta\gamma} \nabla_\gamma v_\alpha. \quad (4.14)$$

Note that in deriving this expression it has been *implicitly assumed* that the material is incompressible. The new term that is proportional to  $D \ln T / Dt$  thus appears in Eq. (4.13) over the traditional isothermal dumbbell model, as has been noted in purely continuum theories [30]. Bird [48] later generalized Eq. (4.13) as

$$\sigma_{\alpha\beta} + \frac{\zeta}{4K(T)} \left[ \sigma_{\alpha\beta}^{(c)} - \sigma_{\alpha\beta} \frac{d \ln K(T)}{d \ln T} \frac{D \ln T}{Dt} - n k_B T \delta_{\alpha\beta} \left( \frac{d \ln K(T)}{d \ln T} - 1 \right) \frac{D \ln T}{Dt} \right] = \frac{\zeta n k_B T}{2K(T)} A_{\alpha\beta}, \quad (4.15)$$

making clear an implicit nonlinear temperature dependence of the spring factor. Of course, this constitutive equation for the extra stress tensor field must ultimately be coupled with macroscopic balance equations, such as Eqs. (4.4) and (4.5). In practise, Eq. (4.4) is foregone in favor of the purely entropic form of the temperature equation, (4.7).

The linear dependence of the spring factor in Eq. (4.13) was also addressed by Gupta and Metzner [49], who pointed out that the quantity



$\zeta/4/K(T) D \ln T/Dt$  appearing there is of insufficient magnitude and of the wrong sign to quantify experimental data. They cite the assumption of constant  $\mu$ , according to Eq. (4.12), as the source of the error, since  $\text{tr} \langle \mathbf{R}\mathbf{R} \rangle_0$  actually increases with increasing temperature. This produces a decrease in the stiffness parameter,  $\mu$ , which can be better expressed with the empirical relationship

$$\mu = \nu T^{-(B+1)}, \quad (4.16)$$

where  $B$  is a number greater than  $-1$  and  $\nu$  is a positive constant. Eq. (4.15) then becomes

$$\sigma_{\alpha\beta} + \frac{\zeta}{4K(T)} \left[ \sigma_{\alpha\beta}^{(c)} + B\sigma_{\alpha\beta} \frac{D \ln T}{Dt} \right] = - (B+1) \frac{\zeta n k_B T}{4K(T)} \delta_{\alpha\beta} \frac{D \ln T}{Dt}. \quad (4.17)$$

This constitutive equation has been used by Luo and Tanner [50] and McClelland and Finlayson [51] for numerical simulations of non-isothermal film blowing and extrusion, respectively, with some apparent degree of success. These studies couple Eq. (4.17) with the momentum balance (4.5) and the temperature equation, (4.7), as already mentioned.

Wiest [52] extended Eq. (4.15) for the Rouse model and obtained a generalization of this equation for a discrete spectrum of relaxation times. In a subsequent work with Phan-Thien [53], a non-isothermal version of the Curtiss-Bird model is obtained. Sugeng *et al.* [54] assert that the non-isothermal constitutive equation described above applies well to fluids with a low degree of elasticity; however, if the elasticity of the material is high, as typical in polymer processing operations, then the elastic effects are comparable in magnitude to the thermal effects and this constitutive equation is no longer valid. Under these circumstances, they propose a non-isothermal generalization of the Phan-Thien/Tanner constitutive equation,

$$\sigma_{\alpha\beta} + \frac{\zeta}{4K(T)} \left[ \sigma_{\alpha\beta}^{(c)} - \sigma_{\alpha\beta} \frac{D \ln T}{Dt} \right] + \frac{\epsilon}{n k_B T} \sigma_{\gamma\gamma} \sigma_{\alpha\beta} + \frac{\zeta \phi}{4K(T)} (A_{\alpha\gamma} \sigma_{\gamma\beta} + A_{\gamma\beta} \sigma_{\alpha\gamma}) = \frac{\zeta n k_B T}{2K(T)} A_{\alpha\beta}, \quad (4.18)$$

where the parameter  $\epsilon$  accounts for the “elongational behavior” of the

model and  $\phi$  affects the “shear behavior.” Note that in this expression, the spring factor is taken as that of Eq. (4.11).

The constitutive equations cited above are restricted to incompressible fluids, and are limited in the neglect of the viscous flow of the surrounding medium, which can lead to substantial viscous heat generation [63]. The generalization to Jeffreys-type constitutive equations is difficult with bead-spring models due to the added degree of complexity and associated nonlinearities of incorporating a solvent viscosity into the expression for the extra stress tensor. An extension of these results to more sophisticated polymer models also turns out to be difficult because it is not clear how to incorporate spatial temperature variations in the kinetic theory [54, 52, 53].

## 4.2.6 Heat Conduction in Polymeric Fluids

When studying non-isothermal flows of polymeric fluids, one must consider not only the production of heat within the material due to viscous heating and entropic effects, but also the transport or conduction of that thermal energy from a given material point within the medium to another. This heat conduction is very important in industrial operations, greatly affecting the processibility of a given material and its final properties [115, 61, 62, 63, 116, 117, 51]. The experimental investigation of heat conduction in flowing polymeric liquids is quite difficult, however, especially considering that heat conduction is a transport process that can be quite slow, and hence can be obscured by other thermally driven transport and relaxational processes, such as thermally induced convection, if the temperature gradients involved are very large.

In all theoretical studies of heat conduction in polymeric materials, a Fourier-type of heat conduction is *a priori* assumed, with  $\mathbf{q}$  of Eq. (4.4) taken proportional to an anisotropic thermal conductivity tensor,

$$\mathbf{q} = -\boldsymbol{\alpha} \cdot \nabla T. \quad (4.19)$$

Some direct experiments have been made of Fourier-type heat conduction in sheared polymeric liquids [118, 119] to try to determine the effect of polymer conformation on the anisotropic thermal conductivity tensor. These measurements seem to show that the thermal conductivity

parallel to the backbone of a macromolecule is higher than perpendicular to it. But only data for a few materials, *e. g.*, polyethylene [119], are available. Theoretical approaches to account for the effects of the microstructure on the thermal conductivity tensor assume the most general form of this tensor which is compatible with the Cayley/Hamilton theorem [120, 2],

$$\boldsymbol{\alpha} = a_1 \boldsymbol{\delta} + a_2 \langle \mathbf{RR} \rangle + a_3 \langle \mathbf{RR} \rangle \cdot \langle \mathbf{RR} \rangle, \quad (4.20)$$

where the  $a_i$  are, in general, functions of the invariants of  $\langle \mathbf{RR} \rangle$  as well as  $\rho$  and  $T$ . From the requirement of a non-negative local rate of entropy production, as quantified by Inequality (8),  $-\mathbf{q} \cdot \nabla T \geq 0$ , it follows that  $a_1 \geq 0$  and  $a_2 + a_3 \geq 0$  [121], but microscopic considerations should be made to apply Eq. (4.20) to specific polymers; *e. g.*, solid polymers or polymeric fluids. Leonov [120] applied Eq. (4.20) to amorphous solid polymers and states that  $a_1$  is the thermal conductivity of an isotropic (undeformed) system, whereas  $a_2$  and  $a_3$  are functions of the first and the second invariants of the tensor  $\langle \mathbf{RR} \rangle$ . For a dilute polymeric solution, van den Brule [122] found that  $a_1$  is the thermal conductivity of the solvent,  $a_2$  can be related to the mass fraction of the polymers and the other microscopic parameters of the model, and  $a_3 = 0$ . Most authors believe the Onsager reciprocal relations imply that  $\boldsymbol{\alpha}$  is symmetric, but this belief has been attacked by others [123].

It is evident that there is still an enormous gap between theoretical and experimental studies concerning the heat conduction in polymeric materials. Only few data on specific substances are available; however, even data on the same substances show significant scattering due to systematic errors related to the different experimental techniques used in the various measurements [117]. Furthermore, most theoretical efforts and experimental interpretations have *assumed* that the heat flux is due solely to Fourier-type conduction, ignoring other possibilities of thermally driven diffusive processes. Recently, Bird *et al.* [124] have examined thermally induced diffusion (the *Soret effect*) in dilute polymer solutions. Nevertheless, in order to keep the present analysis as short and to the point as possible, we also restrict our attention in this paper to Fourier-type conduction; however, the formalism used herein can have much to say about non-Fourier-type heat conduction in the future.

## 4.3 Fundamental Balance Equations for Non-isothermal Polymeric Materials

Our aim in this section is to derive a thermodynamically consistent set of evolution equations for the basic field variables necessary to describe a flowing polymeric liquid using the double generator GENERIC structure, in a similar vein to the preceding analysis in terms of a single generator [94, 2]. Doing thus allows one to achieve a definite splitting between energetic and entropic elasticity potentials, and allows one to obtain a more symmetric dissipation bracket [97]. The resulting equations are free of the restrictions of the previous theories of fluids whose heat flux is solely of Fourier-type, since no *a priori* assumptions are made regarding incompressibility, purely entropic elasticity, time-temperature superposibility, *etc.* Explicit non-isothermal counterparts of popular isothermal viscoelastic fluid models which are thermodynamically consistent are derived. In so doing, common errors and inconsistencies in previously proposed non-isothermal models are exposed and discussed.

### 4.3.1 Thermodynamics of Polymeric Materials at Quasi-Equilibrium

Our starting point is to choose a set of variables which is sufficient to describe completely the thermodynamic state of a polymeric liquid at quasi-equilibrium; *i. e.*, a partial thermodynamic equilibrium where most of the internal degrees of freedom are equilibrated within the time scale of interest, subject to the constraint that the remaining degrees of freedom remain, on the same time scale, frozen at non-equilibrium values [97]. The variable set  $x$  we choose is  $x = [\rho, \epsilon, \mathbf{c}]$ , where  $\rho$  is the mass density of the fluid with units of mass/length<sup>3</sup>,  $\epsilon$  is the internal energy density with units of energy/length<sup>3</sup>, and  $\mathbf{c}$  is the contravariant conformation tensor field expressing the degree of orientation and elongation of the polymer chain with units of length<sup>2</sup>. (Herein, we neglect all but a single relaxation mode, for simplicity, although fluids with multiple relaxation modes can be similarly described through additional conformation tensor fields [2].) It is also necessary to express a thermodynamic potential function for these materials, which we take as the entropy density,  $s$ , which is a function of the thermodynamic

variables  $x$ . A Gibbs relation may then be written down so as to define the temperature, pressure, and entropic potential as, respectively,

$$T \equiv \left( \frac{\partial s}{\partial \epsilon} \right)^{-1}, \quad p \equiv -\epsilon + \left( \frac{\partial s}{\partial \epsilon} \right)^{-1} \left( s - \rho \frac{\partial s}{\partial \rho} \right), \quad (4.21)$$

$$\mathbf{z} \equiv -T \frac{\partial s}{\partial \mathbf{c}}. \quad (4.22)$$

The variable set and its associated thermodynamic potential which were chosen above are the proper quantities to use in the GENERIC structural equation, as described in the next subsection; however, they are not necessarily the most natural choice for modelling polymeric materials. Indeed, since important physical parameters of these models are typically written as functions of temperature, such as the spring factor of Eq. (4.11), it is practical to define a new thermodynamic potential,  $\omega$ , which depends on  $\rho$ ,  $T$ , and  $\mathbf{c}$ , as

$$\omega = s - \frac{\partial s}{\partial \epsilon} \epsilon. \quad (4.23)$$

This new potential is thus a Legendre transformation of the entropy density, and is known as a Massieu function [76]. Consequently, Eq. (4.23) implies the relations

$$\frac{\partial \omega}{\partial \rho} = \frac{\partial s}{\partial \rho}, \quad (4.24)$$

$$\frac{\partial \omega}{\partial T} = \frac{\epsilon}{T^2}, \quad (4.25)$$

$$\frac{\partial \omega}{\partial \mathbf{c}} = \frac{\partial s}{\partial \mathbf{c}}, \quad (4.26)$$

$$p = T \left( \omega - \rho \frac{\partial \omega}{\partial \rho} \right). \quad (4.27)$$

Thermodynamic potentials for polymeric liquids have been presented and applied to  $n$ -alkanes in Chap. 2. The entropic potential has been computed for PE and PIB in Chap. 3 adapting the RIS approximation.

### 4.3.2 The Double Generator GENERIC Structure

The GENERIC structure manifests itself through a global master equation [96],

$$\frac{dF}{dt} = \{F, E\} + [F, S], \quad (4.28)$$

written in terms of the Poisson,  $\{\cdot, \cdot\}$ , and dissipation,  $[\cdot, \cdot]$ , brackets, and two generators,  $E$  and  $S$ , which are global functionals of the dynamic variables chosen for the system description. Here we treat the variables of the preceding subsection as field variables,  $x(\mathbf{r}, t)$ , implying that locally (*i. e.*, for each material point) the fluid is in a quasi-equilibrium state. Furthermore, these field variables need to be supplemented with the momentum density vector field,  $\mathbf{u}$ , so that macroscopic flow phenomena can be described.  $F$  is an arbitrary functional of these variables, with the form  $F[x] = \int f(x) d^3r$  which is possessed by the total energy,  $E$ , and total entropy,  $S$ , as well. The Poisson bracket is bilinear, anti-symmetric, and satisfies the Jacobi identity, and the dissipation bracket is bilinear, symmetric or antisymmetric depending on the parities of the phenomena under consideration, and guarantees a positive rate entropy of production. Note that  $\mathbf{u}$  can be interpreted as  $\rho \mathbf{v}$ , where  $\mathbf{v}$  is the common velocity vector field.

This global equation can also be expressed in the form of a local operator equation [96, 1],

$$\frac{\partial x}{\partial t} = L \frac{\delta E}{\delta x} + M \frac{\delta S}{\delta x}, \quad (4.29)$$

where  $L$  is the Poisson operator associated with the reversible dynamics,  $M$  is a metric matrix associated with the dissipation, and  $\delta/\delta x$  denotes a functional derivative, defined as

$$\frac{\delta F}{\delta x} \equiv \frac{\partial f}{\partial x}, \quad (4.30)$$

for the present article. In general, the functional  $F$  may depend on spatial gradients of  $x$  as well as  $x$  itself, and in this case the definition of Eq. (4.30) should be altered accordingly [2]. Eq. (4.29) is complemented by the mutual degeneracy requirements

$$L \frac{\delta S}{\delta x} = 0, \quad (4.31a)$$

$$M \frac{\delta E}{\delta x} = 0, \quad (4.31b)$$

which express the fact that the operator  $L$  lies in the null space of the generator of the irreversible dynamics,  $S$ , and vice versa for the operator  $M$  and the generator  $E$ . In what follows we will adopt the double generator GENERIC formalism to derive a set of fully dynamically consistent time evolution equations for polymeric materials.

### 4.3.3 Derivation of the Non-isothermal Flow Equations

We now wish to derive a macroscopic set of thermodynamically consistent non-isothermal flow equations for a polymeric fluid using the operator form of the master equation, Eq. (4.29), since it turns out to be easiest to specify the proper dissipative contributions to the dynamics using this form [97]. The reversible dynamics, as described by the  $L$  operator, have already been expressed in terms of an antisymmetric operator matrix in [1]. This operator can be obtained through a rigorous transformation from the Poisson bracket for elastic materials, which was postulated *ad hoc* in [125] for an incompressible material and derived directly from the principle of least action for a compressible one [94]. This operator, in terms of the variable set  $x = [\rho, \mathbf{u}, \epsilon, \mathbf{c}]$ , is [1]

$$L = - \begin{pmatrix} 0 & \nabla_\epsilon \rho & 0 & 0 \\ \rho \nabla_\alpha & \nabla_\epsilon u_\alpha + u_\epsilon \nabla_\alpha & L_{23} & L_{24} \\ 0 & L_{32} & 0 & 0 \\ 0 & L_{42} & 0 & 0 \end{pmatrix}. \quad (4.32)$$

The unspecified elements in the operator matrix of Eq. (4.32) are

$$L_{23} = \nabla_\alpha p + \epsilon \nabla_\alpha - 2 \nabla_\beta c_\gamma \beta z_{\alpha\gamma}, \quad (4.33a)$$

$$L_{32} = p \nabla_\epsilon + \nabla_\epsilon \epsilon - 2 c_\gamma \beta z_\gamma \epsilon \nabla_\beta, \quad (4.33b)$$

$$L_{24} = -(\nabla_\alpha c_\eta \zeta) - \nabla_\beta c_\beta \eta \delta_{\alpha\zeta} - \nabla_\beta c_\beta \zeta \delta_{\alpha\eta}, \quad (4.33c)$$

$$L_{42} = (\nabla_\epsilon c_{\alpha\beta}) - c_{\alpha\gamma} \nabla_\gamma \delta_{\beta\epsilon} - c_{\beta\gamma} \nabla_\gamma \delta_{\alpha\epsilon}. \quad (4.33d)$$

Note that the Einstein summation convention has been introduced in this and subsequent expressions.

The generators to be used in Eq. (4.29) are

$$E[\rho, \mathbf{u}, \epsilon, \mathbf{c}] = \int \left[ \frac{u_\gamma u_\gamma}{2\rho} + e_m(\rho, \mathbf{c}) + \epsilon \right] d^3r, \quad (4.34)$$

$$S[\rho, \epsilon, \mathbf{c}] = \int s(\rho, \epsilon, \mathbf{c}) d^3r. \quad (4.35)$$

The function  $e_m$  depends on the variables indicated, and can quantify the energetic effects of an external magnetic field, for example, upon the system. Note that  $L$  as defined by Eq. (4.32) satisfies degeneracy condition (4.31a).

The last element of Eq. (4.29) to be specified is the metric matrix,  $M$ . For the linear dissipative processes considered here,  $M$  is constructed through the operation [97]

$$M = C D C^T, \quad (4.36)$$

where

$$D = \begin{pmatrix} 0 & 0 & 0 & 0 \\ 0 & T Q_{\beta\alpha\gamma\epsilon} & 0 & 0 \\ 0 & 0 & T^2 \alpha_{\alpha\beta} & 0 \\ 0 & 0 & 0 & T \Lambda_{\rho\delta\gamma\epsilon} \end{pmatrix}, \quad (4.37)$$

$$C = \begin{pmatrix} -1 & 0 & 0 & 0 \\ 0 & \nabla_\beta & 0 & 0 \\ -\frac{1}{2} v_\alpha v_\alpha + \frac{\partial e_m}{\partial \rho} & (\nabla_\beta v_\alpha) & \nabla_\alpha & \frac{\partial e_m}{\partial c_{\rho\delta}} \\ 0 & 0 & 0 & -1 \end{pmatrix}, \quad (4.38)$$

and  $C^T$  is the operator transpose of  $C$  [97]. The decomposition of Eq. (4.36) splits the metric matrix into distinct submatrices with either thermodynamic ( $D$ ) or mechanical ( $C$ ) nature.  $C$  is defined using the generator  $E$  [97], and has essentially the same form regardless of the physical system under consideration.  $D$  is the matrix of phenomenological coefficients, which is symmetric (for the present system) and positive semidefinite. The phenomenological coefficient matrices,  $\mathbf{Q}$ ,  $\alpha$ , and  $\Lambda$  represent viscous, conduction, and relaxational effects, respectively. They are system specific, and will be defined for various polymeric fluid models in the next section. Note that  $D$  was determined with the restrictions that the materials exhibited Fourier-type heat flux only, that mass is conserved, that the principle of material objectivity holds, that chain migration effects are negligible on process time scales, and that the material does not display non-affine motion. (This last restriction will be removed in the next section.) Evaluating Eq. (4.36), we obtain

$$M = \begin{pmatrix} 0 & 0 & 0 & 0 \\ 0 & -\nabla_\beta T Q_{\beta\alpha\gamma\epsilon} \nabla_\gamma & M_{23} & 0 \\ 0 & -T (\nabla_\beta v_\alpha) Q_{\beta\alpha\gamma\epsilon} \nabla_\gamma & M_{33} & -T \frac{\partial e_m}{\partial c_{\rho\delta}} \Lambda_{\rho\delta\eta\zeta} \\ 0 & 0 & M_{43} & T \Lambda_{\alpha\beta\eta\zeta} \end{pmatrix}, \quad (4.39)$$

where the unspecified elements in this operator matrix are

$$M_{23} = \nabla_\beta T Q_{\beta\alpha\gamma\epsilon} (\nabla_\gamma v_\epsilon), \quad (4.40a)$$

$$M_{33} = TQ_{\beta\alpha\gamma\epsilon}(\nabla_\beta v_\alpha)(\nabla_\gamma v_\epsilon) - \nabla_\alpha \alpha_{\alpha\beta} T^2 \nabla_\beta + T \frac{\partial e_m}{\partial c_{\rho\delta}} \Lambda_{\rho\delta\gamma\epsilon} \frac{\partial e_m}{\partial c_{\gamma\epsilon}}, \quad (4.40b)$$

$$M_{43} = -T \Lambda_{\alpha\beta\gamma\epsilon} \frac{\partial e_m}{\partial c_{\gamma\epsilon}}. \quad (4.40c)$$

Note that degeneracy condition (4.31b) is satisfied for the metric matrix. Furthermore, for  $M$  to be symmetric,  $Q_{\alpha\beta\gamma\epsilon} = Q_{\gamma\epsilon\alpha\beta}$ ,  $\Lambda_{\alpha\beta\gamma\epsilon} = \Lambda_{\gamma\epsilon\alpha\beta}$ , and  $\alpha_{\alpha\beta} = \alpha_{\beta\alpha}$ .

The evolution equations for the system variables are obtained from Eq. (4.29) after evaluating the functional derivatives of the generators,

$$\frac{\delta E}{\delta x} = \begin{bmatrix} -\frac{1}{2}v_\alpha v_\alpha + \frac{\partial e_m}{\partial \rho} \\ v_\epsilon \\ 1 \\ \frac{\partial e_m}{\partial c_{\eta\zeta}} \end{bmatrix}, \quad \frac{\delta S}{\delta x} = \begin{bmatrix} \frac{\partial \omega}{\partial \rho} \\ 0 \\ 1/T \\ \frac{\partial \omega}{\partial c_{\eta\zeta}} \end{bmatrix}. \quad (4.41)$$

They are

$$\frac{\partial \rho}{\partial t} = -\nabla_\gamma(\rho v_\gamma), \quad (4.42a)$$

$$\rho \frac{\partial v_\alpha}{\partial t} = -\rho v_\beta \nabla_\beta(v_\alpha) - \nabla_\alpha p + \nabla_\beta \sigma_{\alpha\beta} + \rho b_\alpha, \quad (4.42b)$$

$$\begin{aligned} \frac{\partial \epsilon}{\partial t} &= -\nabla_\gamma(\epsilon v_\gamma) - p \nabla_\gamma v_\gamma - \nabla_\gamma q_\gamma + 2z_{\gamma\alpha} c_{\gamma\beta} \nabla_\beta v_\alpha \\ &\quad + Q_{\alpha\beta\gamma\epsilon}(\nabla_\alpha v_\beta)(\nabla_\gamma v_\epsilon) + \Lambda_{\alpha\beta\gamma\epsilon} \frac{\partial e_m}{\partial c_{\alpha\beta}} \frac{\partial e_m}{\partial c_{\gamma\epsilon}} \\ &\quad + \Lambda_{\alpha\beta\gamma\epsilon} \frac{\partial e_m}{\partial c_{\alpha\beta}} z_{\gamma\epsilon}, \end{aligned} \quad (4.42c)$$

$$\begin{aligned} \frac{\partial c_{\alpha\beta}}{\partial t} &= -v_\gamma \nabla_\gamma c_{\alpha\beta} + c_{\gamma\alpha} \nabla_\gamma v_\beta + c_{\gamma\beta} \nabla_\gamma v_\alpha \\ &\quad - \Lambda_{\alpha\beta\gamma\epsilon} \frac{\partial e_m}{\partial c_{\gamma\epsilon}} - \Lambda_{\alpha\beta\gamma\epsilon} z_{\gamma\epsilon}, \end{aligned} \quad (4.42d)$$

where the extra stress tensor field is given by

$$\sigma_{\alpha\beta} = 2z_{\alpha\gamma} c_{\gamma\beta} + Q_{\beta\alpha\gamma\epsilon} \nabla_\gamma v_\epsilon + 2c_{\beta\gamma} \frac{\partial e_m}{\partial c_{\gamma\alpha}}, \quad (4.43)$$

the body force vector field by

$$b_\alpha = -\nabla_\alpha \frac{\partial e_m}{\partial \rho} + \frac{1}{\rho} \frac{\partial e_m}{\partial c_{\eta\zeta}} \nabla_\alpha c_{\eta\zeta}, \quad (4.44)$$

and  $\mathbf{q}$  is the heat flux vector field of Eq. (4.19). Note that if  $e_m(\rho, \mathbf{c}) = \rho \hat{e}_m(\mathbf{c})$ , then  $\mathbf{b} = \mathbf{0}$ , and that if  $\hat{e}_m$  contains an explicit spatial dependence,  $\hat{e}_m(\mathbf{c}, \mathbf{r})$ , then  $\mathbf{b} = -\partial \hat{e}_m / \partial \mathbf{r}|_{\mathbf{c}}$ .

The first equation, (4.42a), is the continuity equation expressing conservation of mass. The second equation, (4.42b), is the linear momentum balance of Eq. (4.5), given the realization that the total stress tensor field is defined as  $\mathbf{T} = \boldsymbol{\sigma} - p\boldsymbol{\delta}$ .

The third equation, (4.42c), is the balance expression for the internal energy density. Note that this evolution equation no longer has the form of Eq. (4.4): it does not include all contributions to the extra stress tensor of Eq. (4.43) and has additional relaxational terms not appearing in Eq. (4.4), unless one associates the latter with the controversial radiation term,  $Q$ . This is not very satisfying since these relaxational effects have nothing to do with radiation. Hence we have an explicit example of Lavenda's criticism [41] that the specific radiation energy appearing in the macroscopic balance equation is essentially a consistency factor which "permits the computed constitutive dependent variables to be compatible with the macroscopic balance equations." Consequently, in the presence of a non-vanishing  $e_m$ , the specific energy,  $u$ , of Eq. (4.4) cannot be interpreted as the specific internal energy, but as  $\hat{u} \equiv (\epsilon + e_m)/\rho$ . The time evolution equation for this quantity is given by

$$\begin{aligned} \frac{\partial \rho \hat{u}}{\partial t} &= \frac{\partial \epsilon}{\partial t} + \frac{\partial e_m}{\partial c_{\alpha\beta}} \frac{\partial c_{\alpha\beta}}{\partial t} + \frac{\partial e_m}{\partial \rho} \frac{\partial \rho}{\partial t} \\ &= -\nabla_\gamma(\rho \hat{u} v_\gamma) - p \nabla_\gamma v_\gamma + \sigma_{\alpha\beta} \nabla_\alpha v_\beta - \nabla_\gamma q_\gamma. \end{aligned} \quad (4.45)$$

Only in this sense is Eq. (4.4) consistent with Eq. (4.5) as written, but it is for the internal energy and external potential energy taken together. Hence the balance equations of Rational Thermodynamics are not internally consistent for non-vanishing  $e_m$ , even though they implicitly account for it by incorporating a body force vector field into the linear momentum balance, Eq. (4.5).

The last expression, (4.42d), is an evolution equation for the conformation tensor field. When the extra stress tensor field of Eq. (4.43)

turns out to be linear in  $\mathbf{c}$ , Eq. (4.42d) can be rewritten as a constitutive equation for the extra stress tensor field of the form of those arising from kinetic theory models, as discussed above. By taking the time derivative of the thermodynamic potential,  $s(\mathbf{r}, t) = s(\rho(\mathbf{r}, t), \epsilon(\mathbf{r}, t), \mathbf{c}(\mathbf{r}, t))$ , at a fixed spatial position,

$$\frac{\partial s}{\partial t} = \frac{\partial s}{\partial \rho} \frac{\partial \rho}{\partial t} + \frac{\partial s}{\partial \epsilon} \frac{\partial \epsilon}{\partial t} + \frac{\partial s}{\partial c_{\alpha\beta}} \frac{\partial c_{\alpha\beta}}{\partial t}, \quad (4.46)$$

one can also write down a field equation of change for the entropy density,

$$\begin{aligned} \frac{\partial s}{\partial t} = & -\nabla_{\beta}(s v_{\beta}) - \frac{1}{T} \nabla_{\alpha} q_{\alpha} + \frac{1}{T} Q_{\alpha\beta\gamma\epsilon} (\nabla_{\alpha} v_{\beta}) (\nabla_{\gamma} v_{\epsilon}) \\ & + \frac{2}{T} \Lambda_{\alpha\beta\gamma\epsilon} \frac{\partial e_m}{\partial c_{\alpha\beta}} z_{\gamma\epsilon} + \frac{1}{T} \Lambda_{\alpha\beta\gamma\epsilon} \frac{\partial e_m}{\partial c_{\alpha\beta}} \frac{\partial e_m}{\partial c_{\gamma\epsilon}} \\ & + \frac{1}{T} \Lambda_{\alpha\beta\gamma\epsilon} z_{\alpha\beta} z_{\gamma\epsilon}. \end{aligned} \quad (4.47)$$

Note that this expression is consistent with Eq. (4.3) if

$$\begin{aligned} \rho \sigma_s = & -\frac{1}{T^2} q_{\beta} \nabla_{\beta} T + \frac{1}{T} Q_{\alpha\beta\gamma\epsilon} (\nabla_{\alpha} v_{\beta}) (\nabla_{\gamma} v_{\epsilon}) + \frac{2}{T} \Lambda_{\alpha\beta\gamma\epsilon} \frac{\partial e_m}{\partial c_{\alpha\beta}} z_{\gamma\epsilon} \\ & + \frac{1}{T} \Lambda_{\alpha\beta\gamma\epsilon} \frac{\partial e_m}{\partial c_{\alpha\beta}} \frac{\partial e_m}{\partial c_{\gamma\epsilon}} + \frac{1}{T} \Lambda_{\alpha\beta\gamma\epsilon} z_{\alpha\beta} z_{\gamma\epsilon}. \end{aligned} \quad (4.48)$$

Nevertheless, Eq. (4.47) is a dependent equation, and nothing much is gained at present by writing and solving it. In prior works, writing down an entropy equation and identifying  $\sigma_s$  was very important because it allowed one to impose the second law of thermodynamics upon the entropy production rate to determine constraints upon the material parameters. In the approach advocated herein, however, the second law and its corresponding constraints manifest through the positive semi-definite criterion on the  $D$  matrix.

The set of partial differential equations derived above, together with the proper boundary and initial conditions, describes the non-isothermal flow of a compressible, viscoelastic liquid manifesting entropic and energetic elastic effects, viscous dissipation, and Fourier-type heat conduction. If one desires an explicit equation of change for the temperature, it is given by

$$\frac{\partial T}{\partial t} = \frac{\partial T}{\partial \rho} \frac{\partial \rho}{\partial t} + \frac{\partial T}{\partial \epsilon} \frac{\partial \epsilon}{\partial t} + \frac{\partial T}{\partial c_{\alpha\beta}} \frac{\partial c_{\alpha\beta}}{\partial t}, \quad (4.49)$$

where the partial time derivatives are substituted with Eqs. (4.42a), (4.42c), and (4.42d); however, it too is a moot expression as it is a dependent equation. One must still solve for the variable set  $x$  before evaluating Eq. (4.49). Consequently, one is better off just substituting the calculated values of  $x$  into  $T(\rho, \epsilon, \mathbf{c}) = \partial s / \partial \epsilon$ . Of course, this presumes that the potential  $s$  is a known function. Alternatively, one can take  $T$  instead of  $\epsilon$  as an independent variable. The advantage of this approach is that one knows more about the temperature dependence of the material properties than about their dependence on the internal energy.

Apparently, there is no thermodynamically consistent closed temperature equation of the form of Eq. (4.7), even when  $e_m = 0$ . There is essentially no mathematical reason to assume purely entropic elasticity given an arbitrary potential function  $s$ . If one inverts this potential to obtain an internal energy potential,  $\epsilon(\rho, s, \mathbf{c})$ , and then defines  $T = \partial \epsilon / \partial s = f(\rho, s, \mathbf{c})$ ,  $f$  can be inverted with respect to  $s$  to give an expression for  $f^{-1}(\rho, T, \mathbf{c})$ , which can be substituted into the potential  $\epsilon$  to give  $\rho u(\rho, T, \mathbf{c})$ . Now it is hard to accept that  $u$  loses all dependence on the variables  $\rho$  and  $\mathbf{c}$  in this process. For instance, the thermodynamic potential associated with Eq. (4.54) below does not seem to show any signs of this behavior. Consequently, the temperature equation (4.7) must be viewed as applicable only within the limitations imposed by the assumption of purely entropic elasticity.

In the lack of any explicit expressions for the entropic potential, one must ultimately resort to experimental evidence or molecular simulations to see whether or not the assumptions of purely entropic elasticity are valid. Astarita and Sarti [46] make a case for an experimental verification, but the results appear inconclusive, as mentioned above. If there is no explicit temperature equation, then one runs into the problem of specifying boundary conditions for solving the evolution equations of variable set  $x$ . Although boundary conditions in terms of the temperature are easily set, boundary conditions on the internal energy are more difficult to assign. Also, if one does not assume incompressibility, then one no longer has a Poisson equation for the pressure which can be solved simultaneously with the evolution equations for the variables  $\mathbf{v}$ ,  $\epsilon$ , and  $\mathbf{c}$ . The news is not all bad, however, as allowing for compressibility in the material has an important mathematical consequence in that it guarantees that the resulting evolution equation for the extra stress tensor (found by substituting Eq. (4.43) into Eq. (4.42d) when  $\sigma$  is lin-

ear in  $\mathbf{c}$ ) is always purely hyperbolic [126, 127], hence easing some of the difficulties experienced in numerical computations. Still, the best line of progress in the future seems to involve molecular simulations of both simple and viscoelastic fluids in order to determine, in some fashion, the functional forms of the entropic potentials. Once this is accomplished, and the thermodynamic potential is known, the temperature equation of (4.49) can be used after elimination of the variable  $\epsilon$  from the set of evolution equations for the variables  $\rho$ ,  $\mathbf{v}$ , and  $\mathbf{c}$ . Hence one is again allowed to specify boundary and initial conditions on the temperature as opposed to the internal energy density.

Since boundary and initial conditions for  $\epsilon$  are harder to specify than those for  $T$ , an explicit temperature equation of the form of Eq. (4.9) is very practical from a computational standpoint at present because it does not apparently require knowledge of the thermodynamic potential, provided that the heat capacity has been determined experimentally. This equation may then be solved along with the evolution equations for  $\rho$ ,  $\mathbf{c}$ , and  $\mathbf{v}$ , which form a closed set provided that the variable  $\epsilon$  can be eliminated everywhere in favor of  $\rho$ ,  $\mathbf{c}$ , and  $T$ . This independence of the set of evolution equations potential is illusory, however, except for incompressible fluids where the continuity equation is eliminated in favor of a Poisson equation for the pressure. The procedure of Peters [92], and implicitly that of Braun [91], is to take the time derivative of the potential  $\omega$ , (4.23):

$$\frac{\partial s}{\partial t} = \frac{\partial \omega}{\partial t} + \frac{\partial}{\partial t} \left( \frac{\partial s}{\partial \epsilon} \epsilon \right). \quad (4.50)$$

However, the time derivatives appearing in this expression are time derivatives at fixed spatial positions, as defined analogously to Eq. (4.46). Hence Eq. (4.50) yields nothing more than an identity. Assuming incompressibility, Peters takes  $\partial/\partial t$  as the material derivative,  $D/Dt$ . The quantity  $Ds/Dt$  is then set equal to the proper terms on the right-hand side of Eq. (4.47) and a temperature equation derived, in terms of our nomenclature, as

$$\begin{aligned} \rho c \frac{DT}{Dt} &= Q_{\alpha\beta\gamma\epsilon} (\nabla_\alpha v_\beta) (\nabla_\gamma v_\epsilon) - \nabla_\beta q_\beta + T \frac{\partial 2c_{\alpha\gamma} z_{\alpha\beta}}{\partial T} (\nabla_\gamma v_\beta) \\ &+ 2\Lambda_{\alpha\beta\gamma\epsilon} \frac{\partial e_m}{\partial c_{\alpha\beta}} z_{\gamma\epsilon} - \Lambda_{\alpha\beta\gamma\epsilon} \frac{\partial e_m}{\partial c_{\alpha\beta}} T \frac{\partial z_{\gamma\epsilon}}{\partial T} + \Lambda_{\alpha\beta\gamma\epsilon} z_{\alpha\beta} z_{\gamma\epsilon} \\ &- \Lambda_{\alpha\beta\gamma\epsilon} z_{\alpha\beta} T \frac{\partial z_{\gamma\epsilon}}{\partial T} + \Lambda_{\alpha\beta\gamma\epsilon} \frac{\partial e_m}{\partial c_{\alpha\beta}} \frac{\partial e_m}{\partial c_{\gamma\epsilon}}, \end{aligned} \quad (4.51)$$

where

$$\frac{\rho c}{T} = 2 \frac{\partial \omega}{\partial T} + T \frac{\partial^2 \omega}{\partial T^2}. \quad (4.52)$$

Setting  $e_m = 0$  gives an expression similar, but not identical, to Eqs. (4.8) and (4.9). The difference lies in the terms proportional to  $\Lambda$ , the relaxation matrix, which were not explicitly written down in [91], and the requirement of a closure approximation in [92] to produce a microstructural interpretation of the extra stress tensor field, thus allowing the derivative on the right-hand side of Eq. (4.9) to be evaluated.

One must realize, however, that the temperature equation given above is mathematically restricted to incompressible materials in order to obtain a closed set of evolution equations for the variables  $\mathbf{v}$ ,  $\mathbf{c}$ , and  $T$  without knowledge of the functional form of the potential  $\omega$ . (However, a sufficiently accurate experimental determination of  $c$  is required as well if  $\omega$  is unknown. The incompressibility assumption then allows one to evaluate the pressure from the corresponding Poisson equation without knowledge of  $\omega$ .) Consequently, caution must be exercised when employing temperature equations of the form of Eqs. (4.7), (4.9), and (4.51).

It should be possible to obtain from Eq. (4.50) a temperature equation for a compressible material, but  $\omega$  cannot be mathematically eliminated from it in the process, and therefore no practical advantages ensue other than replacing energy boundary/initial conditions with temperature ones. Since  $\omega$  cannot be mathematically eliminated from this equation, one has, in effect, Eq. (4.49). In order to eliminate effectively  $\omega$  from this equation *a posteriori*, one can define a thermodynamic function with respect to derivatives of the pressure, similarly to the heat capacity of Eq. (4.52). One can then use the temperature equation sans  $\omega$  after experimentally determining this additional thermodynamic function along with  $c$ . Unfortunately, this does not eliminate the pressure from the momentum equation, which implies that one must still know the potential  $\omega$  in order to solve the full system of evolution equations.

Problems also arise in the literature on account of poor bookkeeping. For instance, take  $\epsilon(\rho, s, \mathbf{c})$  as the thermodynamic potential. Defining  $T = \partial\epsilon/\partial s$ , one obtains a function for  $T = f(\rho, s, \mathbf{c})$ . Inverting this function, one can obtain a function for  $s = f^{-1}(\rho, T, \mathbf{c})$ , which can be substituted into  $\epsilon(\rho, s, \mathbf{c})$  to give  $\epsilon(\rho, f^{-1}(\rho, T, \mathbf{c}), \mathbf{c})$ , which then leads to  $\epsilon'(\rho, T, \mathbf{c})$ ; however,  $\epsilon$  and  $\epsilon'$  are two distinct functions. Indeed, defining the Helmholtz free energy density as the Legendre transformation of the

internal energy density,  $a = \epsilon - Ts$ , one finds that

$$\frac{\partial a}{\partial \mathbf{c}} = \frac{\partial \epsilon}{\partial \mathbf{c}} = \frac{\partial \epsilon'}{\partial \mathbf{c}} - \frac{\partial \epsilon'}{\partial f^{-1}} \frac{\partial f^{-1}}{\partial \mathbf{c}}. \quad (4.53)$$

One must always be careful to distinguish between  $\epsilon$  and  $\epsilon'$ , as well as their time derivatives and corresponding evolution equations.

## 4.4 Constitutive Equations for Non-isothermal Polymer Models

In order to apply Eqs. (4.42a)-(4.42d) to obtain models for specific polymeric materials, constitutive assumptions for the Massieu function of Eq. (4.23) have to be determined and the phenomenological coefficients,  $\mathbf{Q}$ ,  $\boldsymbol{\alpha}$ , and  $\mathbf{\Lambda}$  have to be specified. Doing thus results in a thermodynamically consistent set of evolution equations for the system variables, which may, in principle, be solved for a given process or flow field after specifying the proper boundary and initial conditions.

Several key examples of non-isothermal polymeric fluid models can be realized by taking the Massieu function of Eq. (4.23) as a sum of two contributions,

$$\omega(\rho, T, \mathbf{c}) = \omega_0(\rho, T) - \frac{1}{2T} \rho \alpha_1 K(T) \text{tr} \mathbf{c} + \frac{1}{2} \rho \alpha_1 k_B \ln(\det \mathbf{c}), \quad (4.54)$$

where  $\omega_0(\rho, T)$  is the contribution that is independent of the elasticity of the material, and the remaining terms represent the Boltzmann entropy of the microstructure [77, 94, 95, 2]. The parameter  $\alpha_1$  in the above equation is a measure of the degree of elasticity per unit mass of the polymeric fluid, which gives a quantitative measure of the strength of elastic forces per unit mass in the material. As an example, for a solution of dumbbells,  $\alpha_1$  is given by the number of dumbbells per unit volume divided by the mass density. It is taken herein as a material constant; *i. e.*, it is not a function of temperature. The spring constant,  $K$ , is taken as an arbitrary function of temperature. Note that, for this particular  $\omega$ , the pressure of Eq. (4.27) reduces to

$$p = T(\omega_0 - \rho \partial \omega_0 / \partial \rho). \quad (4.55)$$

The function  $e_m$  is taken as vanishing.

The matrix  $\boldsymbol{\alpha}$  in Eqs. (4.19) and Eq. (4.42c) is the thermal conductivity tensor of the polymeric fluid. It is, in principle, anisotropic, and assumes the most general form realizable through the Cayley/Hamilton theorem, Eq. (4.20) (with  $\mathbf{c} = \langle \mathbf{R}\mathbf{R} \rangle$ ), where the coefficients  $a_i$ ,  $i = 1, 2, 3$ , are taken as functions of  $\rho$ ,  $T$ , and the invariants of  $\mathbf{c}$ . For the models under consideration herein, a suitable choice of these coefficients would be to take  $a_1$  as the isotropic thermal conductivity,  $k$ ,  $a_2 = 3/2/m\rho\alpha_1\zeta k_B$  [122], where  $m$  is the mass of a dumbbell bead, and  $a_3 = 0$ . Of course, the most intuitive approach would be to treat these coefficients as parameters to be fit using experimental data, but given the problems associated with the necessary experiments described earlier and the possibility of a non-Fourier-type heat flux (which creates the additional problem of distinguishing non-conventional transport processes from the traditional ones), perhaps molecular simulations provide a more ready alternative.

The matrix  $\mathbf{Q}$  is also anisotropic in general. A sufficient condition for  $\mathbf{Q}$  to result in a materially objective extra stress tensor field is for  $\mathbf{Q}$  to be objective and for  $Q_{\alpha\beta\gamma\epsilon} = Q_{\alpha\beta\epsilon\gamma}$ . A general expression for  $\mathbf{Q}$  in terms of the stated variables is [2]

$$Q_{\alpha\beta\gamma\epsilon} = \eta(T)(\delta_{\alpha\gamma}\delta_{\beta\epsilon} + \delta_{\alpha\epsilon}\delta_{\beta\gamma}) + (\kappa(T) - 2/3\eta(T))\delta_{\alpha\beta}\delta_{\gamma\epsilon} + \text{H.O.T.}, \quad (4.56)$$

where the bulk ( $\kappa$ ) and shear ( $\eta$ ) viscosity coefficients now depend on temperature, and H.O.T. represents terms that are higher order in the conformation tensor, which are not required for the models described in the remainder of this article. Again, the extent and nature of these higher-order terms is dictated by the Cayley/Hamilton theorem, and an explicit expression may be found in [2]. An explicit temperature dependence of the viscosity parameters could be taken as an Arrhenius form, *e. g.*,

$$\eta(T) = \eta_0 \exp(A_0/k_B T), \quad (4.57)$$

where  $A_0$  is an activation energy.

### 4.4.1 The Non-isothermal Maxwell and Oldroyd-B Models

Given the above definitions, only the relaxation matrix,  $\mathbf{\Lambda}$ , remains to be specified to determine completely a viscoelastic fluid model. For



both the Maxwell and Oldroyd-B models, this matrix is that which generalizes the relaxation matrix corresponding to the isothermal upper-convected Maxwell model [125, 128, 2],

$$\Lambda_{\alpha\beta\gamma\epsilon} = \frac{1}{2\rho\alpha_1\lambda(T)K(T)}(c_{\alpha\gamma}\delta_{\beta\epsilon} + c_{\alpha\epsilon}\delta_{\beta\gamma} + \delta_{\alpha\gamma}c_{\beta\epsilon} + \delta_{\alpha\epsilon}c_{\beta\gamma}). \quad (4.58)$$

In this expression,  $\lambda$  is the relaxation time of the viscoelastic material, which is also dependent on the temperature. The system of evolution equations is then given by Eqs. (4.42a), (4.42b),

$$\frac{\partial\epsilon}{\partial t} = -\nabla_\gamma(\epsilon v_\gamma) - p\nabla_\gamma v_\gamma - \nabla_\gamma q_\gamma + \sigma_{\alpha\beta}\nabla_\alpha v_\beta, \quad (4.59)$$

$$c_{\alpha\beta}^{(c)} = -\frac{1}{\lambda(T)}c_{\alpha\beta} + \frac{k_B T}{\lambda(T)K(T)}\delta_{\alpha\beta}, \quad (4.60)$$

where  $\mathbf{c}^{(c)}$  is defined analogously to Eq. (4.14) and the extra stress tensor is given by

$$\sigma_{\alpha\beta} = \rho\alpha_1 K(T)c_{\alpha\beta} - \rho\alpha_1 k_B T \delta_{\alpha\beta} + Q_{\alpha\beta\gamma\epsilon}\nabla_\gamma v_\epsilon. \quad (4.61)$$

The Maxwell model results for  $\mathbf{Q} = \mathbf{0}$ , and the Oldroyd-B model for  $\mathbf{Q}$  as given by Eq. (4.56).

The linear expression for the extra stress tensor of Eq. (4.61) can be inverted and substituted into Eq. (4.60) to obtain an evolution equation for the extra stress tensor. Doing thus, there results

$$\lambda(T)\widehat{\sigma}_{\alpha\beta}^{(c)} + \left[1 - \lambda(T)\frac{D\ln K(T)}{Dt}\right]\sigma_{\alpha\beta} = \rho\alpha_1 k_B T \lambda(T) \left[2A_{\alpha\beta} + \left(\frac{D\ln K(T)}{Dt} - \frac{D\ln T}{Dt}\right)\delta_{\alpha\beta}\right]. \quad (4.62)$$

for the non-isothermal Maxwell model, and

$$\begin{aligned} \lambda(T)\widehat{\sigma}_{\alpha\beta}^{(c)} + \left[1 - \lambda(T)\frac{D\ln K(T)}{Dt}\right]\sigma_{\alpha\beta} = & \\ \rho\alpha_1 k_B T \lambda(T) \left[2A_{\alpha\beta} + \left(\frac{D\ln K(T)}{Dt} - \frac{D\ln(T)}{Dt}\right)\delta_{\alpha\beta}\right] & \\ + 2\eta(T)A_{\alpha\beta} + \tilde{\kappa}(T)A_{\epsilon\epsilon}\delta_{\alpha\beta} & \\ + 2\lambda(T)\eta(T)\widehat{A}_{\alpha\beta}^{(c)} + \lambda(T)\tilde{\kappa}(T)(A_{\epsilon\epsilon}\widehat{\delta}_{\alpha\beta})^{(c)} & \end{aligned}$$

$$\begin{aligned} & + 2\lambda(T)\frac{D\eta(T)}{Dt}A_{\alpha\beta} + \lambda(T)\frac{D\tilde{\kappa}(T)}{Dt}A_{\epsilon\epsilon}\delta_{\alpha\beta} \\ & - 2\lambda(T)\eta(T)\frac{D\ln K(T)}{Dt}A_{\alpha\beta} \\ & - \lambda(T)\tilde{\kappa}(T)\frac{D\ln K(T)}{Dt}A_{\epsilon\epsilon}\delta_{\alpha\beta}, \end{aligned} \quad (4.63)$$

for the non-isothermal Oldroyd-B model, with  $\widehat{\sigma}_{\alpha\beta}^{(c)}$  defined as  $\sigma_{\alpha\beta}^{(c)} + \sigma_{\alpha\beta}\nabla_\gamma v_\gamma$  and  $\tilde{\kappa}(T) = \kappa(T) - 2/3\eta(T)$ .

The first expression above corresponds to the constitutive expression of Bird, (4.15), provided that  $\rho\alpha_1 = n$ ,  $\lambda(T) = \zeta/4/K(T)$ , and that the fluid is taken as incompressible. If  $K(T)$  is taken as a linear function of temperature, according to Eq. (4.11), then the constitutive equation of Marrucci, (4.13), is obtained. The constitutive equation of Gupta and Metzner results from taking  $K(T)$  as expressed by Eqs. (4.11) and (4.16). A generalization of Eq. (4.62) in terms of multiple conformation tensor fields reproduces the result of Wiest [52]. Furthermore, Phan-Thien [129] has shown under what conditions this type of constitutive equations is consistent with the notion of time-temperature superposition. Eq. (4.63) represents the extension of the kinetic theory models to Jeffreys type fluids, which could not be addressed easily through a kinetic theory approach. It also goes beyond the Simple Fluid Theory discussed earlier.

Two points are now evident. First, these evolution equations for the extra stress tensor field contain an additional term over the usual upper-convected derivative employed in engineering analyses. (Note that the first term on the right-hand side of Eqs. (4.62) and (4.63) is  $\widehat{\sigma}^{(c)}$  and not the usual  $\sigma^{(c)}$ .) Ergo, whether or not it is explicitly stated in these works, an incompressible fluid has been assumed. Indeed, in some it is explicitly stated that the fluid *is* compressible, at least slightly, leading to incorrect applications of the governing evolution equations, especially when one considers that the additional term in the convected derivative actually has profound implications on the mathematical character of the constitutive equation for the extra stress tensor field [127]. Second, by comparing Eqs. (4.60), (4.62), and (4.63), it is obvious that using the conformation tensor field as the system variable, as opposed to the extra stress tensor field, results in a much more natural and mathematically simpler set of evolution equations: time derivatives of the temperature appear explicitly in the constitutive equations for the extra stress tensor

field, but not in the evolution equations for  $\mathbf{c}$ . This simplicity of the conformation tensor field evolution equation carries over into the numerical solution of the equation set, and represents a key advantage of using the conformation tensor field as the appropriate system variable. Although, traditionally, the extra stress tensor field has been the variable of interest, since it was directly measurable, as optical experiments now begin to play the dominant role in rheological measurements it is more natural to use a structural variable which can be directly related to the measured optical quantities, such as birefringence and dichroism. Furthermore, as industry begins to model processes involving residual orientation and flow-induced crystallization of polymeric materials, a microstructural variable is a more natural choice than a kinematical one for quantifying the process dynamics. Furthermore, working on a purely macroscopic level in terms of a conformation tensor allows one to avoid making dubious closure approximations to obtain the constitutive equation for the extra stress tensor field, as in [92]. It is also no more difficult, and perhaps less so, to specify proper boundary and initial conditions on  $\mathbf{c}$  than on  $\boldsymbol{\sigma}$ . Hence any preference which one might have once had for writing constitutive equations for the extra stress tensor field instead of a microstructural variable field should have vanished.

The addition of a Newtonian viscosity contribution to the Maxwell Model to form the Oldroyd-B Model is a more important modification for non-isothermal polymeric materials than for isothermal ones because viscous heating can dominate elastic effects in typical processing operations [54, 109, 51, 110]. The elastic effects are reversible in nature: elongating the polymer chains results in a release of heat to the environment, but returning them to their initial configurations requires exactly as much heat as was originally given off. Viscous heat is irreversible; once generated, it is not absorbed by returning the material to its original configuration, but must be conducted or radiated from the system.

If one wants to assume incompressibility and to work in terms of the temperature variable and its explicit evolution equation, given the caveat mentioned earlier, Eq. (4.51) leads to

$$\begin{aligned} \rho c \frac{DT}{Dt} &= -\nabla_{\beta} q_{\beta} + \rho \alpha_1 T \frac{\partial K(T)}{\partial T} c_{\alpha\beta} A_{\alpha\beta} - \rho \alpha_1 k_B T \nabla_{\gamma} v_{\gamma} \\ &+ \frac{T^2}{2\lambda(T)K(T)} \left( \frac{\rho \alpha_1 K(T)^2}{T^2} c_{\gamma\gamma} - \frac{6\rho \alpha_1 k_B K(T)}{T} \right) \end{aligned}$$

$$\begin{aligned} &+ \rho \alpha_1 k_B^2 c_{\gamma\gamma}^{-1} \Big) \\ &- \frac{T^2}{2\lambda(T)K(T)} \left( \frac{\rho \alpha_1 K(T)}{T} \frac{\partial K(T)}{\partial T} c_{\gamma\gamma} - \frac{3\rho \alpha_1 k_B K(T)}{T} \right. \\ &\left. - 3\rho \alpha_1 k_B \frac{\partial K(T)}{\partial T} + \rho \alpha_1 k_B^2 c_{\gamma\gamma}^{-1} \right) \end{aligned} \quad (4.64)$$

for the Maxwell Model, and the same as above with the term

$$Q_{\alpha\beta\gamma\epsilon}(\nabla_{\alpha} v_{\beta})(\nabla_{\gamma} v_{\epsilon}) = 2\eta(T)A_{\alpha\beta}A_{\alpha\beta} + \tilde{\kappa}(T)A_{\gamma\gamma}A_{\epsilon\epsilon} \quad (4.65)$$

added to the right-hand side for the Oldroyd-B Model, after neglecting the higher-order terms in Eq. (4.56). Note that the Cayley-Hamilton theorem can be used to eliminate  $\mathbf{c}^{-1}$  from this equation,

$$c_{\zeta\zeta}^{-1} = \frac{1}{I_3}(c_{\zeta\epsilon}c_{\epsilon\zeta} - I_1c_{\zeta\zeta} + 3I_2), \quad (4.66)$$

with  $I_1 = \text{trc}$ ,  $I_2 = 1/2[(\text{trc})^2 - \text{tr}(\mathbf{c} \cdot \mathbf{c})]$ , and  $I_3 = \text{detc}$ , thus revealing a behavior which is higher-order in  $\mathbf{c}$ . The conformation tensor field can be eliminated from this equation in favor of  $\boldsymbol{\sigma}$ , so that one has the variable set  $[\mathbf{v}, \boldsymbol{\sigma}, T]$  to solve for, subject to the proper Poisson equation for the pressure; however, given the forms of the constitutive equations for the extra stress tensor field, Eqs. (4.62) and (4.63), solving in terms of the variable set  $[\mathbf{v}, \mathbf{c}, T]$  is clearly preferred for the reasons discussed above.

An interesting point is that the heat capacity of Eq. (4.64) is given by Eq. (4.52). For the potential of Eq. (4.54), this amounts to

$$\begin{aligned} c &= \frac{T}{\rho} \left( 2 \frac{\partial \omega_0}{\partial T} + T \frac{\partial^2 \omega_0}{\partial T^2} \right) - \frac{1}{2} \alpha_1 T \text{trc} \frac{\partial^2 K(T)}{\partial T^2} \\ &\equiv c_0 - \frac{1}{2} \alpha_1 T \text{trc} \frac{\partial^2 K(T)}{\partial T^2}. \end{aligned} \quad (4.67)$$

Note that  $c$  reduces to  $c_0$  when  $K(T)$  is a linear function of  $T$ . When  $K(T)$  is nonlinear in  $T$ , if one wishes to solve the set of evolution equations using the temperature equation of (4.51) as one of its members, then one can take the experimentally measured heat capacity as  $c_0$  (cf. Chap. 6, p. 125). In this case Eq. (4.67) should be used in the calculations for nonlinear  $K(T)$ . It would be interesting to see a definitive set of experiments exploring the effects of deformation on the heat capacity of polymeric materials, as we are aware of none.

### 4.4.2 The Non-isothermal Giesekus Model

Another very popular isothermal viscoelastic constitutive equation is the Giesekus model [130]. This model considers a solution of Hookean dumbbells subject to an anisotropic mobility tensor,

$$\zeta_{\alpha\beta}^{-1} = \frac{1}{\zeta} \left[ (1 - \beta(T))\delta_{\alpha\beta} + \beta(T) \frac{K(T)}{k_B T} c_{\alpha\beta} \right], \quad (4.68)$$

where  $\beta(T)$  is an empirical, temperature dependent function. The condition  $0 \leq \beta(T) \leq 1$  enforces the stresses to decay upon a cessation of deformation and transfers directly from the isothermal case. The relaxation matrix,  $\mathbf{\Lambda}$ , for the Giesekus model is [131, 2]

$$\begin{aligned} \Lambda_{\alpha\beta\gamma\epsilon} &= \frac{1}{2\rho\alpha_1\lambda(T)K(T)} \times \\ &\times \left[ (1 - \beta(T))(c_{\alpha\gamma}\delta_{\beta\epsilon} + c_{\alpha\epsilon}\delta_{\beta\gamma} + c_{\beta\gamma}\delta_{\alpha\epsilon} + c_{\beta\epsilon}\delta_{\alpha\gamma}) \right. \\ &\left. + \frac{2\beta(T)K(T)}{k_B T} (c_{\alpha\gamma}c_{\beta\epsilon} + c_{\alpha\epsilon}c_{\beta\gamma}) \right]. \end{aligned} \quad (4.69)$$

The last term on the right hand side is a second-order correction to the Hookean dumbbell relaxation matrix, Eq. (4.58). Inserting this expression into the partial differential equation (4.42d),

$$\begin{aligned} c_{\alpha\beta}^{(c)} &= -\frac{1 - \beta(T)}{\lambda(T)} c_{\alpha\beta} + \frac{1 - \beta(T)}{\lambda(T)K(T)} k_B T \delta_{\alpha\beta} \\ &- \frac{2\rho\alpha_1\beta(T)K(T)^2}{k_B T} c_{\alpha\gamma}c_{\beta\gamma} + 2\rho\alpha_1\beta(T)K(T)c_{\alpha\beta}, \end{aligned} \quad (4.70)$$

and using the definition for the extra stress tensor field, Eq. (4.61) (with  $\mathbf{Q} = \mathbf{0}$ ), yields the non-isothermal generalization of the Giesekus model,

$$\begin{aligned} \lambda(T)\widehat{\sigma}_{\alpha\beta}^{(c)} + \sigma_{\alpha\beta} \left[ 1 - \lambda(T) \frac{D \ln K(T)}{Dt} \right] + \frac{\beta(T)}{\rho\alpha_1 k_B T} \sigma_{\alpha\epsilon} \sigma_{\epsilon\beta} = \\ \rho\alpha_1 k_B T \lambda(T) \left[ 2A_{\alpha\beta} + \left( \frac{D \ln K(T)}{Dt} - \frac{D \ln(T)}{Dt} \right) \delta_{\alpha\beta} \right]. \end{aligned} \quad (4.71)$$

Once again, we notice the complexity of this constitutive equation compared to the corresponding evolution equation for the conformation tensor field because of the appearance of the time derivatives of the temperature field in this expression.

### 4.4.3 The Non-isothermal FENE-P Model

The FENE-P model is another popular isothermal viscoelastic fluid constitutive equation. Here, the linearly elastic spring law in Eq. (4.54) is replaced by a nonlinear spring law [2],

$$\begin{aligned} \omega(\rho, T, \mathbf{c}) &= \omega_0(\rho, T) + \frac{1}{2T} \rho\alpha_1 K(T) b(T)^2 \ln \left( 1 - \frac{\text{tr } \mathbf{c}}{b(T)^2} \right) \\ &+ \frac{1}{2} \rho\alpha_1 k_B \ln(\det \mathbf{c}), \end{aligned} \quad (4.72)$$

where  $b(T)$  is the maximum allowable chain extension, which is taken as a temperature dependent parameter. The evolution equation for the conformation tensor is then

$$c_{\alpha\beta}^{(c)} = -\frac{1}{\lambda(T)} \left( \frac{b(T)^2}{b(T)^2 - \text{tr } \mathbf{c}} \right) c_{\alpha\beta} + \frac{k_B T}{\lambda(T)K(T)} \delta_{\alpha\beta}, \quad (4.73)$$

and the corresponding expression for the extra stress tensor field is

$$\sigma_{\alpha\beta} = \rho\alpha_1 K(T) \left( \frac{b(T)^2}{b(T)^2 - \text{tr } \mathbf{c}} \right) c_{\alpha\beta} - \rho\alpha_1 k_B T \delta_{\alpha\beta}. \quad (4.74)$$

Note that this expression is nonlinear in the conformation tensor, and hence it is difficult to invert this relationship to obtain a constitutive equation in terms of the extra stress tensor field.

### 4.4.4 The Non-isothermal Phan-Thien and Tanner Model

The Phan-Thien/Tanner model considers the dependence of the relaxation time on the internal microstructure of the fluid, and allows a slippage of the polymer chains with respect to the surrounding medium, often referred to as non-affine motion. For a general conformation tensor theory, what exactly is meant by non-affine motion depends critically on the exact interpretation of the conformation tensor. For instance, if one considers the conformation tensor as a contravariant deformation tensor, “non-affine motion” might be taken to mean a “slip” of the deformation tensor relative to the kinematical motion of the fluid particles; *i. e.*, the deformation of the material particle does not keep

up with that required by the particle convection. If the conformation tensor is taken as the second moment of the orientational distribution function of a solution of dumbbells, then “non-affine motion” may be taken to mean that the end-to-end orientation vector of the dumbbell does not convect directly with the local fluid particles.

Non-affine motion is accounted for in the metric matrix by considering couplings between the gradient of the momentum density,  $\nabla \mathbf{u}$ , and the entropic potential,  $\mathbf{z}$ , tensor fields, under the realization that these two fields have opposite parities [94, 132, 121, 2]; *i. e.*, they have opposite signs under a time inversion. This inversion is related to the properties of the microstructure of the material, and how the microstructural constituents are affected by suddenly reversing the direction of time – see [40] for further details. The gradient of the momentum density changes sign under this transformation, but the entropic potential does not. Hence the corresponding elements in the  $M$  matrix are actually antisymmetric instead of symmetric! This represents a departure from the properties of the GENERIC structure which have been considered thus far: only phenomena with like parities were considered [1]. However, this additional structural requirement for phenomena of opposite parities actually arises from a detailed statistical treatment of the system on a fine-grained level of description [133]. During a projection operator transformation to a more coarse-grained level of description, the parities of the processes involved survive without alteration. Consequently, the  $D$  matrix of Eq. (4.37) is supplemented by an *antisymmetric* contribution,

$$D = \begin{pmatrix} 0 & 0 & 0 & 0 \\ 0 & TQ_{\beta\alpha\gamma\epsilon} & 0 & TX_{\epsilon\gamma\beta\alpha} \\ 0 & 0 & T^2\alpha_{\alpha\beta} & 0 \\ 0 & -TX_{\alpha\beta\gamma\epsilon} & 0 & T\Lambda_{\rho\delta\gamma\epsilon} \end{pmatrix}. \quad (4.75)$$

This antisymmetric contribution may be an artifact of working on too coarse a level of description with too few degrees of freedom. In [132], such an antisymmetric contribution to the dissipative dynamics arose when passing from an inertial to a non-inertial system description. On a more detailed level of description, in terms of a larger number of degrees of freedom, it may turn out that  $D$  remains symmetric.

Taking the operator product of Eq. (4.36), the metric matrix turns out to be

$$M = \begin{pmatrix} 0 & 0 & 0 & 0 \\ 0 & -\nabla_\beta T Q_{\beta\alpha\gamma\epsilon} \nabla_\gamma & M_{23} & -\nabla_\beta X_{\epsilon\gamma\beta\alpha} T \\ 0 & M_{32} & M_{33} & M_{34} \\ 0 & -X_{\alpha\beta\gamma\epsilon} T \nabla_\gamma & M_{43} & T \Lambda_{\alpha\beta\eta\zeta} \end{pmatrix}, \quad (4.76)$$

with

$$M_{23} = \nabla_\beta T Q_{\beta\alpha\gamma\epsilon} (\nabla_\gamma v_\epsilon) + \nabla_\beta X_{\epsilon\gamma\beta\alpha} T \frac{\partial e_m}{\partial c_{\gamma\epsilon}}, \quad (4.77a)$$

$$M_{32} = -T (\nabla_\beta v_\alpha) Q_{\beta\alpha\gamma\epsilon} \nabla_\gamma + \frac{\partial e_m}{\partial c_{\alpha\beta}} X_{\alpha\beta\gamma\epsilon} T \nabla_\gamma, \quad (4.77b)$$

$$M_{34} = -T \frac{\partial e_m}{\partial c_{\rho\delta}} \Lambda_{\rho\delta\eta\zeta} - (\nabla_\beta v_\alpha) X_{\epsilon\gamma\beta\alpha} T, \quad (4.77c)$$

$$M_{43} = -T \Lambda_{\alpha\beta\gamma\epsilon} \frac{\partial e_m}{\partial c_{\gamma\epsilon}} + X_{\alpha\beta\gamma\epsilon} T (\nabla_\gamma v_\epsilon), \quad (4.77d)$$

and element  $M_{33}$  as given by Eq. (4.40b). Note that the additional terms do not contribute to the entropy production rate in the (3, 3) element of  $M$  (a known result for processes with opposite parities [40, 2]), and that the antisymmetry of  $M$  requires that  $X_{\alpha\beta\gamma\epsilon} = X_{\gamma\epsilon\alpha\beta}$ .

The non-isothermal Phan-Thien/Tanner model can now be obtained by setting  $e_m = 0$ ,  $\mathbf{Q} = \mathbf{0}$ , and using the Massieu function of Eq. (4.54), along with the phenomenological matrices [2],

$$X_{\alpha\beta\gamma\epsilon} = \frac{a(T) - 1}{2} (c_{\alpha\gamma} \delta_{\beta\epsilon} + c_{\alpha\epsilon} \delta_{\beta\gamma} + c_{\beta\gamma} \delta_{\alpha\epsilon} + c_{\beta\epsilon} \delta_{\alpha\gamma}), \quad (4.78)$$

$$\Lambda_{\alpha\beta\gamma\epsilon} = \frac{1}{2\rho\alpha_1\lambda(T)K(T)} \left( 1 + \frac{\epsilon}{a(T)} \frac{K(T)}{k_B T} c_{\delta\delta} - 3 \frac{\epsilon}{a(T)} \right) \times \\ \times (c_{\alpha\gamma} \delta_{\beta\epsilon} + c_{\alpha\epsilon} \delta_{\beta\gamma} + \delta_{\alpha\gamma} c_{\beta\epsilon} + \delta_{\alpha\epsilon} c_{\beta\gamma}). \quad (4.79)$$

The parameter  $a(T)$  lies in the range  $[-1, 1]$ , and characterizes the degree of non-affine polymer motion. It is a function of temperature since, in general, the non-affine motion varies with the rigidity of the polymer chains. One then obtains Eqs. (4.42a), (4.42b), (4.59), and

$$c_{\alpha\beta}^{(a)} \equiv \frac{\partial c_{\alpha\beta}}{\partial t} + v_\gamma \nabla_\gamma c_{\alpha\beta} - \frac{a(T) + 1}{2} (c_{\alpha\gamma} \nabla_\gamma v_\beta + c_{\beta\gamma} \nabla_\gamma v_\alpha) \\ - \frac{a(T) - 1}{2} (c_{\alpha\gamma} \nabla_\beta v_\gamma + c_{\beta\gamma} \nabla_\alpha v_\gamma) = -\Lambda_{\alpha\beta\gamma\epsilon} z_{\gamma\epsilon}, \quad (4.80)$$

with the extra stress tensor field given by

$$\sigma_{\alpha\beta} = 2c_{\beta\gamma}z_{\alpha\gamma} + X_{\alpha\beta\gamma\epsilon}z_{\gamma\epsilon}. \quad (4.81)$$

Again, the extra stress tensor field of Eq. (4.81) is linear in  $\mathbf{c}$ , so we may obtain an explicit constitutive equation for the stress tensor field,

$$\begin{aligned} & \lambda(T) \frac{1}{a(T)} \widehat{\sigma_{\alpha\beta}^{(a)}} + \frac{1}{a(T)} \sigma_{\alpha\beta} \times \\ & \times \left[ 1 + \frac{\epsilon}{a(T)^2 \rho \alpha_1 k_B T} \sigma_{\gamma\gamma} - \lambda(T) \left( \frac{D \ln a(T)}{Dt} + \frac{D \ln K(T)}{Dt} \right) \right] \\ & = \rho \alpha_1 k_B T \lambda(T) \\ & \times \left[ 2a(T) A_{\alpha\beta} + \left( \frac{D \ln K(T)}{Dt} - \frac{D \ln T}{Dt} \right) \delta_{\alpha\beta} \right], \end{aligned} \quad (4.82)$$

after taking  $\mathbf{\Lambda}$  in Eq. (4.80) as given by Eq. (4.58). This expression reduces to the isothermal Phan-Thien/Tanner model if temperature and density variations are absent. Eq. (4.82) is an extension of the constitutive equation of Sugeng *et al.*, Eq. (4.18), since the degree of non-affine motion,  $a(T) = (1 - \phi)$ , is an explicit function of temperature, the fluid is compressible, and  $K(T)$  is an arbitrary function of temperature.

## 4.5 Conclusions

In this chapter we have used a modern theoretical approach to non-equilibrium thermodynamics to derive a set of mechanically and thermodynamically consistent evolution equations for a non-isothermal polymeric liquid. This set of evolution equations for the system variables arises from a master equation for the system dynamics in which the basic principles of mechanics and thermodynamics are embedded *a priori*. This set of equations accounts for a compressible, viscoelastic fluid with energetic as well as entropic elasticity, viscous dissipation, Fourier-type heat conduction, and relaxation of the internal microstructure. In so doing, several inconsistencies and disadvantages of prior theoretical work on non-isothermal polymeric materials were revealed and discussed. In the presence of a non-vanishing elastic potential, the balance equations of Rational Thermodynamics were seen to be internally inconsistent. The temperature equation universally used in engineering analyses of

non-isothermal polymer flows was seen to rest on dubious assumptions. It was pointed out that the implicit assumption of incompressibility in prior theoretical work changes the mathematical character of the constitutive equation for the extra stress tensor field. The use of the conformation tensor field, instead of the extra stress tensor field, as one of the system variables results in a simpler set of evolution equations, with practical implications regarding its numerical solution in processing geometries. The set of evolution equations derived herein was shown to produce non-isothermal counterparts of several popular isothermal viscoelastic fluid models.

In the following Chaps. 5 and 6 we will compute numerical solutions of the time evolution equations derived in Chap. 4. In this context we focus on so called rheological flows. Furthermore, we will give a microscopic interpretation of the friction coefficients appearing in these time evolution equations. The rheological behaviour of amorphous polymers both in the liquid and in the solid state is a fascinating topic which has attracted many investigators, theoretical and experimental. For general reviews on rheology of liquids and solids the reader is referred to the standard textbooks in the field [26, 55, 56]. Theoretical developments in the field of rheology have a long history and are mainly directed towards the development of new constitutive equations for the extra stress tensor in the material, see *e. g.* [134, 135, 136, 137, 138, 139, 140, 60, 141]. In Chap. 4, [2, 24] it has been shown that a large number of such constitutive equations can be recast into modern formalisms of non-equilibrium thermodynamics. In these approaches the principles of classical mechanics and the laws of thermodynamics are embedded *a priori*. This ensures the thermodynamic admissibility and mechanical consistency of the evolution equations. Experimental progress in rheology is mainly concerned with the construction and development of new rheometers to measure the viscosity as a function of the applied deformation, *e. g.* [142, 143, 144, 145]. However the application of rheoptics is becoming more important, *e. g.* [57, 58, 59, 146]. This method allows to understand the mechanical properties of complex materials via an optical investigation of the internal microstructure. This is interesting because these methods are faster and cheaper than the conventional mechanical measurements. Furthermore, optical measurements can be used in arbitrary deformations of the material which is not the case for mechanical measurements which are performed in pure shear or pure elongational deformations only. This is of importance in process-

ing and engineering because the product control by means of optical methods may be cheaper and perhaps more reliable than mechanical quality checks. In what follows we discuss the rheology of amorphous polymers for homogenous deformations adopting the continuum mechanics description of Chap. 4. To apply this description to a specific material, constitutive relationships for the material's free energy and the phenomenological matrices have to be adopted. Our approach allows the prediction of rheological as well as rheoptical behaviour of the amorphous material. Furthermore, a large class of well established constitutive equations in polymer rheology is treated in a unique manner. We have focussed on isothermal and incompressible viscoelastic materials in Chap. 5. In this case the rheological spring constant of the material is a linear function of temperature and the phenomenological coefficients which appear in the material description are assumed to be independent of temperature. Thus the polymer is viewed as a material of purely entropic elasticity and the extra stress tensor is a linear function of temperature. In Chap. 6 we discuss non-isothermal and compressible viscoelastic materials.

## Chapter 5

# Enhanced Constitutive Models for Polymer Melts and Microscopic Interpretation of the Phenomenological Coefficients

### Abstract

In the present chapter an alternative representation of the enhanced viscoelastic fluid models in terms of the conformation tensor is introduced. We show the equivalence of this representation with the originally proposed formulation in terms of the extra stress tensor. Furthermore, we give a microscopic interpretation of the phenomenological coefficients appearing in these models and we explain how they may be obtained from atomistic simulations.

## 5.1 Introduction

Recently the performance of enhanced constitutive models for isothermal and incompressible polymer melts in a cross-slot flow has been discussed intensively. In this analysis a continuum formulation in terms of the extra stress tensor has been adopted to discuss and to evaluate a new class of viscoelastic fluid models of differential type (the so called fixed viscosity or Feta-models) and to compare the predictions with the Giesekus and the PTT model [60]. At the same time it has become possible to generate relaxed configurations of unstrained and strained atomistic polymer melts via Monte Carlo (MC) simulations [22] and to employ molecular dynamics (MD) simulations [23] to extract friction coefficients, relaxation times, and viscosities from the atomistic polymer melts. This is an important point since it allows to study, to test, and to develop new phenomenological relationships in polymer rheology. Up to now only the unstrained MC configurations have been subjected to MD simulations but a similar procedure should also be possible for strained MC configurations. Thus, additional phenomenological parameters appearing in the constitutive relationships may be determined by projection of the atomistic simulations onto the phenomenological relationships, similar as in [23]. As a first step in this direction we give an alternative presentation of the recently proposed enhanced constitutive models for polymer melts in terms of a conformation tensor to have a link between atomistic simulations and macroscopic material properties. This is reasonable since in atomistic simulations the conformation of the polymers can be extracted at once but it is more difficult to obtain the extra stress from such simulations [22, Figs. 15, 16].

Recent studies in non-equilibrium thermodynamics [2, 24] of complex materials have shown how to relate the polymer's conformation to the purely mechanical extra stress tensor from which the material functions (viscosities and normal stress coefficients) can be extracted. In these studies it has been shown that one has to solve a time evolution equation for the conformation tensor to recover the transient and the static system response to homogenous deformations. The extra stress tensor and the viscometric functions are calculated *a posteriori* from the thermodynamic properties of the fluid: the density, temperature and conformation tensor. In what follows we present an alternative approach to enhanced constitutive models based on a conformation tensor description. Furthermore, we give a microscopic interpretation of

the phenomenological coefficients which appear in these fluid models and we suggest how these quantities may be extracted from atomistic simulations of polymer melts. The fact that we can relate the phenomenological material parameter to the internal microstructure of the melt represents an important advantage of the conformation tensor over the traditional extra stress description. Another point in favour of the conformation tensor approach is the full thermodynamic consistency of the evolution equations. Moreover, using the conformation tensor avoids numerical instabilities which are encountered in viscoelastic fluid models with a deformation dependent relaxation time when working in terms of the extra stress tensor [147].

The present chapter is organized as follows. In Sec. 5.2 we present the time evolution equation for the conformation tensor and the we explain how the extra stress is related to the thermodynamic potential of the material. In Sec. 5.3 we give the constitutive relations for the thermodynamic potential and the phenomenological matrices for rotational diffusivity and non-affine motion. With the conformation tensor equation and the constitutive assumptions we recover the modified upper convected Maxwell models (Sec. 5.4). We discuss the phenomenological relationships for the variable relaxation time and we explain the main features of the enhanced viscoelastic fluid models. Sec. 5.5 deals with the interpretation of the phenomenological coefficients in terms of the material's microstructure. We introduce a mobility tensor to account for anisotropic drag and we give a relationship which relates the degree of non-affine motion to the conformation tensor. We discuss how the phenomenological relationships may be extracted from atomistic MD simulations. Conclusions and discussions are given in the final Sec. 5.6.

## 5.2 Conformation Tensor Formulation

To treat the rheology of amorphous polymeric materials we study the evolution equation for the conformation tensor equation [2, 24], Eqs. (4.42d), (4.80), pp. 79, 94

$$\begin{aligned} \frac{\partial c_{\alpha\beta}}{\partial t} &= -v_\gamma \nabla_\gamma c_{\alpha\beta} + c_{\gamma\alpha} \nabla_\gamma v_\beta + c_{\gamma\beta} \nabla_\gamma v_\alpha - X_{\alpha\beta\gamma\epsilon} \nabla_\gamma v_\epsilon \\ &\quad - \Lambda_{\alpha\beta\gamma\epsilon} z_{\gamma\epsilon}, \end{aligned} \quad (5.1)$$

for homogenous velocity gradients,  $\nabla \mathbf{v} = \text{const}$ . In the above equation<sup>1</sup>  $\mathbf{c}$  is the second rank contravariant conformation tensor,  $\mathbf{v}$  is the velocity,  $\mathbf{X}$  characterizes the degree of non-affine motion, and  $\mathbf{\Lambda}$  is the rotational viscosity. The orientational field

$$\mathbf{z} = -T \left. \frac{\partial \omega_1}{\partial \mathbf{c}} \right|_{\rho, T}, \quad (5.2)$$

is defined in terms of the thermodynamic potential,  $\omega_1 \equiv \omega_1(\rho, T, \mathbf{c})$ , depending on density  $\rho$ , temperature  $T$ , and conformation  $\mathbf{c}$  (Eqs. (4.22), (4.26) pp. 75, 75). Here we are using the Massieu function as a thermodynamic potential since it depends on measurable variables and it arises naturally from the Legendre transformation of the entropy density (generator in the GENERIC formalism [24]). With the specification of constitutive relationships for the Massieu function and the phenomenological matrices the recently proposed viscoelastic fluid models in Ref. [60] may be recovered as we will show in Sec. 5.4. The conformation tensor is the second moment of the end-to-end vector of the polymer chains,  $\mathbf{c} = \langle \mathbf{R}\mathbf{R} \rangle$ . Hence it describes the elongation and the orientation of the polymer coils in the material. If the chain ends are taken as the material points representing the polymer in a continuum formulation, and these points are envisioned as undergoing an affine deformation described by the deformation gradient tensor  $\mathbf{F}$ , one can readily show that  $\mathbf{c} = \mathbf{F} \cdot \mathbf{F}^T$  [22]. In this case  $\mathbf{c}$  may be interpreted as the elastic Cauchy tensor. The form of the extra stress tensor arises naturally through a systematic modeling approach in terms of the Hamiltonian framework [2] or the GENERIC formalism [24], Eq. (4.81), p. 95

$$\sigma_{\alpha\beta} = 2z_{\alpha\gamma} c_{\gamma\beta} + X_{\alpha\beta\gamma\epsilon} z_{\gamma\epsilon}, \quad (5.3)$$

where the first term is the elastic contribution to the extra stress tensor arising from the Poisson operator and the second term takes into account additional stresses due to slip of the material. This second term originates from the irreversible contribution to the overall dynamics. Note that here we are neglecting viscous dissipation of the deforming continuum (similar as in [60]) which can be easily incorporated into the analysis. The above Eq. (5.3) is an important relationship establishing the connection between the polymer conformation and the extra stress of the material. The viscometric functions, *i. e.* the viscosities and normal stress coefficients, are defined in the usual way in terms of

<sup>1</sup>In Eq. (5.1) and in what follows we adopt the Einstein summation convention.



the extra stress tensor. They are calculated from the thermodynamic properties of the melt (density, temperature, and conformation) and the relevant relaxation time after Eq. (5.1) for the conformation tensor has been solved for homogenous deformations. An important issue of the conformation tensor approach followed in this work is to guarantee the positive-definiteness of the internal variable,  $\mathbf{c}$  [2]. This allows to extract information from the underlying internal microstructure and to compute rheoptical properties of the deforming material. Furthermore, it gives a more natural interpretation of theoretical aspects concerning the relaxation-time/microstructure dependence as we will see in Sec. 5.5.

### 5.3 Constitutive assumptions

For the Massieu function we adopt the relationship for the Hookean dumbbell Eq. (4.54), p. 85. With the Massieu function (4.54) and the definition of the orientational field (5.2) we obtain

$$z_{\alpha\beta} = \frac{1}{2}\rho\alpha_1 K\delta_{\alpha\beta} - \frac{1}{2}\rho\alpha_1 k_B T c_{\alpha\beta}^{-1}. \quad (5.4)$$

This quantity is the thermodynamic conjugate variable to the extensive conformation tensor and may be viewed as an orienting field acting on the coils in the strained polymer melt. The conformation tensor,  $\mathbf{c}$ , and the orienting field,  $\mathbf{z}$ , are the appropriate thermodynamic variables to the description of complex fluids and they can be extracted from atomistic simulations of polymer melts to test and to improve constitutive relationships such as Eq. (4.54) [22, Figs. 8-10]. To recover the enhanced viscoelastic fluid models the phenomenological matrices for rotational diffusivity and non-affine motion are taken according to Eqs. (4.58), (4.78), pp. 87, 94. The relaxation time  $\lambda \equiv \lambda_0 \lambda(\text{trc})$  and the degree of non-affine motion  $-1 \leq a(\text{trc}) \leq 1$  are now functions of the first invariant of the conformation tensor. In the models discussed in [60], the parameter  $a = 1 - \xi$  characterizing the polymer slip has been assumed to be constant. This point will be addressed in Sec. 5.5. The relaxation matrix can be generalized to account for anisotropic drag (an important phenomenon in the realistic description of polymer melts) as we will discuss below. Inserting Eqs. (5.4), (4.78) into Eq. (5.3) we recover Eq. (4.81), p. 95 where the degree of non affine motion is allowed to be a function of the first invariant of the conformation tensor. Note that

the Hookean approximation gives a linear relationship between conformation tensor and extra stress tensor which can be inverted easily to express  $\lambda(\text{trc})$  in terms of the extra stress tensor.

Following [60] we collect some examples for the function  $\lambda(\text{tr}\boldsymbol{\sigma})$  in Tab. 5.1. In the first column we report the name of the viscoelastic constitutive equation. In the second column we give the functional form of the variable relaxation time in terms of the extra stress tensor.

**Table 5.1:** *The relaxation time as a function of the stress tensor for some viscoelastic fluid models (from Ref. [60]).*

Model	$\lambda(\text{tr}\boldsymbol{\sigma})$
Maxwell	1
PTT I	$\left(1 - \frac{\epsilon}{a^2 \rho \alpha_1 k_B T} \sigma_{\delta\delta}\right)^{-1}$
PTT II	$\exp\left[-\left(\frac{\epsilon}{a^2 \rho \alpha_1 k_B T} \sigma_{\delta\delta} - 3\frac{\epsilon}{a}\right)\right]$
Cox-Merz	$\left(1 - \frac{\epsilon}{a^2 \rho \alpha_1 k_B T} \sigma_{\delta\delta}\right)^{\frac{1}{2}}$
Ellis	$\left[1 + A \left(\frac{\epsilon}{a^2 \rho \alpha_1 k_B T} \sigma_{\delta\delta}\right)^{\bar{a}}\right]^{-b}$
Marrucci-a	$1 - \left(\frac{\epsilon}{a^2 \rho \alpha_1 k_B T} \sigma_{\delta\delta} - 3\frac{\epsilon}{a}\right)$

In Tab. 5.2, p. 105 the relaxation time functions are expressed in terms of the conformation tensor. In the expressions for the relaxation time functions the parameters  $a$ ,  $\epsilon$  denote the degree of non-affine motion and the strength of the material response on the conformation, respectively. The quantities  $A$ ,  $\bar{a}$ ,  $b$  are further numbers taken as fit parameters in [60]. The most simple case,  $\lambda(\text{trc}) = 1$ , corresponds to the linear viscoelastic Maxwell model (*cf.* Sec. 4.4.1, p. 86).

**Table 5.2:** *The relaxation time as a function of the conformation tensor for some viscoelastic fluid models.*

Model	$\lambda(\text{trc})$
Maxwell	1
PTT I	$\left(1 - \frac{\epsilon}{a} \frac{K}{k_B T} c_{\delta\delta} - 3 \frac{\epsilon}{a}\right)^{-1}$
PTT II	$\exp\left[-\left(\frac{\epsilon}{a} \frac{K}{k_B T} c_{\delta\delta} - 3 \frac{\epsilon}{a}\right)\right]$
Cox-Merz	$\left(1 + \frac{\epsilon}{a} \frac{K}{k_B T} c_{\delta\delta} - 3 \frac{\epsilon}{a}\right)^{\frac{1}{2}}$
Ellis	$\left[1 + A \left(\frac{\epsilon}{a} \frac{K}{k_B T} c_{\delta\delta} - 3 \frac{\epsilon}{a}\right)^{\tilde{a}}\right]^{-b}$
Marrucci-a	$1 - \left(\frac{\epsilon}{a} \frac{K}{k_B T} c_{\delta\delta} - 3 \frac{\epsilon}{a}\right)$

In the following Sec. 5.4 we want to discuss the stress tensor description of the viscoelastic fluid models reported in the above Tabs. 5.1, 5.2 to show the relation to Ref. [60]. Having established the equivalence between the two descriptions in terms of the mechanical stress tensor and the conformation tensor we discuss how the phenomenological coefficients appearing in the constitutive equations could be determined (Sec. 5.5).

## 5.4 Stress Tensor Formulation

With the constitutive assumption for the Massieu function (4.54) we obtained a linear relationship between the conformation tensor and the extra stress Eq. (4.81). With the relations for the phenomenological matrices (4.58), (4.78) we can write down the constitutive equation for

the modified upper convected Maxwell models [148]

$$\sigma_{\alpha\beta}^{(a)} + \frac{\sigma_{\alpha\beta}}{\lambda_0 \lambda(\text{tr}\boldsymbol{\sigma})} = \frac{2\eta}{\lambda_0 \lambda(\text{tr}\boldsymbol{\sigma})} A_{\alpha\beta}, \quad (5.5)$$

where  $\eta = a^2 \alpha_1 \rho k_B T \lambda_0$  is the zero shear viscosity,  $\mathbf{A} = 1/2 \cdot (\nabla \mathbf{v} + \nabla \mathbf{v}^T)$  is the symmetric part of the velocity gradient, and  $\lambda(\text{tr}\boldsymbol{\sigma})$  is any one of the functions in Tab. 5.1. In the limit of small deformations the above constitutive equations reduce to the linear viscoelastic Maxwell model. Note that the modified upper convected Maxwell models do not account for anisotropic drag; a point which is addressed in Sec. 5.5. Second normal stress differences arise from the Gordon Schowalter derivative in Eq. (5.5). We emphasize that working in terms of the conformation tensor is preferable since it avoids numerical instabilities as encountered, e. g., in the White Metzner models [147], another example of viscoelastic fluid models falling into the class of Eq. (5.5).

In Figs. 5.2 and 5.1, pp. 107, 108 we report the dependence of the relaxation time on  $\text{tr}\boldsymbol{\sigma}$  and  $\text{trc}$  to clarify the relationship between the extra stress description and the conformation tensor approach. We have taken  $a = 1$  for all curves. In Fig. 5.2a we portray the variable relaxation times of the models introduced in Tab. 5.1 as a function of the first invariant of the extra stress tensor. All curves start out at equilibrium, i. e.  $\text{tr}\boldsymbol{\sigma} = 0$ . The overall relaxation time,  $\lambda = \lambda_0 \lambda(\text{trc})$ , is equivalent to  $\lambda_0$  for small stress values and approaches zero as the extra stress tensor becomes very large, and hence a Newtonian constitutive assumption arises in this limit. In Fig. 5.2b we have drawn the stress dependence of the relaxation time for the Cox-Merz rule (*cf.* p. 109) and the modified Ellis model. This last model has been proposed as an approximation to the Cox-Merz rule to achieve numerical stabilization and to gain more flexibility in describing first normal stress differences [60]. The parameters  $A, \tilde{a}, b$  have been chosen equal to 2, 2, 1, respectively. For this value of  $b$  the Ellis model reduces to a modified Maxwell model [148] and  $\tilde{a}$  represents the sensitivity of the fluid relaxation time to increasing stress beyond a critical stress level [2]. In Fig. 5.1 we report the dependence of the relaxation time on the first invariant of the conformation tensor,  $\text{trc}$ . The curves start out at equilibrium,  $\text{trc} = 3$ , since in this state we have globular coils,  $\mathbf{c} = \boldsymbol{\delta}$ . Due to the linear relationship between conformation and extra stress the curves have been only shifted along the  $x$ -axis.

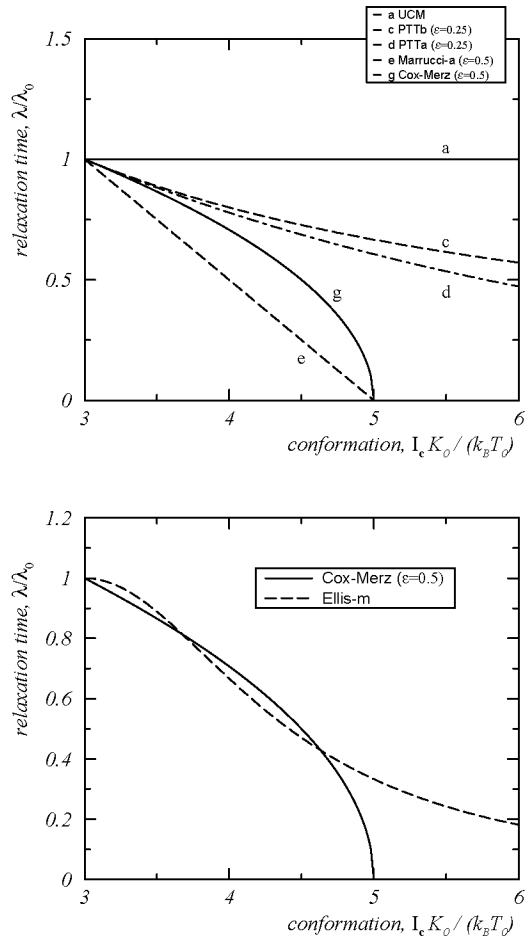


**Figure 5.1:** The dependence of the relaxation time,  $\lambda/\lambda_0$ , on the first invariant of the conformation tensor,  $I_c = \text{tr} \mathbf{c}$ , for some viscoelastic fluid models with variable relaxation time in Tab. 5.1 with  $a = 1$ . For the Ellis-m model we took  $A = 2$ ,  $\tilde{a} = 2$ ,  $b = 1$ .

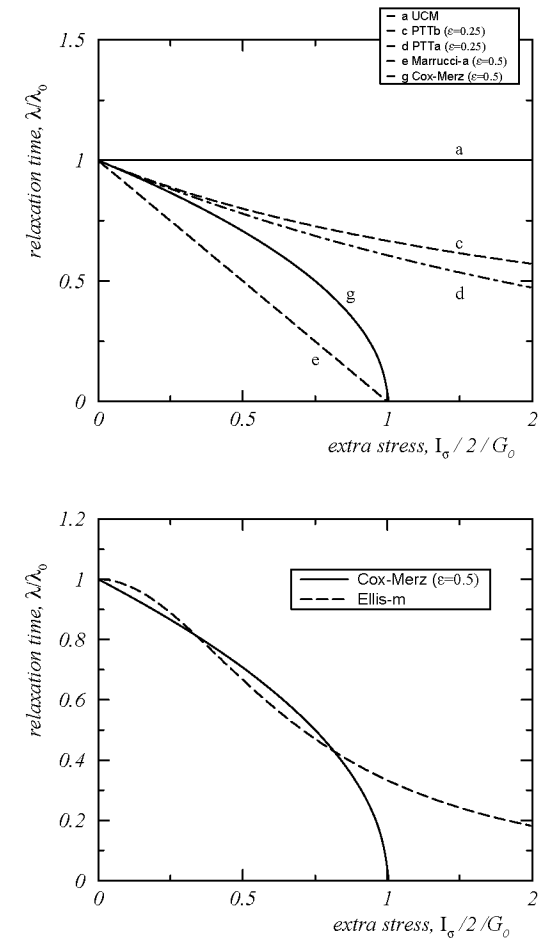


**Figure 5.2:** The same as Fig. 5.2 for the dependence of the relaxation time on the first invariant of the extra stress tensor,  $I_\sigma = \text{tr} \boldsymbol{\sigma}$  (Tab. 5.2).

The Cox-Merz rule (*cf.* p. 106) has been suggested as a way of obtaining an improved relation between the linear viscoelastic properties and the viscosity. This empiricism predicts that the magnitude of the complex viscosity is equal to the viscosity at corresponding values of frequency and shear rate  $\eta(\dot{\gamma}) = |\eta^*(\omega)|_{\omega=\dot{\gamma}}$  [142, p. 150]. Since we are not considering oscillatory shear flows in the present work we do not study the Cox Merz rule in more detail.

Fig. 5.3 shows the steady state viscosity for some of the viscoelastic fluid models Eqs. (5.1), (5.5) with  $\lambda(\text{tr}\epsilon)$ ,  $\lambda(\text{tr}\sigma)$  from Tabs. 5.2, 5.1. The material parameters  $a$ ,  $\epsilon$  are the same as in Figs. 5.2, 5.1. All models predict the so called shear thinning behaviour. A detailed presentation of viscoelastic material models in shear and elongational can be found in [26, 55, 56].

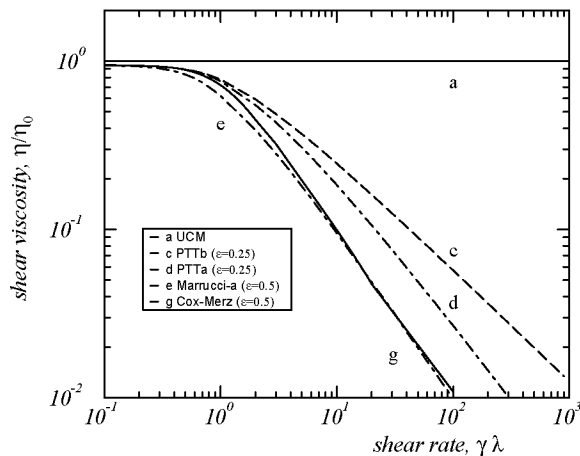


**Figure 5.3:** The nonlinear viscosity function for some viscoelastic fluid models with variable relaxation time. The parameters  $a$ ,  $\epsilon$  are the same as in Figs. 5.1, 5.2.

The modified Maxwell models (5.5) are equivalent to the enhanced viscoelastic fluid models (Feta) models [60, Eq. (34)]. In addition to the variable relaxation time  $\lambda(\text{tr}\sigma)$  also the elastic modulus,  $G(\text{tr}\sigma)$ , is

taken to be deformation dependent in these models

$$\eta(\text{tr}\sigma) = \lambda(\text{tr}\sigma)G(\text{tr}\sigma), \quad (5.6)$$

where  $\eta(\text{tr}\sigma)$  denotes the nonlinear steady state shear viscosity function. The quantity  $\eta(\text{tr}\sigma)$  is chosen in such a way to have an accurate description of the steady state non-linear shear viscosity. The functional dependence of both  $\lambda(\text{tr}\sigma)$  and  $G(\text{tr}\sigma)$  is arbitrary as long as the product of both quantities satisfies the above requirement. This allows for a saver numerical treatment of the equations and gives more flexibility in describing first normal stress differences. The reason for this is that a single power-law exponent cannot accurately describe the shear rate dependency of both the shear viscosity and first normal stress difference and, in practice, different functionalities have been used for the viscosity and the elastic modulus. This is similar to an approach followed by Deiber and Schowalter where different functionalities have been used for the viscosity and the relaxation time [149, 147]. A drawback of the examples treated thus far in [60] is that the second normal stress differences are zero [60, p. 401].

## 5.5 Determination of Phenomenological Coefficients

### 5.5.1 Bead-Friction Coefficient, Relaxation Times, and Viscosity

In the phenomenological matrices Eqs. (4.58), (4.78) there are several quantities which are material dependent and which have to be determined from atomistic simulations of polymer melts to gain a reliable prediction of the material's macroscopic properties. These quantities include the relaxation time,  $\lambda_0$ , the characteristic spring constant,  $K$ , the degree of non-affine motion,  $a$ , and the strength of the material's response on the conformation,  $\epsilon$ . A further phenomenological coefficient,  $\beta_\zeta$ , is introduced into the fundamental time evolution equation (5.1) if we take into account the phenomenon of anisotropic drag. To determine these phenomenological coefficients we can benefit from the conformation tensor description introduced in Sec. 5.2 and to use it in combination with MC and MD simulations. The conformation of the

polymers can be easily extracted from these simulations and it can be studied as a function of the other thermodynamic properties of the melt [22]. This allows to test and to determine new constitutive relations for the phenomenological coefficients. The mesoscopic bead friction coefficient,  $\zeta$ , and the relaxation time,  $\lambda_0$ , appearing in Eq. (4.58) have been determined from MD simulations of relaxed MC configurations of unstrained and unentangled atomistic polymer melts invoking the Rouse model [23]. The characteristic elastic constant,  $K$ , in Eq. (4.58) is proportional to the inverse mean squared end-to-end distance of the polymer chains and it has been calculated from the RIS models. Furthermore, it can be extracted from bulk MD runs, from end-bridging MC runs, or from MC sampling of continuous unperturbed chains (CUC) and the different results may be compared [23].

### 5.5.2 Isotropic and Anisotropic Drag Coefficient

The relaxation matrix (4.58) does not take into account the phenomenon of anisotropic drag which is necessary for a realistic description of the physical properties of a polymer melt. This effect occurs due to the alteration in the flow field that one monomer in the chain feels due to the motion of the other monomers [16]. In a similar spirit to the concept of hydrodynamic interaction the Giesekus model takes into account the effect on a given polymer chain (represented as a dumbbell) due to the presence of the confining interactions with the other chains. This effect is modeled by introducing an anisotropic hydrodynamic drag force under flowing conditions. Thus, a new phenomenon is added to relaxation matrix (4.58) discussed above, namely, that the surrounding, flow oriented chains in the melt would create this anisotropy in the effective molecular drag. According to this postulate, the usually constant, inverse hydrodynamic drag coefficient in kinetic theory which is basically inversely proportional to the relaxation time, is replaced with an anisotropic, conformation-dependent “mobility tensor”

$$\zeta_{\alpha\beta}^{-1} = \frac{1}{\zeta} \left( (1 - \beta_\zeta) \delta_{\alpha\beta} + \beta_\zeta \frac{K}{k_B T} c_{\alpha\beta} \right), \quad (5.7)$$

where  $\beta_\zeta$  is an empirical constant which lies within the range of  $0 \leq \beta_\zeta \leq 1$  [2, 24]. The dependence on the conformation tensor is necessary in order for the mobility tensor to become isotropic (*i. e.* proportional to the identity tensor) at equilibrium, since there is no preferred direction

of orientation under quiescent conditions. The scalar drag coefficient,  $\zeta$ , is known from MD simulations of detailed atomistic PE melts and it is independent of chain length beyond a chain length of  $N \approx 70$  [23]. It would be interesting to do a similar analysis with an oriented polymer melt invoking the relation for the anisotropic drag (5.7) and to verify if the value  $\beta_\zeta \approx 0.2 - 0.3$  [60] may be recovered.

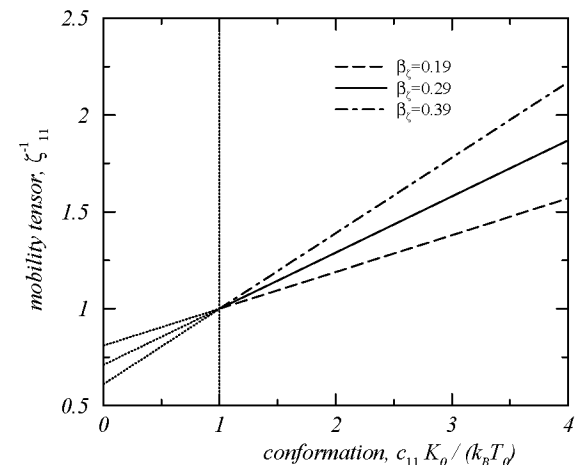


**Figure 5.4:** The 11-component of the mobility tensor,  $\zeta^{-1}$ , as a function of the 11-component of the dimensionless conformation tensor,  $\tilde{c}_{11}$ , for several values of the phenomenological Giesekus parameter,  $\beta_\zeta$ , according to Eq. (5.7). This situation corresponds to a purely diagonal conformation tensor as encountered in elongational flow. The curves have been extrapolated to  $\tilde{c}_{11} = 0$ .

For a purely diagonal orientational field,  $\mathbf{z}$ , corresponding to an uniaxial elongation we have plotted the relationship between the 11-component of the mobility tensor and the 11-component of the conformation tensor for several values of the Giesekus parameter,  $\beta_\zeta$ , (Fig. 5.4). The curves start out at  $\tilde{c}_{11} = 1$  and have been extrapolated to  $\tilde{c}_{11} = 0$ . The phenomenological parameter  $\beta_\zeta$  may be obtained from the intersection of the MD simulation data with the  $x$ -axis or from their slope.

The relaxation matrix for the Giesekus model is obtained with the constitutive relation for the anisotropic drag (5.7)

$$\Lambda_{\alpha\beta\gamma\epsilon} = \frac{1}{2\rho\alpha_1\lambda_0\lambda(\mathbf{c})K} \left[ (1 - \beta_\zeta)(c_{\alpha\gamma}\delta_{\beta\epsilon} + c_{\alpha\epsilon}\delta_{\beta\gamma} + c_{\beta\gamma}\delta_{\alpha\epsilon} + c_{\beta\epsilon}\delta_{\alpha\gamma}) + \frac{2\beta_\zeta K}{k_B T} (c_{\alpha\gamma}c_{\beta\epsilon} + c_{\alpha\epsilon}c_{\beta\gamma}) \right], \quad (5.8)$$

which has a similar form to the relaxation matrix associated with the hydrodynamic interaction [2, p. 251]. It may be used with the conformation tensor equation (5.1) to study further viscoelastic fluid models.

Next we want to discuss another possibility to describe second normal stress coefficients in polymer melts, *i. e.* we want to study non affine motion.

### 5.5.3 Degree of Non-affine Motion and Strength of Material Response

In the examples discussed in [60], the parameter  $a$  characterizing the degree of non-affine motion in the phenomenological matrix (4.78) has been assumed to be constant. However, the polymer molecule's rigidity/aspect ratio varies strongly with deformation, which implies that a variable parameter  $a$  might be a more appropriate choice. In fact Hinch [150] and Rallison and Hinch [151] have proposed models based on a modification of the FENE dumbbell model which utilizes a mixed convected derivative with the parameter  $a$  given as [151]

$$a = \frac{\text{trc}}{\beta_a R_G^2 + \text{trc}}, \quad (5.9)$$

where  $\beta_a$  is a numerical factor of the order of unity and  $R_G$  is the undistorted radius of gyration of the chain. Similar as with the end-to-end distance it may be obtained from the RIS models, from bulk MD runs, from end-bridging MC runs or from MC sampling of CUCs [23]. In Fig. 5.5 we portray the degree of non-affine motion as a function of the first invariant of the conformation tensor,  $\text{trc} = I_c$ , for three different values of the parameter  $\beta_a$ . We took  $R_G^2 = 1/6 R^2 \equiv 1.145$  valid for long PE chains.

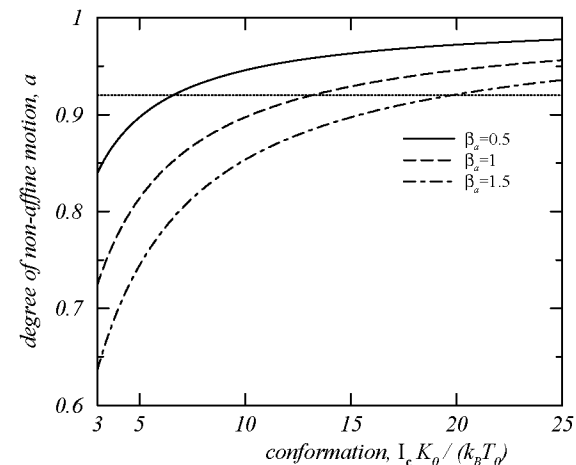


**Figure 5.5:** The dependence of the degree of non-affine motion,  $a$ , on the trace of the dimensionless conformation tensor,  $\text{trc}$ , for several values of the phenomenological coefficient  $\beta_a$  and  $R_G^2 = 1.145$  according to Eq. (5.9). The horizontal line,  $a = 0.92$ , is the constant value adopted in Ref. [60].

We notice that the polymer slip varies strongly with the conformation of the polymers as the deformation sets in. As the polymer coils are stretched and the trace of the conformation tensor increases the degree of non-affine approaches quickly the limiting value  $a = 1$ . Thus, a constant value for the degree of non-affine motion, *e. g.*  $a = 0.92$  [60], has to be viewed with scepticism especially if we are working in the nonlinear viscoelastic regime. Note that in simple shear the mixed convected derivative  $-1 < a < 1$  is characterized by a non-monotonic shear-stress versus shear rate behaviour. During the start-up of steady shearing one observes oscillations between large positive and negative values in the shear stress for high shear rates if that derivative is adopted. In a similar way as proposed for the constitutive relation for the anisotropic drag (5.7) the relation of Rallison and Hinch (5.9) could be invoked to determine a numerical value for the parameter  $\beta_a$ . The right hand side of Eq. (5.9) is obtained from the viscosity ratio of the strained and the unstrained polymer melt. Disposing of a relationship between

the degree of non-affine motion and the conformation tensor one can map the chain conformations and the relaxation times as obtained from MD simulations of strained configurations on one of the constitutive assumptions in Tab. 5.2 to determine the phenomenological parameter  $\epsilon$  governing the strength of the material's dependence on the polymer conformation.

## 5.6 Conclusions

In this chapter we have given an alternative approach to enhanced constitutive models for polymer melts in terms of the conformation tensor description. This is preferable over the traditional continuum approach in terms of the extra stress tensor because we have a direct link to the internal microstructure of the material's constituents and it allows to discuss rheoptical and mechanical properties independent from each other. Phenomenological coefficients arising from the dissipative contribution to the system dynamics can be extracted from atomistic simulations of the polymer melts. This is due to the fact that the conformation tensor can be readily obtained from atomistic simulations and the trajectories can be mapped on constitutive relationships of polymer rheology. We have presented such phenomenological relationships and we suggested possibilities to extract microscopic parameters from MD simulations of strained polymer melts.

The spring constant is related to the energetic elasticity of the polymer and it can be calculated directly in the framework of the RIS approximation. The relaxation times and the mesoscopic friction coefficient, may be obtained from atomistic configurations of the melt invoking the Rouse model or the reptation model depending whether we have an entangled or an unentangled melt. To determine the coefficient quantifying the strength of anisotropic drag in the melt MD runs of relaxed oriented configurations of the melt should be performed. The trajectories of these MD runs can be mapped on the Giesekus form of the anisotropic mobility tensor. A similar recipe may be appropriate to determine the Rallison/Hinch parameter quantifying the strength of non-affine motion in the system as a function of the polymer's aspect ratio.

## Chapter 6

# Rheology of Non-isothermal and Compressible Viscoelastic Materials

### Abstract

We present a numerical study of non-isothermal fiber spinning processes taking into account compressibility and energetic elasticity of the processed material. For the thermodynamic potential we adopt a combination of a FOV free energy and the thermodynamic potential of a Hookean dumbbell. The basic equations of motion arise from modern frameworks of non-equilibrium thermodynamics and are solved for homogenous deformations. We discuss the morphology and the physical and thermodynamic properties of the processed sample. Accounts on non-isothermal stress relaxation experiments and the problem of critical cooling are given.

## 6.1 Introduction

Non-isothermal rheology [61, 62, 57, 63], *i. e.* the rheological response in the presence of changing temperature, is an important problem, both as a basic study in rheology and as an applied problem in polymer processing. Lots of basic work in rheology, both experimental and theoretical has dealt with isothermal flows, with the temperature held constant during any one measurement/calculation. However, it is well known that the final properties of a finished article are strongly dependent on the details of the processing operation as defined by the deformation and thermal histories of the processed material. In what follows we discuss the rheological response of a deformed amorphous polymer which is simultaneously quenched to a temperature slightly above the glass temperature. We will study the macroscopic deformation, the internal structure, and the thermodynamic properties of the sample during the process and we will show how different processing conditions influence the physical state and the internal microstructure (morphology) of the final article thus produced. The study of this work applies especially to homopolymers<sup>1</sup> since they tend to be most clearly in one state or another (*e. g.* viscous, rubberlike, or glassy) and are thus suitable candidates for our study.

In this work we start from a full set of time evolution equations for non-isothermal polymeric materials with entropic and energetic elasticity as obtained from a general framework of non-equilibrium thermodynamics [2, 24], Chap. 4. This is preferable over traditional modeling procedures which combine balance equations for the density, the momentum, and the internal energy with a constitutive equation for the extra stress, *e. g.* [115, 48, 49, 152, 153], because it ensures the thermodynamic consistency of the evolution equations and it allows to extract information on the internal microstructure (morphology) of the material. The problem is quite complicated since besides non-isothermal effects and entropic elasticity we have to take into account compressibility and energetic elasticity of the processed polymer. This is important since density variations about 10% are not unusual in polymers and can be even higher when phase transitions are involved. In addition to that small density variations have a dramatic effect on the relaxation time spectrum [20, 21, 154]. We take into account energetic elasticity

<sup>1</sup>A polymer which is derived from a single monomer is called a homopolymer.



of the material since the Theory of Purely Entropic Elasticity [43, 44], Sec. 4.2.4 is not adequate to capture the complicated frictional behaviour of polymeric materials [46, 14]. In principle, energetic elasticity accounts for the relative spatial position of the material's constituents and models of Physical Chemistry [10, 11, 83] have to be adapted to capture the thermally induced energetic effects present in polymeric materials. However, it is worth doing so since there are only few studies in polymer rheology considering explicitly energetic elasticity of the material [48, 49]. Finally we adopt a thermal and a caloric equation of state of the quiescent material to include the  $\rho pT$ -behaviour and the heat capacity into our treatment [8, 9, 5, 7, 78]. This is important since the  $\rho pT$ -behaviour is related to important material properties as the sound velocity and the thermal expansion of the material and compression work is done against the pressure of the material.

Our theoretical analysis may be relevant in the context of property enhancement by molecular orientation. It is well known that temperatures not too far above the glass temperature are the best ones for inducing high levels of orientation by macroscopic deformation of the material. At more elevated temperatures the relaxation processes are too fast, and at temperatures very near to the glass temperature the sample can fail by brittle fracture if it is deformed. One is thus motivated to seek out the best temperature and deformation strategies in a temperature regime somewhat above the glass temperature. In experimental studies substantially higher stresses could be achieved under non-isothermal conditions. However, in many cases it proved difficult to extract the samples from the oven in their highly stressed states; the processed material showed a so called glassy response. In the cases where it was possible to conserve the highly oriented state stresses about 40% higher than in the isothermal runs were achieved [57]. Here we want to study incompressible and compressible processes where the material is simultaneously deformed and quenched from the rubbery state, thereby freezing in high levels of molecular orientation. Our theoretical analysis shows that it should be possible to conserve the high orientation induced by such a process.

In Sec. 6.2 we present the equations of motion for a non-isothermal and compressible amorphous polymer with entropic and energetic elasticity and we give the definition of the pressure, the heat capacity, and the orientational field in terms of the thermodynamic potential. Fur-

thermore, we define the material properties needed for the subsequent sections. Sec. 6.3 is devoted to the constitutive relations we need to solve the equations of motion. We take a thermodynamic potential for the polymer, we write down the constitutive relations for the phenomenological matrices, and we give phenomenological relations for the temperature dependence of the relaxation time we use in our calculations. In Sec. 6.4 we give a treatment of some aspects of non-isothermal rheology. A short account on non-isothermal stress relaxation experiments is given. Furthermore, we discuss an alternative non-isothermal fiber spinning process to produce highly oriented glassy fibers and we look at a deformation process with small simultaneous compression. Finally, we give a short treatment of the problem of critical cooling rates. Numerical examples appropriate to PE are given. In the final Sec. 6.5 we present conclusions and we give an outlook.

## 6.2 General Relationships

### 6.2.1 Non-isothermal Rheology of Viscoelastic Materials

In the framework of non-isothermal rheology we study the evolution equations [24] for the density,  $\rho$ , the temperature,  $T$ , and the elastic Cauchy tensor,  $\mathbf{c}$ ,

$$\frac{\partial \rho}{\partial t} = -\nabla_{\gamma}(\rho v_{\gamma}), \quad (6.1)$$

$$\rho c \frac{DT}{Dt} = Q_{\alpha\beta\gamma\epsilon}(\nabla_{\alpha} v_{\beta})(\nabla_{\gamma} v_{\epsilon}) + \rho c R + T \frac{\partial 2c_{\alpha\gamma} z_{\alpha\beta}}{\partial T} (\nabla_{\gamma} v_{\beta}) - T \frac{\partial p}{\partial T} \nabla_{\gamma} v_{\gamma} + \Lambda_{\alpha\beta\gamma\epsilon} z_{\alpha\beta} z_{\gamma\epsilon} - \Lambda_{\alpha\beta\gamma\epsilon} z_{\alpha\beta} T \frac{\partial z_{\gamma\epsilon}}{\partial T}, \quad (6.2)$$

$$\frac{\partial c_{\alpha\beta}}{\partial t} = -v_{\gamma} \nabla_{\gamma} c_{\alpha\beta} + c_{\gamma\alpha} \nabla_{\gamma} v_{\beta} + c_{\gamma\beta} \nabla_{\gamma} v_{\alpha} - \Lambda_{\alpha\beta\gamma\epsilon} z_{\gamma\epsilon}. \quad (6.3)$$

Eq. (6.1) is the ordinary continuity equation. Eq. (6.2) is the temperature equation for a compressible material with entropic and energetic elasticity. In that equation  $D/Dt$  is the material time derivative,  $R$  is a time dependent external cooling rate of units temperature/time and  $\mathbf{Q}$ ,  $\mathbf{\Lambda}$  denote the phenomenological matrices for viscous flow and rotational

diffusivity, respectively. In this equation we adopted a constitutive relation for the heat flux vector,  $\mathbf{q} = -1/3\rho c R \mathbf{r}$ . Furthermore, the field  $e_m$  (Eq. (4.34), p. 77), is taken to be independent of  $\mathbf{c}$ . All works on non-isothermal rheology using an external cooling rate in the temperature equation (e. g. [115, 49]) make use of a non-Fourier type heat flux without stating it explicitly (cf. Sec. 4.2.6, p. 72). The first term on the right hand side of Eq. (6.2) is the temperature rise due to viscous dissipation. The second, third, and fourth term describe temperature variations due to external heating or cooling, elastic stresses, and compression/dilatation of the material, respectively. Note that here the elastic contribution to the extra stress (third term) is allowed to be a nonlinear function of temperature. Hence we allow explicitly for energetic elasticity. The last two terms account for temperature variations due to relaxational phenomena. In the case of purely entropic elasticity this equation reduces to the temperature equation of Astarita [43], Eq. (4.7), p. 67. Eq. (6.3) is the conformation tensor equation describing the macroscopic state of deformation of the material. The first three terms on the right hand side arise from the (contravariant) codeformational derivative and the last term describes the relaxation of the internal microstructure. We left out the momentum equation (4.42b), p. 79 since it is satisfied for elongational flows taking an appropriate expression for the function  $e_m(\rho)$ . In the above equations the pressure, heat capacity, and orientational field are denoted with  $p$ ,  $c$ , and  $\mathbf{z}$ , respectively. These quantities are defined in terms of the Massieu function,  $\omega \equiv \omega(\rho, T, \mathbf{c})$  [24], Chaps. 2, 4. The form of the pressure

$$p = T \left( \omega - \rho \left. \frac{\partial \omega}{\partial \rho} \right|_{T, \mathbf{c}} \right), \quad (6.4)$$

arises naturally through the Poissonian structure of reversible dynamics as has been shown in the framework of the single generator Bracket formalism and the double generator GENERIC structure. The heat capacity is

$$\frac{\rho c}{T} = 2 \left. \frac{\partial \omega}{\partial T} \right|_{\rho, \mathbf{c}} + T \left. \frac{\partial^2 \omega}{\partial T^2} \right|_{\rho, \mathbf{c}}, \quad (6.5)$$

which can be recovered from the definition of the heat capacity in terms of the Helmholtz free energy using  $\omega \equiv -a/T$ . The orientational field is the conjugate variable to the conformation tensor

$$\mathbf{z} = -T \left. \frac{\partial \omega}{\partial \mathbf{c}} \right|_{\rho, T}, \quad (6.6)$$

and has dimensions force/length<sup>4</sup>. It can be regarded as the tensorial force density per unit length in the material. We designate the diagonal elements of  $\mathbf{z}$  as direct forces and the off-diagonal elements as shear forces in analogy to the elements of the extra stress tensor. Similar to the definition of the shear stresses  $z_{21}$  is the 1-component of the force density per unit length acting on a face of a cubical element which is perpendicular to the 2-direction.

The form of the extra stress tensor is recovered from a systematic modeling approach through the Bracket formalism or the GENERIC [2, 24]. It can be calculated a posteriori from the conformation tensor and the orientational field,

$$\sigma_{\alpha\beta} = 2z_{\alpha\gamma}c_{\gamma\beta} + Q_{\beta\alpha\gamma\epsilon}\nabla_{\gamma}v_{\epsilon}, \quad (6.7)$$

where the fourth order tensor  $\mathbf{Q}$  denotes the viscous contribution to the extra stress. Note that here we are disregarding effects of non-affine motion. Consideration of this effect leads to additional terms in the temperature equation (6.2), the equation of the elastic Cauchy tensor (6.3) and the definition of the extra stress tensor (6.7).

To quantify the material properties related to the basic equations of motion (6.1)-(6.3) we recall the definition of the viscosity, the orientation factor (related to the birefringence) and the tensorial force density in the deforming specimen.

## 6.2.2 Material Properties

Since we are studying mainly elongational deformations in this work it suffices to recall the material properties for this kind of flow. For uniaxial extensional flow the velocity gradient tensor has diagonal components,  $\dot{\epsilon}$ ,  $-\dot{\epsilon}/2$ ,  $-\dot{\epsilon}/2$ . The elongational viscosity is  $\eta_e = (\sigma_{11} - \sigma_{22})/\dot{\epsilon}$ , and the amorphous orientation factor is  $f = (|c_{11} - c_{22}|)/\text{trc}$  [146]. The force density in the spinline per unit length is identical to the orientational field, Eq. (6.6) and can be evaluated once a constitutive assumption for the Massieu function has been specified.

In the next section we will adopt constitutive relations for the Massieu function and the phenomenological matrices. Then we will study the above set of equations for homogenous deformations assuming adiabatic conditions.

## 6.3 Constitutive Assumptions

### 6.3.1 Thermodynamic Potential

The fundamental time evolution equations for the polymeric material (6.1)-(6.3) have been constructed such that they obey the basic principles of mechanics and laws of thermodynamics. To apply them to a special material a thermodynamic potential has to be specified. Similar as in previous works [2, 24], Chap. 4 we take the Massieu function as a sum of two contributions,

$$\omega(\rho, T, \mathbf{c}) = \omega_0(\rho, T) + \omega_1(\rho, T, \mathbf{c}), \quad (6.8)$$

where  $\omega_0(\rho, T)$  is the liquid contribution that is independent of the elasticity of the material, and  $\omega_1(\rho, T, \mathbf{c})$  represents the contribution of the internal microstructure. For the liquid contribution to the Massieu function we adopt an expression which leads to a generalization of the equation of state proposed by Flory, Orwoll and Vrij (FOV-equation) [8, 9]. For the elastic contribution we take the expression for a Hookean dumbbell which has been used in [2, 24]. It has proven to be useful in non-equilibrium thermodynamics to recover most of the well established rheological fluid models including those with variable relaxation time (*e. g.* the PTT model) and those with anisotropic drag (*e. g.* the Giesekus model), Sec. 4.4.2, p. 91.

In their theoretical derivation of a temperature equation for non-isothermal polymeric liquids Wapperom and Hulsen [64] take into account the temperature dependence of various thermodynamic properties: For the liquid contribution to (6.8) a thermodynamic potential of the Tait (thermal) equation of state has been adopted [64, p. 1008, Eq. (39)]. For the dependence of the shear modulus on the thermodynamic variables a phenomenological relationship has been used [64, p. 1006, Eq. (35)]. The elastic contribution to (6.8) has been described with the potential of the Hookean dumbbell and the FENE-P dumbbell. The dependence of the mean squared end-to-end distance,  $\langle R^2 \rangle$ , on temperature and density has also been considered. Usually, as strain induced crystallization sets in a strong variation of the temperature coefficient  $d \ln \langle R^2 \rangle / dT$  is observed [64, p. 1007]. The density dependence of  $\langle R^2 \rangle$  is caused by intermolecular forces [64, p. 1007 and references therein].

### Liquid Contribution

For the liquid contribution to the total Massieu function we take the thermodynamic potential of Eq. (2.17), p. 14. The thermal equation of state in terms of the reduced thermodynamic variables (2.16) corresponds to the modified FOV equation (2.18). Upon substitution of the thermodynamic potential (2.17) into (6.5) we find a linear relationship between heat capacity and temperature

$$c_0 = \alpha_0 k_B (q_0 + q_1 T), \quad (6.9)$$

where  $q_0 = \check{c} \Delta \Gamma$ ,  $q_1 = 2\check{c} \Gamma^2 / T^*$ , and  $\check{c} = p^* / \alpha_0 / \rho^* / k_B / T^*$  is a characteristic constant with order of magnitude one (*cf.* Sec. 2.3.2). The parameters  $q_0$ ,  $q_1$  take the values 1.4827 J/g/K,  $1.2045 \cdot 10^{-3}$  J/g/K<sup>2</sup>, respectively [78]. In Sec. 2.3.2, p. 13 we have reported values of the coefficients for PE appearing in the Massieu function (2.17) and in the equations of state (2.18), (6.9).

Having specified the liquid contribution to the thermodynamic potential (first term in Eq. (6.8)) we want to turn our attention to the material's elastic properties (second term in Eq. (6.8)).

### Elastic Contribution

For the elastic part of the Massieu function we adopt the following expression for a Hookean dumbbell [2, 24]

$$\omega_1(\rho, T, \mathbf{c}) = -\frac{1}{2T} \rho \alpha_1 K(T) (\text{tr} \mathbf{c} - 3) + \frac{1}{2} \rho \alpha_1 k_B \ln(\det \mathbf{c}), \quad (6.10)$$

where  $\text{tr} \mathbf{c}$  and  $\det \mathbf{c}$  denote the trace and the determinant of the conformation tensor, respectively. The constant  $\alpha_1$  is a measure of the degree of elasticity and gives a quantitative measure of the strength of elastic forces per unit mass. The nonlinear spring constant of a flexible macromolecule determines the entropic and the energetic potential and is defined as

$$K(T) = \frac{k_B T}{\text{tr} \langle \mathbf{R} \mathbf{R} \rangle_0}, \quad (6.11)$$

where  $\mathbf{R}$  is the end-to-end vector of the polymer chain or the distance between crosslinks or entanglement points and  $\langle \mathbf{R} \mathbf{R} \rangle_0$  is the second

moment of the equilibrium end-to-end vector evaluated at temperature  $T$ . This function contains details about the chemical structure of the polymer under consideration and it has been calculated (*cf.* Chap. 3) adopting the RIS models of physical chemistry [10, 11, 83]. In Tab. 6.1 we report the coefficients of a polynomial fit to the characteristic ratio of PE (the denominator in Eq. (6.11)).

**Table 6.1:** *Coefficients in the polynomial fit of the characteristic ratio for PE,  $C_\infty = \sum_{i=0}^6 c_i T^i$ , for  $100 < T [C^\circ] < 250$ .*

$i$	$c_i$	$i$	$c_i$
0	8.30784367	4	$5.33287318 \cdot 10^{-10}$
1	-0.0147529154	5	$-8.72025919 \cdot 10^{-13}$
2	$5.09101339 \cdot 10^{-5}$	6	$6.2992149 \cdot 10^{-16}$
3	$-1.9319202 \cdot 10^{-7}$		

Inserting Eq. (6.10) into (6.6) we calculate the force density per unit length in the specimen

$$z_{\alpha\beta} = \frac{1}{2} \rho \alpha_1 K(T) \delta_{\alpha\beta} - \frac{1}{2} \rho \alpha_1 k_B T c_{\alpha\beta}^{-1}, \quad (6.12)$$

where  $\delta$  denotes the unit tensor. Substituting Eq. (6.10) into (6.5) we recover the conformational contribution to the heat capacity

$$c_{\text{conf}} = -\frac{1}{2} \alpha_1 T (\text{trc} - 3) \frac{\partial^2 K(T)}{\partial T^2}. \quad (6.13)$$

For the total heat capacity we obtain

$$c = \alpha_0 k_B (q_0 + q_1 T) - \frac{1}{2} \alpha_1 T (\text{trc} - 3) \frac{\partial^2 K(T)}{\partial T^2}, \quad (6.14)$$

where the first term arises from the liquid contribution to the Massieu function, Eq. (6.9), and the second one from the conformational contribution, Eq. (6.13). In the undeformed state,  $\text{trc} = 3$ , the heat capacity reduces to the measured value [78]. In Tab. 6.2 we present thermodynamic properties of PE for  $p_0 = 100$  bar and  $T_0 = 443.15$  K according to the thermodynamic potential of Eq. (6.8).

**Table 6.2:** *Thermodynamic properties of PE at  $p_0 = 100$  bar and  $T_0 = 443.15$  K according to Eq. (2.17).  $\beta$ ,  $\gamma$ ,  $\kappa$ , and  $c$  denote thermal expansion, temperature coefficient of the pressure, isothermal compressibility, and heat capacity, respectively.  $C_\infty = \lim_{n \rightarrow \infty} \langle R^2 \rangle_0 / n l^2$  is the characteristic ratio,  $l = 1.53$  Å.  $T_m$ ,  $T_g$  are melting and glass temperature.*

$\rho$ [ $\frac{\text{g}}{\text{mole}}$ ]	0.8283	$c$ [ $\frac{\text{J}}{\text{gK}}$ ]	2.71
$\gamma$ [ $\frac{\text{MPa}}{\text{K}}$ ]	0.9503	$C_\infty$	6.6588
$\beta$ [ $10^{-4} \frac{1}{\text{K}}$ ]	4.9023	$T_m$ [K]	$403.15 \pm 10$
$\kappa$ [ $10^{-4}$ MPa]	5.1585	$T_g$ [K]	$353.15 \pm 10$

Having discussed the thermodynamic properties of the quiescent PE melt we come to the specification of the phenomenological matrices accounting for relaxation and viscous dissipation of the internal microstructure.

### 6.3.2 Phenomenological Matrices

For the phenomenological matrices we have at our disposal several expressions which have been proposed for isothermal, incompressible viscoelastic materials and which have been generalized to non-isothermal and compressible viscoelastic materials [2, 24]. For the relaxation matrix,  $\mathbf{\Lambda}$ , we adopt the constitutive relationship of the Giesekus model

$$\Lambda_{\alpha\beta\gamma\epsilon} = \frac{1}{2\rho\alpha_1\lambda(T)K(T)} \left[ (1-\beta)(c_{\alpha\gamma}\delta_{\beta\epsilon} + c_{\alpha\epsilon}\delta_{\beta\gamma} + c_{\beta\gamma}\delta_{\alpha\epsilon} + c_{\beta\epsilon}\delta_{\alpha\gamma}) + \frac{2\beta K(T)}{k_B T} (c_{\alpha\gamma}c_{\beta\epsilon} + c_{\alpha\epsilon}c_{\beta\gamma}) \right], \quad (6.15)$$

where  $\beta$  is a number between zero and one. The last term on the right hand side is a second-order correction to the relaxation matrix

for the Maxwell model and describes an anisotropic drag experienced by the chains as the material deforms. In general, the parameter  $\beta$  is allowed to be an arbitrary function of temperature. Here, however, we wish to take a constant value for this phenomenological parameter [153],  $\beta = 0.29$ .

For the temperature dependence of the relaxation time we take the following empirical relationships

$$\frac{\lambda(\rho, T)}{\lambda_r} = \frac{T_r \rho_r}{T \rho} \exp \left[ \frac{A_0}{R} \left( \frac{1}{T} - \frac{1}{T_r} \right) \right], \quad (6.16)$$

$$\log \left( \frac{\lambda(T)}{\lambda_r} \right) = \frac{c_1(T - T_r)}{c_2 + T - T_r}, \quad (6.17)$$

which are plotted in Fig. 6.1. Eq. (6.16) is the equation of Ferry [20], where  $\lambda_r$  is the characteristic relaxation time of the system at temperature  $T_r$  and density  $\rho_r$ ,  $A_0$  is the activation energy for viscous flow,

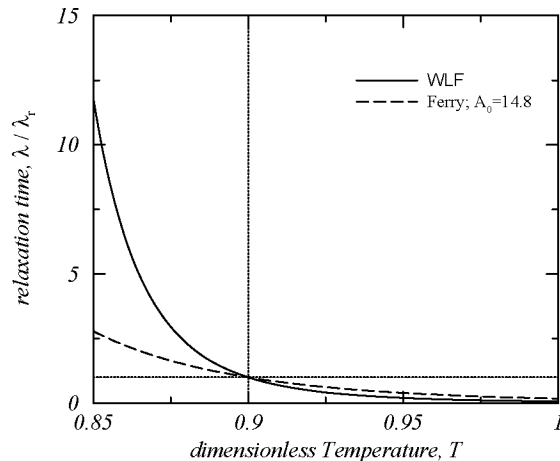


**Figure 6.1:** Temperature dependence of the relaxation time according to the equation of Ferry (6.16) and the WLF equation (6.17). For the reference temperature we took  $T_r = 443.15$  K.

$R$  is the ideal gas constant, and we have used the Arrhenius form for the temperature dependence of the viscosity. The reference temperature may be taken as the melting temperature  $T_r = T_m$ ; the activation

energy is  $A_0 = 13$  kcal/mole [155]. Eq. (6.17) is the WLF equation [21] where  $T_r$  is a reference temperature, e. g. the melting point, and  $c_1 = 8.86$ ,  $c_2 = 101.6$  K. This equation has been proven to fit quite well the relaxation time spectrum for a large class of glass forming materials as they are supercooled. In Fig. 6.1 we have plotted the normalised relaxation times according to Eqs. (6.16), (6.17) for  $T_0 = 443.15$  K. For simplicity we took  $T_r/T_0 = 0.9$ . Effects of cooling rate on the relaxation time can be easily incorporated into the present analysis by adopting the appropriate modification of the WLF equation [62, 57].

To describe viscous dissipation of the material we have the following expression for the viscous dissipation matrix

$$\mathbf{Q}_{\alpha\beta\gamma\epsilon} = \eta(T)(\delta_{\alpha\gamma}\delta_{\beta\epsilon} + \delta_{\alpha\epsilon}\delta_{\beta\gamma}), \quad (6.18)$$

where  $\eta(T)$  denotes the shear viscosity. A well established temperature dependence of the viscosity is the Arrhenius form

$$\eta(T) = \eta_0 \exp \left( \frac{A_0}{RT} \right). \quad (6.19)$$

The above expression for the phenomenological matrix  $\mathbf{Q}$  can be modified to include bulk viscous effects and higher order terms.

At this point we have at our disposal all constitutive relationships which are necessary to solve the set of time evolution equations (6.1)-(6.3) and we can begin to study particular applications.

## 6.4 Applications

The time evolution equations (6.1)-(6.3) have been solved in reduced form introducing dimensionless quantities,  $\tilde{\rho} = \rho/\rho_0$ ,  $\tilde{T} = T/T_0$ ,  $\tilde{\mathbf{c}} = K(T_0)/(k_B T_0) \cdot \mathbf{c}$ . The quantities  $\rho_0$ ,  $T_0$  denote density and temperature at the start-up of deformation. For the thermodynamic potential (6.8) and the phenomenological matrices (6.15), (6.18) the time evolution equations Eqs. (6.1)-(6.3) have been solved for homogenous velocity gradients,  $\nabla \mathbf{v}$ , and density, temperature fields,  $\rho$ ,  $T$  using a fourth order Runge-Kutta scheme. In this case we have a system of eleven ordinary differential equations for the homogenous conformation tensor, the temperature and the mass density. The coefficients appearing in the

system equations are functions of temperature and density according to the phenomenological relationships given in Sec. 6.3 (Eqs. (6.16), (6.17) and (6.19)).

### 6.4.1 Non-isothermal Stress Relaxation

Astarita and Sarti [46] and Sarti and Esposito [14] performed non-isothermal stress relaxation experiments under adiabatic conditions to test the validity of the Theory of Purely Entropic Elasticity [43, 44]. In these experiments they measured the temperature rise and the forces in a specimen during shear- and elongational-deformations and how these quantities change during relaxation. For experimental details the reader is referred to the literature [46, 14]. For PVA above its melting temperature and for PIB the temperature remained constant during the relaxational period of the stress relaxation experiment; *i. e.* these materials can be considered to be of purely entropic elasticity in this temperature range. However, for PVA it was found in Ref. [14] that the Theory of Purely Entropic Elasticity fails dramatically near the glass transition temperature. This was seen as a decrease of temperature during the relaxational part of the experiment which compensated the temperature rise during deformation. Thus, the frictional heating behaviour of PVA near  $T_g$  is more complicated than for materials with purely entropic elasticity. Note that in all experimental runs the temperature variations induced by deformation were a few tenths of one Kelvin which is quite difficult to resolve experimentally<sup>2</sup>.

To demonstrate how the above set of equations reduces to the Theory of Purely Entropic Elasticity we performed computer experiments of non-isothermal stress relaxation, Fig. 6.2. In these calculations we adopted the Maxwell model; *i. e.*  $\beta = 0$  in Eq. (6.15) and  $\mathbf{Q} = \mathbf{0}$ . The material is considered as incompressible,  $\rho = \text{const}$ , and the elongation rate was taken as  $\dot{\epsilon}\lambda_0 = 0.1$ , *i. e.* we are working in the regime of small deformations. The phenomenological parameters  $\alpha_0$  and  $\alpha_1$  have been set equal to 30 and 0.03, respectively. The other relevant parameters are collected in Sec. 2.3.2, p. 14, ( $q_0, q_1$  p. 124).

<sup>2</sup>Preliminary attempts have been undertaken to measure temperature variations induced by deformation and stress relaxation (Dr. T. Schweizer, ETH Zurich, personal communication).

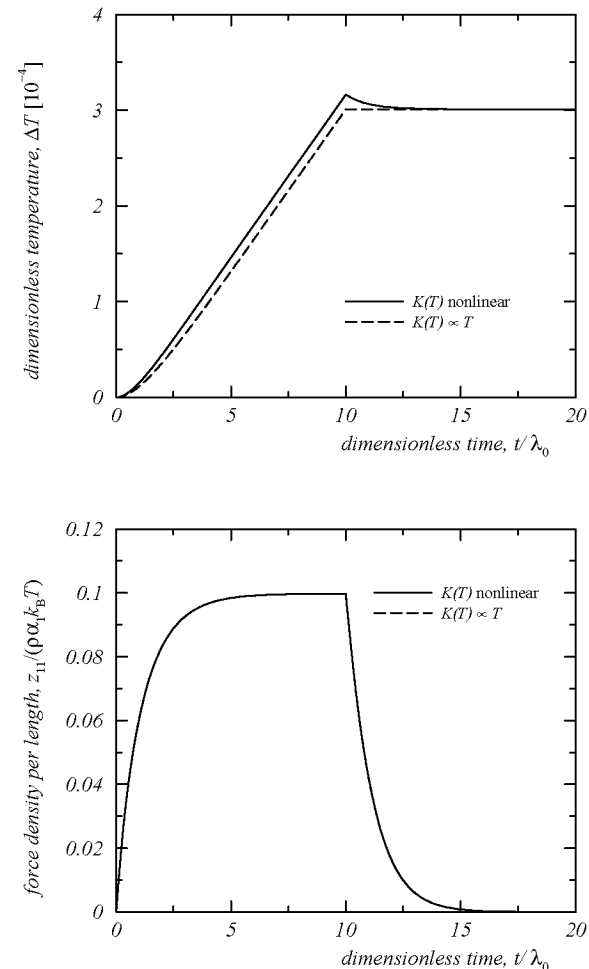


**Figure 6.2:** Temperature rise (a) and 11-component of the force density per unit length (b) in non-isothermal stress-relaxation experiment ( $\dot{\epsilon} = 0.1$ ) for a material with entropic and energetic elasticity (solid line) and purely entropic elasticity (dashed line). The difference of the results for  $K(T) \propto T$  and a nonlinear  $K(T)$  in (b) cannot be resolved.

For the temperature dependence of the relaxation time we took Eq. (6.16) with  $T_r = T_0 = 443.15$  K [153]. Fig. 6.2a shows the temperature course in two non-isothermal stress relaxation experiments. The dashed line is for a material with purely entropic elasticity, *i. e.*  $K(T) \propto T$ . In this run we see that the temperature remains constant during relaxation. However, taking  $K(T)$  to be nonlinear in  $T$  we observe a temperature relaxation after the elongation has been switched off (solid line). The parameters  $\alpha_0$ ,  $\alpha_1$  have been chosen to obtain a temperature rise of approximately  $\Delta T = 0.13$  K corresponding to the experimentally observed value [14]. Note that the temperature rise at the beginning of the experiment is not linear but we observe a temperature rise of higher order. This is confirmed by the experimental results. In Fig. 6.2b we have plotted the force density in the drawing direction as a function of dimensionless time. This quantity relaxes for a linear as well as for a non-linear spring constant. The differences between the linear and the nonlinear spring constant are small for our parameter set as it has been observed by Sarti and Esposito [14].

### 6.4.2 Non-isothermal Fiber Spinning Process

The processing of most thermoplastics involves sequential heating, deforming and cooling. In practice, the final shape, the internal structure and gross physical properties of the article formed are normally found to be dependent on the details of the processing operation as defined by the thermal and deformation histories of the material processed. We want to describe the flow and temperature fields, the physical state (thermodynamic properties) and internal microstructure (morphology) of a material for given deformation and thermal histories (*i. e.* imposed operating conditions for the process) adopting the Maxwell model, *i. e.*  $\beta = 0$ ,  $\mathbf{Q} = 0$ . We have studied two non-isothermal processes, P1 and P2, for a material with a melting temperature of  $T_m = 403.15 \pm 10$  K and a glass temperature of  $T_g = T_m - 50$  K =  $353.15 \pm 10$  K. The initial temperature of both processes,  $T = 443.15$  K, is taken as the reference temperature and corresponds to a dimensionless temperature  $\tilde{T} = 1$ . All thermodynamic quantities are normalized with respect to the initial values (Tab. 6.2, p. 126). In what follows we want to work with dimensionless variables and we will drop the tilde. For the temperature dependence of the relaxation time we took the WLF equation (6.17) with the melting temperature,  $T_m$ , as the reference temperature,

*i. e.*  $\lambda_r = \lambda(T_m) = 1$ . The phenomenological coefficients  $\alpha_0$  and  $\alpha_1$  are 5000 and 0.2, respectively. In the figures to follow we have taken solid lines for P1 and dashed lines for P2.

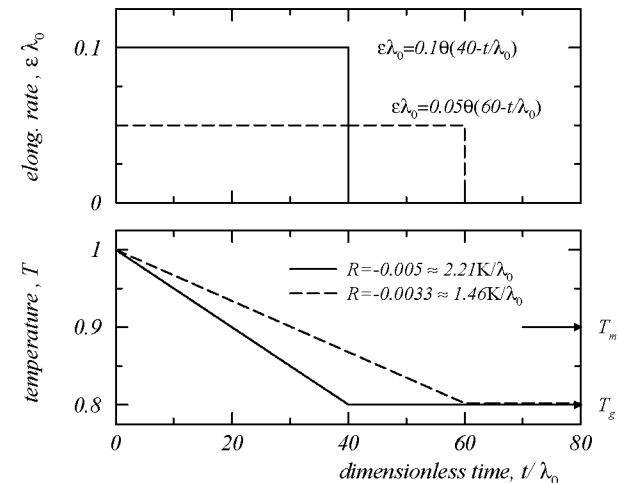


**Figure 6.3:** Deformation- (a) and temperature-history (b) for two non-isothermal processes P1 (solid line) and P2 (dashed line) with different elongation rates,  $\dot{\epsilon}$  and cooling rates,  $R$ . Deformation histories and cooling rates are denoted with each curve;  $\Theta$  denotes the Heavyside step function.

Fig. 6.3 shows the temperature- and deformation-history of the two non-isothermal processes. The deformation history is denoted with each curve in the upper graph (Fig. 6.3a). For P1 we have taken a constant elongation rate  $\dot{\epsilon}\lambda_0 = 0.1$  which is switched off at  $t/\lambda_0 = 40$ . The elongation rate of P2 is  $\dot{\epsilon}\lambda_0 = 0.05$  and it is switched off at  $t/\lambda_0 = 60$ . Fig. 6.3b shows the temperature histories in both processes. As the elongation starts the material is quenched from the initial temperature,  $T_0 = 1$ . The cooling rates in dimensionless units and in units of the relaxation time,  $\lambda_0$ , are reported in the figure. The dimensionless melting temperature and the glass temperature are located at  $T_m = 0.8$  and  $T_g = 0.9$ , respectively and are marked with arrows in Fig. 6.3b. The cooling process stops as the elongation rate is switched off. At the

end of the process the temperature is slightly above the glass transition temperature,  $T_g$ . Note that here we have not taken into account effects of the material's thermodynamic properties on the externally imposed deformation. However, the temperature history is more complicated than the externally imposed cooling rate (cf. we solve Eq. (6.2)!).

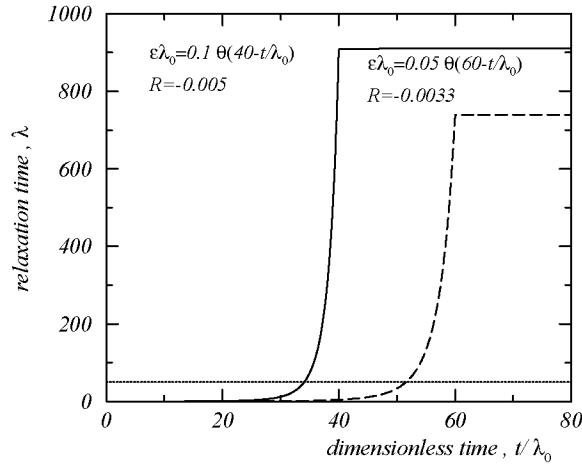


**Figure 6.4:** The time development of the relaxation time in the two processes P1 (solid line) and P2 (dashed line). Note how the time scale of the processes and the rheological time scales overlap each other. The area below the dotted line,  $\lambda = 50$ , marks the average duration of the two processes.

In Fig. 6.4 we portray the time evolution of the relaxation time in both processes. This quantity is a strong function of temperature and it has a strong influence on the material properties. For P2 it has a value of  $\lambda \approx 7 \cdot 10^{-2}$  at the start-up of deformation and it reaches  $\lambda \approx 7 \cdot 10^2$  at the end of the process. The deformation- and temperature histories are denoted with each curve. The dashed horizontal line  $\lambda = 50$  marks the average duration of the processes and is the time scale of P1 and P2. Note how the rheological scales overlap the time scales of the two processes. In what follows we want to look at the mechanical and thermodynamic properties of the processed material.

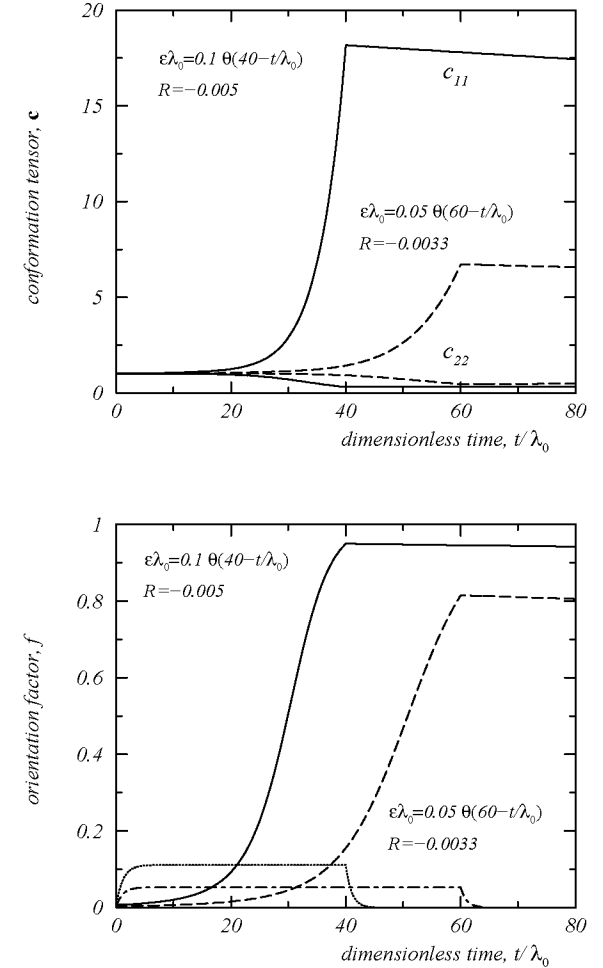
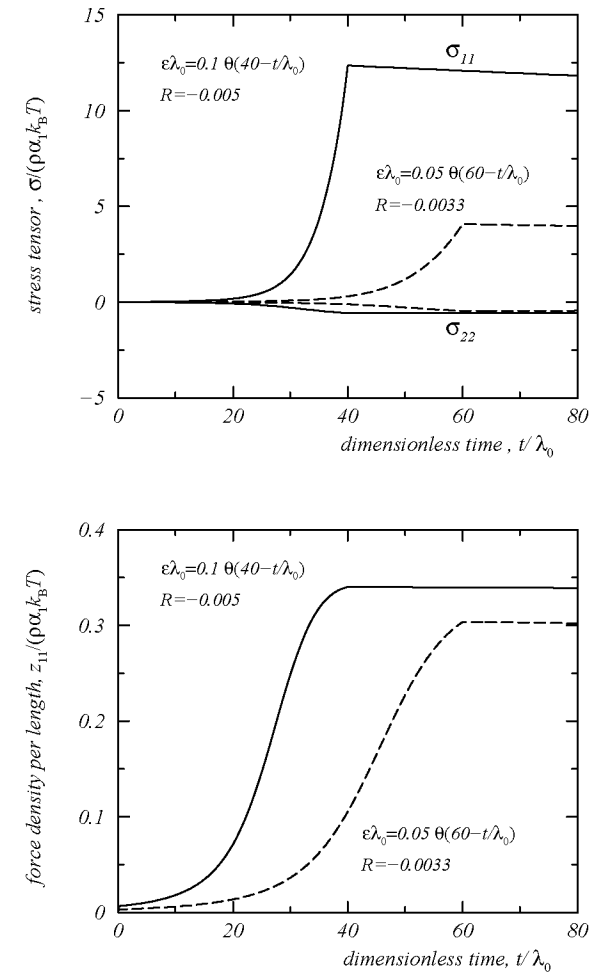


**Figure 6.5:** The conformation tensor (a) and the amorphous orientation factor (b) for the two non-isothermal processes, P1 and P2. The dotted line and the dashed dotted line in (b) are for an isothermal process at  $T = 0.9$  and the deformation histories of P1 and P2, respectively.



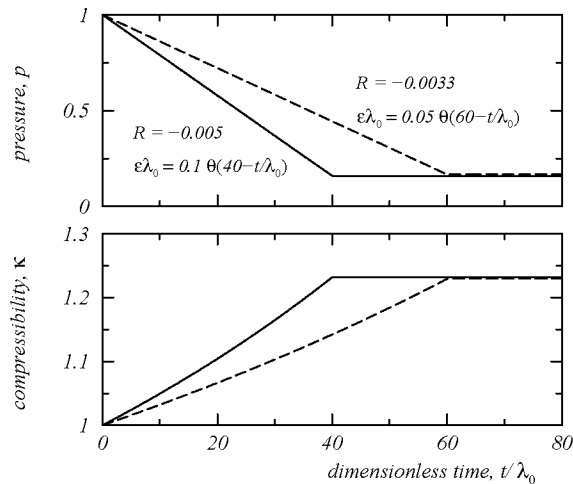
In Fig. 6.5, p. 134 we have plotted the conformation tensor and the amorphous orientation factor. Fig. 6.5a shows the development of the conformation tensor during the processes. This quantity can be viewed as the conformation of the polymer coils or the deformation of the material. In the deformation period of the process the entries of the conformation tensor increase rapidly. During the relaxation phase we observe a slight decrease in  $c_{11}$ . The changes in the conformation tensor during relaxation are more pronounced in P1 than in P2. Fig. 6.5b shows the orientation factor as a function of time for both processes. In this quantity we observe only a small relaxation after the deformation has been switched off. In Fig. 6.5b we have also included the orientation factor for two isothermal processes at constant temperature,  $T = 0.9$ . The deformation histories of these runs correspond to that of P1 (dotted line) and P2 (dot-dashed line). Our calculations show that a deformation with simultaneous quenching yields a higher oriented state than an isothermal process. The application of a deformation with simultaneous quenching to the glass transition temperature,  $T_g$ , may be an alternative to the common high speed fiber spinning process. In that process the orientation in the spinline is induced by rapid deformation, the temperature of the material being constant. The calculations show that a similar effect may be obtained with a slow deformation and a moderate cooling of the material.

Fig. 6.6, p. 136 shows the mechanical properties of the material during the two processes. Fig. 6.6a displays the extra-stress tensor as a function of dimensionless time. This quantity shows essentially the same time evolution as the conformation tensor,  $c$ . Fig. 6.6b displays the force density per unit length in the drawing direction as a function of time. Also in this quantity we observe a strong increase during the process and small variations after elongation and quenching have been switched off. Whereas the conformation tensor (Fig. 6.5a) and the extra-stress tensor (Fig. 6.6a) show some variations during relaxation the orientation factor (Fig. 6.5b) and the force density (Fig. 6.6b) vary only slightly after deformation and quenching have been turned off. From Figs. 6.5 and 6.6 we note that the mechanical properties of the oriented material correlate quite well with the orientation (birefringence) frozen into it, which in turn correlates quite well with the stress induced in the melt at the time of quenching. This is true whether the melt history is isothermal or non-isothermal. Next we want to study the time evolution of the pressure, the compressibility, and the heat capacity of the material during the processes (Figs. 6.7, 6.8).



**Figure 6.6:** The extra-stress tensor (a) and the 11-component of the force density per unit length in the spinline (b) for the two non-isothermal processes, P1 and P2.

We have mapped the thermodynamic properties of the specimen during the processes. If we chose an initial pressure of  $p_0 = 100$  MPa the density of the material is  $\rho \approx 0.83 \text{ g cm}^{-3}$ . All thermodynamic properties are taken relative to the initial values. In Fig. 6.7 we report the thermodynamic properties of the specimen as a function of dimensionless time. Fig. 6.7a shows the pressure decrease during deformation; Fig. 6.7b displays the compressibility as a function of time. The time evolution of the pressure and the compressibility is rather complicated and it can be analyzed by mapping the  $\rho(T)$  and  $\kappa(T)$  curves of the process onto the  $\rho(T)|_{p=\text{const}}$  and the  $\kappa(T)|_{p=\text{const}}$  plane of the quiescent material. Since the processes P1 and P2 are incompressible, the temperature coefficient of the pressure is constant and the thermal expansion is equal to the isothermal compressibility.



**Figure 6.7:** Pressure and isothermal compressibility of the drawn filament in the two processes, P1 and P2, as function of dimensionless time.

In Fig. 6.8 we report the heat capacity of the specimen as a function of dimensionless time. The upper curve shows the heat capacity for P1 and P2. The lower graph shows that part of the heat capacity which is related to conformational changes induced by orientation. These varia-

tions are very large due to the high orientation which is reached in the material. However, since the ratio  $\alpha/\alpha_0$  is very small these effects are not observed in the heat capacity,  $c$ . (Here we have assumed that the relative strength of the liquid contribution to the Massieu function,  $\alpha_0$ , is greater than the relative strength of the conformational contribution,  $\alpha_1$ ;  $\alpha_1/\alpha_0 = 4 \cdot 10^{-5}$ .)

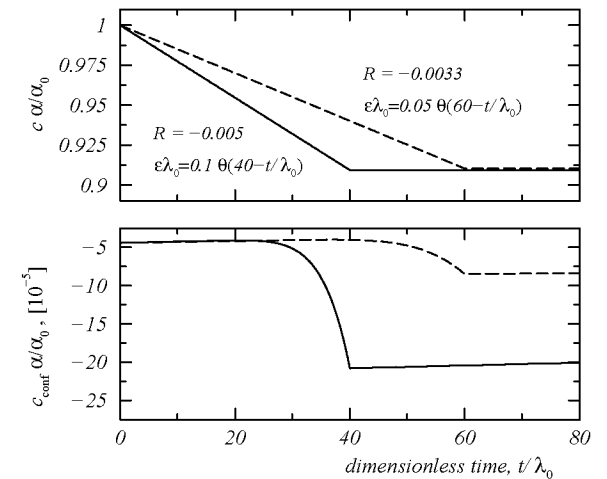


**Figure 6.8:** The heat capacity  $c$  (a), and the conformational contribution to the heat capacity  $c_{\text{conf}}$  (b) of the material as a function of time in the two processes.

In this section we have studied exclusively incompressible processes. However, polymeric materials possess a considerable free volume and the assumption of incompressibility is questionable.

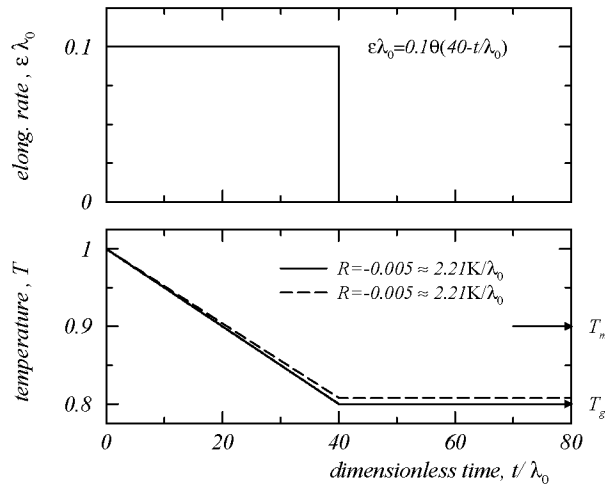
### 6.4.3 Non-isothermal Deformation with Compression

We have studied a compressible process, P3, which has the same elongation rate and the same external cooling rate as P1. In contrast to P1 we have an additional slight compression perpendicular to the stretching

direction. The deformation history of P3 is defined as follows

$$\nabla \mathbf{v} = \begin{pmatrix} \dot{\epsilon} & 0 & 0 \\ 0 & -\frac{1}{2}\dot{\epsilon} + \dot{\delta} & 0 \\ 0 & 0 & -\frac{1}{2}\dot{\epsilon} + \dot{\delta} \end{pmatrix} \Theta(t_0 - t), \quad (6.20)$$

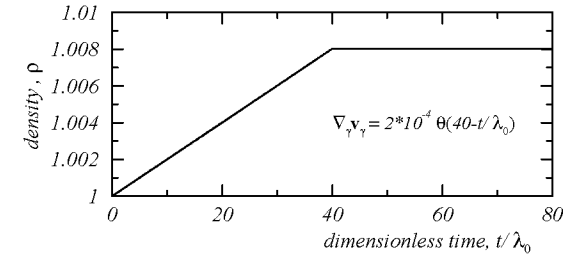
where  $\dot{\epsilon}$ ,  $\dot{\delta}$  denote the elongation rate and the compression rate, respectively.  $\Theta$  is the Heavyside function and  $t_0$  the time when the deformation stops. Here we adopted the Maxwell model, *i. e.*  $\beta = 0$ ,  $\mathbf{Q} = 0$  to describe the processes as in the previous paragraph. The phenomenological parameters,  $\alpha_0$  and  $\alpha_1$ , are taken as 5000 and 0.2, as before.



**Figure 6.9:** Deformation- and temperature-history for non-isothermal processes P1 (solid line) and P3 (dashed line). In P3 there is an additional compression which affects the temperature history of the specimen.

In Fig. 6.9 we display the elongation- and temperature-history of P1 and P3. As before the solid line is for P1 and now the dashed line is for P3 for all figures to follow in this paragraph. Due to the additional density changes taking place in the material the final temperature of P3 is slightly higher than that of P1. In the upper graph we report the elongation history,  $\epsilon\lambda_0$ , of both processes. In the lower figure we have

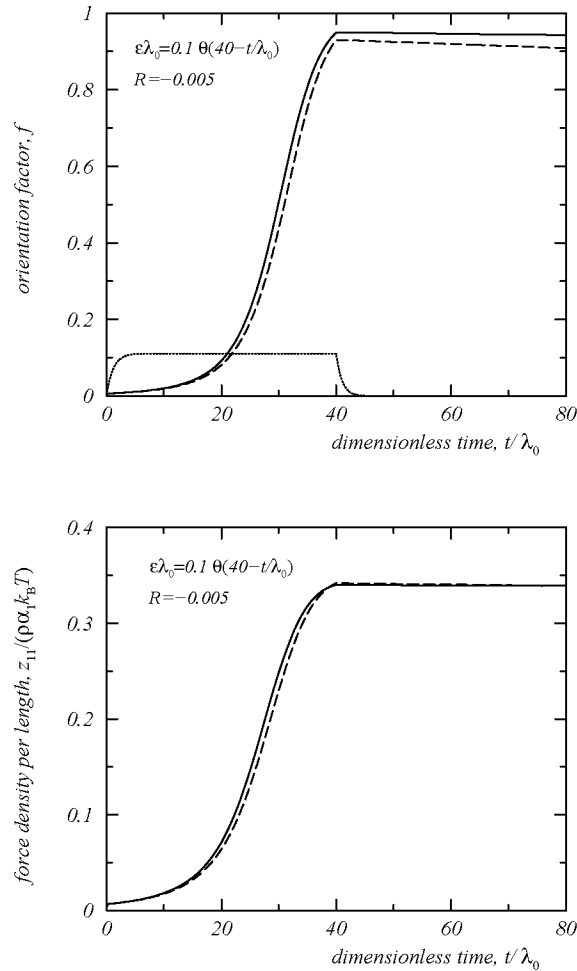
included the cooling rate,  $R$ , in dimensionless units and in units of the relaxation time  $\lambda_0$ . Melting point and glass temperature are denoted with  $T_m$  and  $T_g$ , respectively and are marked with arrows in the lower graph.



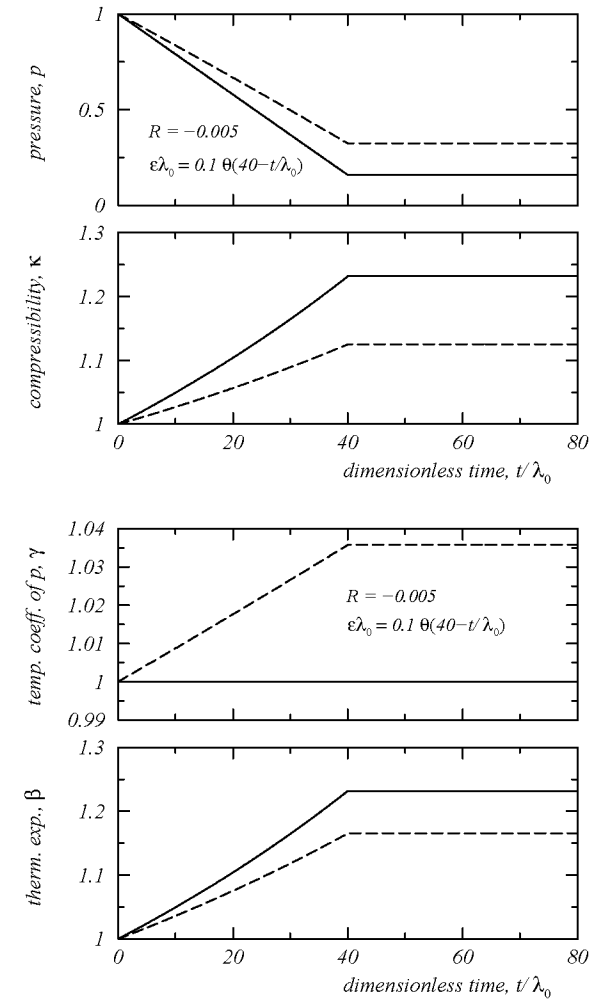
**Figure 6.10:** Density as a function of temperature in P3. The compression,  $\nabla_\gamma v_\gamma$ , is perpendicular to the drawing direction and causes a density increase of 0.8%, approximately.

Fig. 6.10 shows the density rise in the material due to the pressure history of Fig. 6.12a, p. 142. Assuming a compression of the sample in the 2- and 3-direction we obtain a density variation (governed by the continuity equation (6.1)) as shown in Fig. 6.10. The compression as a function of time,  $\nabla_\gamma v_\gamma$ , stops at  $t\lambda_0 = 40$  and is reported in the figure. The pressure history has been taken to yield  $\dot{\delta}\lambda_0 = 10^{-4}$  in Eq. (6.20).

Fig. 6.11a, p. 141 displays the time evolution of the orientation factor in the amorphous material for the non-isothermal processes P1 and P3. Note that the additional compression lowers the final orientation in the material. This is due to the fact that the final temperature in P3 is slightly higher than in P1 which has a drastic effect on the time evolution of the relaxation time. Furthermore, we have included the result of the isothermal and incompressible process with temperature  $T = 0.9$  and density  $\rho = 1$  (dotted line in Fig. 6.11). Fig. 6.11b maps the 11-component of the tensorial force density in the spinline as a function of time. At the beginning,  $t/\lambda_0 \approx 0$ , and towards the end,  $t/\lambda_0 \approx 60$ , of the process, we observe the same force density as in the incompressible run. In the intermediate time interval there are small differences.



**Figure 6.11:** Development of the orientation factor (a) and the 11-component of the force density in the spinline (b) with time in the incompressible process, P1, and in the process with an additional compression, P3.



**Figure 6.12:** Thermodynamic properties of the two processes, P1 and P3: (a) pressure  $p$ , (b) compressibility  $\kappa$ , (c) temperature coefficient of the pressure  $\gamma$ , and (d) thermal expansion coefficient,  $\beta$ .

Figs. 6.12a and 6.12b, p. 142 show the pressure and compressibility of the material as a function of dimensionless time. For the incompressible process, P1, the decrease in pressure  $p$ , and compressibility  $\kappa$ , is more pronounced than for the compressible one, P3. In P3 this effect is compensated due to the additional density variations. Fig. 6.12c and 6.12d display the temperature coefficient of the pressure  $\gamma$ , and the thermal expansion coefficient  $\beta$ , as a function of dimensionless time. For P1 the temperature coefficient of the pressure is constant since the process is incompressible and the thermal expansion coefficient increases with decreasing temperature. In P3, we have an increase of both, the temperature coefficient of the pressure and the thermal expansion coefficient.

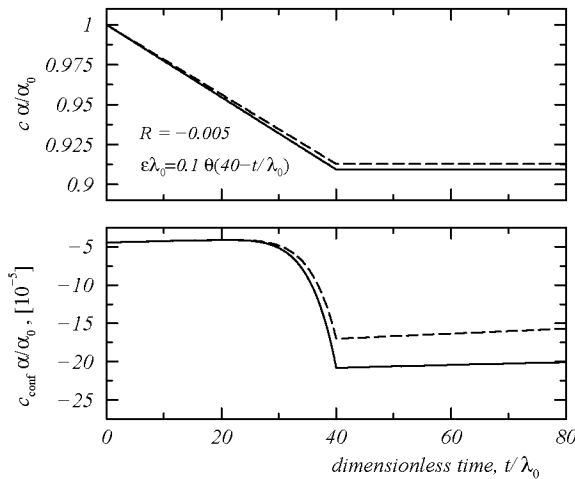


**Figure 6.13:** Development of the heat capacity in the two processes P1 and P3. The lower graph shows the development of the conformational part to the heat capacity.

The time evolution of the heat capacity,  $c$ , and its conformational contribution,  $c_{\text{conf}}$ , are reported in Fig. 6.13. The upper graph shows the total heat capacity during P1 and P3. The lower graph displays the conformational contribution to the heat capacity. Similar as with the incompressible processes we observe large variations in this quantity. Due to the smaller orientation induced in P3 the conformational contribution to  $c$  is less pronounced than in P1.

### 6.4.4 The Problem of Critical Cooling

Following [115, 49, 152, 153] it is instructive to study the macroscopic deformation and the elongational viscosity for an incompressible material with the temperature history  $T = T_0 + Rt$ , where  $R$  is a constant externally imposed cooling rate and  $T_0$  is the initial temperature of the sample. This shows how our theory is related to the other approaches to non-isothermal rheology in the literature. In contrast to previous works in the field we wish to take into account explicitly energetic elasticity and we adopt an approximation of the equation of Ferry (6.16) for the temperature dependence of the relaxation time  $\lambda(T)/\lambda_r = T_r/T \exp[\tau(1 - T/T_r)]$ , with  $T_r = T_0 = 483.15\text{K}$  corresponding to the initial temperature and  $\tau = 20$  [153]. Note that the density has disappeared in the prefactor since the material is incompressible.

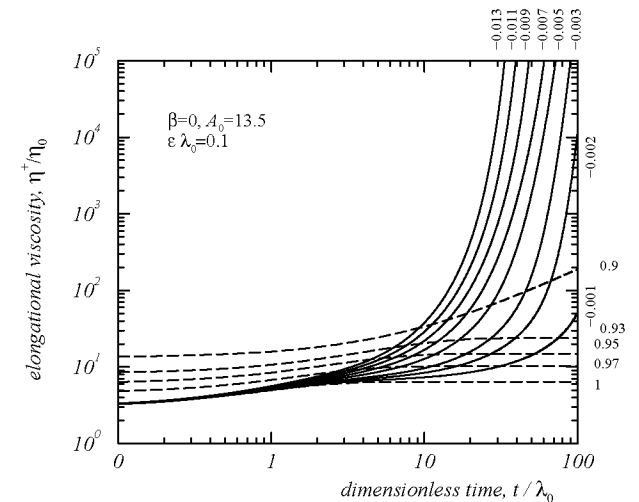


**Figure 6.14:** Oldroyd-B model for inception of steady elongational flow. Dashed lines are isothermal runs, solid lines are non-isothermal runs with initial temperature  $T = 1$ . The temperatures and cooling rates are denoted with each curve as horizontal and vertical strings, respectively.

Fig. 6.14, p. 144 shows the dimensionless elongational viscosity for the Oldroyd-B model. The reference temperature is  $T_0 = 483.15\text{K}$ . The strain rate,  $\dot{\epsilon}\lambda_0$ , the parameter in the equation of Ferry,  $A_0$ , and the Giesekus parameter,  $\beta$ , are reported in the graph. The phenomenological parameter for the strength of elasticity of the material,  $\alpha_1$ , has been set equal to one. The dashed lines are isothermal runs; the temperature of these runs being reported with each curve. The solid lines are non-isothermal runs with an initial temperature of  $T = T_0$ . The dimensionless cooling rate,  $R$ , of these runs is denoted with each curve.

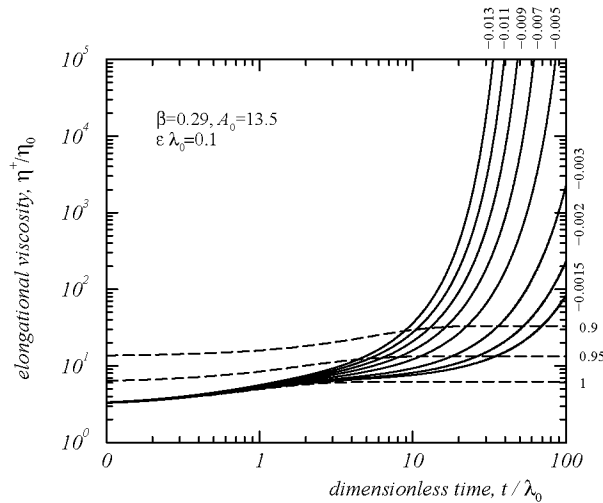


**Figure 6.15:** The same as Fig. 6.14 for the Oldroyd-B model with Giesekus contribution for inception of steady elongational flow.

Fig. 6.15 shows the same predictions for the Giesekus model with an Oldroyd-B contribution. The Giesekus parameter was taken as  $\beta = 0.29$ ; all other parameters are the same as in Fig. 6.14. As before the dashed lines are isothermal runs with the constant temperature denoted with each curve (as horizontal strings) and the solid lines are non-isothermal runs with the cooling rate denoted with each curve (as vertical strings). The strong increase of the elongational viscosity in cooling (a so called blow up in the elongational viscosity) has been ob-

served in several experiments on non-isothermal rheology and has also been explained theoretically (e. g. [62]). Note the differences in the dashed curves  $T = 0.9$ . The Oldroyd-B model predicts a considerable strain hardening effect which is not encountered if a Giesekus contribution is taken into account.

Furthermore, we have studied the Trouton viscosity of the non-isothermal Maxwell model, i. e.  $\beta = 0$ ,  $\mathbf{Q} = 0$ , for different cooling rates  $R$  and elongation rate  $\dot{\epsilon}\lambda_0 = 0.1$  as in [115]. The Trouton viscosity is  $\eta_{el}/\eta_{sh}^0 = (\sigma_{11} - \sigma_{22})/(\dot{\epsilon}\alpha_1\rho k_B T \exp(\tau Rt))$ . In Fig. 6.16 we display the viscosity ratio, as a function of dimensionless time. The strain rate,  $\dot{\epsilon}\lambda_0$ , and the activation energy,  $A_0$ , are reported in the graph.

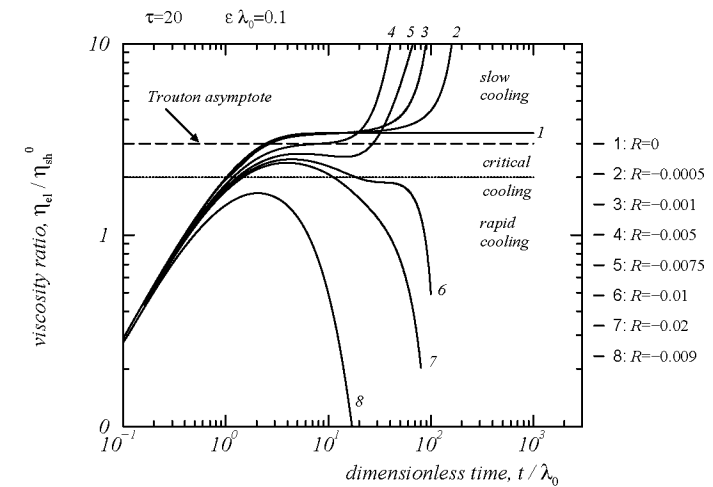


**Figure 6.16:** Viscosity ratio for several non-isothermal runs with different cooling rates.

The long dashed line in Fig. 6.16 is the Trouton asymptote,  $\eta_{el}/\eta_{sh}^0 = 3$ . The solid line 1 is an isothermal run ( $R = 0$ ), the other solid lines, 2...8, are non-isothermal runs with increasing cooling rate ( $R = -0.0005, -0.001, -0.005, -0.0075, -0.009, -0.01, -0.02$ ). As the cooling rate increases the viscosity blows up,  $\eta_{el}/\eta_{sh}^0 \rightarrow \infty$  (curve 2...4). For further increase of the cooling rate, curve 5, we observe the oppo-

site trend. For even higher cooling rates (curve 6...8) the viscosity ratio breaks down,  $\eta_{el}/\eta_{sh}^0 \rightarrow 0$ . This suggests [115] that there may exist a cooling rate (between curve 5 and 6) where the viscosity ratio attains a constant value,  $\eta_{el}/\eta_{sh}^0 = 2$ .

## 6.5 Conclusions

We wish to summarize briefly the results that we obtained by using a continuum approach to non-isothermal rheology of amorphous glass forming polymeric materials. We started from a set of thermodynamic consistent partial differential equations for the density, the temperature, and the elastic Cauchy tensor. To solve this set of equations we adopted constitutive relations for the material's thermodynamic potential and for the phenomenological matrices of rotational diffusivity and viscous dissipation. The characteristic elastic constant of the material was taken as a non-linear function of temperature to allow for energetic elasticity. For the temperature dependence of the relaxation time we adopted the equation of Ferry and the WLF equation for supercooled glass forming liquids. The evolution equations have been solved for arbitrary three dimensional homogenous deformations and results for elongational flows have been presented. We gave a brief account on non-isothermal stress relaxation experiments to illustrate the effect of energetic elasticity on temperature relaxation. Furthermore, we have discussed a non-isothermal fiber spinning process to produce highly oriented glassy fibers with low elongation rates and we simulated non-isothermal stretching with a simultaneous small compression. The material properties and the morphology of the finished article have been discussed for various deformation and temperature histories. We showed that the mechanical and thermodynamic properties of the processed material correlate quite well with the orientation (morphology) frozen into it and that the morphology of the finished product depends on the chosen process conditions. Finally we studied how the elongational viscosity blows up in cooling experiments and we saw that it seems difficult to establish a critical cooling rate in non-isothermal rheology. Further work in this direction should focus on the numerical treatment of more sophisticated rheological models, *e. g.* models with deformation dependent relaxation times and FENE models, the inclusion of

non-affine motion into the system equations, the investigation of higher deformation rates, and the application to other glass forming polymers such as PS and PVA. The discussion of shear flows, nonlinear material properties, and the effects of heating are other interesting points.

## Chapter 7

# Conclusions

In the present thesis we have applied classical equilibrium thermodynamics, Physical Chemistry (RIS approximation), and a modern framework of non-equilibrium thermodynamics (GENERIC) to give a continuum description of non-isothermal and compressible polymeric materials. These methods have been applied to describe the rheology of isothermal polymeric materials with purely entropic elasticity and to discuss alternative industrial processes to produce highly oriented fibers taking into account energetic elasticity of the material. The RIS models have been used as a microscopic input for the macroscopic material description.

In Chap. 2 we presented thermodynamic potentials for polymeric liquids. The thermodynamic potentials depend on the material's density, its temperature and the polymer conformation. For the liquid contribution to the potential we proposed two mathematical expressions leading to a SG and to a modified FOV equation of state, respectively. For the elastic contribution to the potential we adopted the thermodynamic potential of the Hookean spring to capture the material's elastic properties related to the internal microstructure. To apply the elastic part of the potential to linear polymers we adapted the RIS approximation of Physical Chemistry and we calculated the averages of the chain conformation as a function of temperature. Numerical examples appropriate to PE and to hexadecane were given and comparison with experimental data above their melting temperature yielded satisfactory results.

The combination of thermodynamics (Hookean dumbbell) and statistical mechanics (RIS approximation) pursued in Chap. 2 allowed us to determine the entropic and the energetic potential for linear polymers (Chap. 3). A recipe to check the validity of the Theory of Purely Entropic Elasticity emerged from this analysis and numerical examples appropriate to PE and to PIB have been presented. PE cannot be considered to be of purely entropic elasticity since the energetics of the bond conformations is more than 40% of the total elastic energy. PIB was seen to obey the Theory of Purely Entropic Elasticity since the energetic potential is approximately 1% of the total elastic free energy. This result is consistent with experimental findings in non-isothermal stress relaxation experiments. Since the Theory of Purely Entropic Elasticity turned out to be insufficient to the description of polymeric materials a new set of time evolution equations had to be derived. This is the topic of Chap. 4.

In Chap. 4 the recently proposed GENERIC framework of non-equilibrium thermodynamics has been applied to derive a full set of thermodynamically consistent time evolution equations for the dynamical variables. These are the thermodynamic variables of Chap. 2 and the momentum density as an additional dynamical variable to describe macroscopic flow phenomena. Our set of PDE's (Eqs. (4.42a)-(4.42d), p. 79) describes the dynamical behaviour of a non-isothermal, compressible viscoelastic fluid with entropic and energetic elasticity, Fourier-type heat flux, and relaxation of the internal microstructure. Many popular constitutive equations of polymer rheology can be obtained from this set of time evolution equations. Furthermore, modified constitutive equations for non-isothermal and compressible polymeric materials with entropic and energetic elasticity have been derived. They represent counterparts of the established constitutive equations. The conformation tensor equation (4.42d), p. 79 has been solved for arbitrary homogenous deformations assuming incompressibility and isothermal conditions. In this case we deal with a material of purely entropic elasticity. Popular rheological models for amorphous polymeric materials in elongation, stretching, shearing, and mixed flows can be solved numerically. We are able to compute transient and steady state viscosities and to discuss the stress optical rule for the FENE-P, Giesekus, and PTT/PT models. In Cap. 5 possibilities to determine microscopic friction parameters which appear in the time evolution equations have been proposed. Chap. 6 deals with the numerical analysis of the time evolution equations for non-isothermal homogenous deformations.



Chap. 5 deals with isothermal and incompressible polymers in the liquid state. We discussed the recently proposed FETA models and showed how they may be expressed in a conformation tensor formalism. These models can be obtained from the time evolution equations derived in Chap. 4. The equivalence of both approaches has been shown and the advantages of the conformation tensor approach with respect to the stress-tensor description have been addressed. The dependence of mesoscopic friction coefficients appearing in these constitutive equations on the conformation tensor have been analyzed and possibilities to extract these coefficients from atomistic simulations of polymer melts have been suggested.

In Chap. 6 we returned to amorphous polymeric materials. We solved the time evolution equations derived in Chap. 4 for homogeneous deformations taking into account compressibility of the material and non-isothermal conditions (*i. e.* we solved Eqs. (4.42a) and (4.42d), p. 79 together with Eq. (4.51), p. 83). We adopted a thermodynamic potential discussed in Chaps. 2 and 3 and we evaluated thermodynamic material properties under homogeneous deformations. For the temperature dependence of the relaxation time spectrum we took phenomenological relationships. For materials with energetic and entropic elasticity we discuss adiabatic, non-isothermal stress relaxation experiments and we compare our theoretical results with experimental findings. We proposed an alternative fiber spinning processes with simultaneous supercooling to the glass transition temperature for incompressible and compressible materials. We found that small deformations are sufficient to produce highly oriented samples if the material is quenched simultaneously. The practical realization of such processes may be the topic of further studies. The problem of critical cooling in non-isothermal rheology was touched briefly.

Non-equilibrium thermodynamics and statistical mechanics are a possible starting point if one is interested in a continuum description of polymeric materials. Non-isothermal conditions and compressibility effects are included naturally in the framework of non-equilibrium thermodynamics. Statistical mechanics has been adopted to take into account energetic elasticity of the material.

# List of Abbreviations

EIT	Extended Irreversible Thermodynamics
ETH	Eidgenössische Technische Hochschule (Swiss Federal Institute of Technology)
FENE-P	Finitely Extensible Non-linear Elastic - Peterlin
FETA	Fixed Eta (viscosity)
FOV	Flogy Orwoll Vrij
GENERIC	General Equation Non-Equilibrium Reversible Irreversible Coupling
MC	Monte Carlo
MD	Molecular Dynamics
NEMD	Non-Equilibrium Molecular Dynamics
PDE	Partial Differential Equation
PDMS	Polydimethylsiloxane
PE	Polyethylene
PIB	Polyisobutylene
PS	Polystyrene
PTT, PTTI	Phan-Thien/Tanner
PT, PTTII	Phan-Thien
PVA	Poly(Vinyl Acetate)
RIS	Rotational Isomeric State
SG	Spencer Gilmore
UCM	Upper Convected Maxwell
WLF	Williams Landel Ferry

# List of Figures

2.1	Density of PE (SG equation) . . . . .	12
2.2	Density for PE and $C_{16}H_{34}$ (FOV equation) . . . . .	15
2.3	Temperature coefficient of $p$ for PE and $C_{16}H_{34}$ . . . . .	17
2.4	Thermal expansion for PE and $C_{16}H_{34}$ . . . . .	18
2.5	Isothermal compressibility for PE and $C_{16}H_{34}$ . . . . .	19
2.6	End-to-end vector for $n$ -alkanes . . . . .	24
2.7	Second moment of the end-to-end vector . . . . .	26
2.8	Isotherms for PE and $C_{16}H_{34}$ . . . . .	28
2.9	Heat capacity of PE . . . . .	29
2.10	Characteristic ratio for $n$ -alkanes . . . . .	31
2.11	Temperature coefficient vs. chain length . . . . .	32
2.12	Temperature coefficient vs. temperature . . . . .	33
2.13	Spring constant . . . . .	34
3.1	Energetic elasticity of $n$ -alkanes . . . . .	41
3.2	Heat capacity of $n$ -alkanes . . . . .	42
3.3	Characteristic ratio vs. temperature for $n$ -alkanes . . . . .	46
3.4	Spring constant of $n$ -alkanes . . . . .	47
3.5	Energetic vs. entropic- / total elastic energy for $n$ -alkanes . . . . .	48
3.6	Characteristic ratio vs. temperature for PIB . . . . .	50
3.7	Spring constant of PIB . . . . .	51
3.8	Energetic vs. entropic- / total elastic energy for PIB . . . . .	52
5.1	Relaxation time vs. extra stress . . . . .	107
5.2	Relaxation time vs. conformation . . . . .	108
5.3	Nonlinear shear viscosity for viscoelastic fluid models . . . . .	109
5.4	Anisotropic mobility tensor . . . . .	112
5.5	Degree of non-affine motion . . . . .	114

6.1	Temperature dependence of the relaxation times . . . . .	127
6.2	Non-isothermal stress relaxation experiments . . . . .	130
6.3	Process history for P1 and P2 . . . . .	132
6.4	Relaxation time . . . . .	133
6.5	Morphology . . . . .	134
6.6	Mechanical properties . . . . .	136
6.7	Thermodynamic properties . . . . .	137
6.8	Heat capacity . . . . .	138
6.9	Process history for P1 and P3 . . . . .	139
6.10	Density . . . . .	140
6.11	Morphology and mechanical properties . . . . .	141
6.12	Thermodynamic properties . . . . .	142
6.13	Heat capacity . . . . .	143
6.14	Viscosity in non-isothermal elongation (Oldroyd-B) . . . . .	144
6.15	Viscosity in non-isothermal elongation (Giesekus) . . . . .	145
6.16	Viscosity ratio in elongation . . . . .	146

# Bibliography

- [1] H. C. Öttinger and M. Grmela. Dynamics and thermodynamics of complex fluids: II. Illustrations of a general formalism. *Phys. Rev. E*, 56:6633–6655, 1997.
- [2] A. N. Beris and B. J. Edwards. *Thermodynamics of Flowing Systems*. Oxford University Press, New York, 1994.
- [3] R. S. Spencer and G. D. Gilmore. Equation of state for polystyrene. *J. Appl. Phys.*, 20:502–506, 1949.
- [4] R. S. Spencer and G. D. Gilmore. Equation of state for high polymers. *J. Appl. Phys.*, 21:523–526, 1950.
- [5] P. J. Flory, R. A. Orwoll, and A. Vrij. Statistical thermodynamics of chain molecule liquids. I. An equation of state for normal paraffin hydrocarbons. *J. Am. Chem. Soc.*, 86:3507–3514, 1964.
- [6] P. J. Flory, R. A. Orwoll, and A. Vrij. Statistical thermodynamics of chain molecule liquids. II. Liquid mixtures of normal paraffin hydrocarbons. *J. Am. Chem. Soc.*, 86:3515–3520, 1964.
- [7] R. A. Orwoll and P. J. Flory. Equation-of-state parameters for normal alkanes. Correlation with chain length. *J. Am. Chem. Soc.*, 89:6814–6822, 1967.
- [8] G. T. Dee and D. J. Walsh. Equations of state for polymeric liquids. *Macromolecules*, 21:811–815, 1988.
- [9] G. T. Dee, T. Ougizawa, and D. J. Walsh. The pressure-volume-temperature properties of polyethylene, poly(dimethylsiloxane), poly(ethylene glycol) and poly(propylene glycol) as a function of molecular weight. *Polymer*, 33:3462–3469, 1992.
- [10] P. J. Flory. *Statistical Mechanics of Chain Molecules*. Hanser Publishers, Munich, 1988.
- [11] P. J. Flory. Foundations of rotational isomeric state theory and general methods for generating configurational averages. *Macromolecules*, 7:381–392, 1974.
- [12] W. L. Mattice and U. W. Suter. *Conformational Theory of Large Molecules, The Rotational Isomeric State Model in Macromolecular Systems*. John Wiley and Sons Inc., New York, 1994.
- [13] M. Rehahn, W. L. Mattice, and U. W. Suter. *Rotational Isomeric State Models in Macromolecular Systems*, volume 131/132 of *Adv. Polym. Sci.* Springer, 1997.
- [14] G. C. Sarti and N. Esposito. Testing thermodynamic constitutive equations for polymers by adiabatic deformation experiments. *J. Non-Newtonian Fluid Mech.*, 3:65–76, 1977.
- [15] P. E. Rouse. A theory of the linear viscoelastic properties of dilute solutions of coiling polymers. *J. Chem. Phys.*, 21:1272–1280, 1953.
- [16] R. B. Bird, R. C. Armstrong, and O. Hassager. *Dynamics of Polymeric Liquids, Vol. 2, Kinetic Theory*. Wiley-Interscience, New York, second edition, 1987.
- [17] M. Doi and S. F. Edwards. *The Theory of Polymer Dynamics*. Clarendon Press, Oxford, 1988.
- [18] H. C. Öttinger. *Stochastic Processes in Polymeric Fluids*. Springer, Berlin, 1996.
- [19] H. Leaderman. Textile materials and the time factor i. mechanical behaviour of textile fibers and plastics. *Text. Res.*, 11:171–193, 1941.
- [20] J. D. Ferry. Mechanical properties of substances of high molecular weight. VI. dissipation in concentrated polymer solutions and its dependence on temperature concentration. *J. Am. Chem. Soc.*, 72:3746–3752, 1950.
- [21] M. L. Williams, R. F. Landel, and J. D. Ferry. The temperature dependence of relaxation mechanisms in amorphous polymers and other glass-forming liquids. *J. Am. Chem. Soc.*, 77:3701–3707, 1955.

- [22] V. G. Mavrantzas and D. N. Theodorou. Atomistic simulation of polymer melt elasticity: Calculation of the free energy of an oriented polymer melt. *Macromolecules*, 31:6310–6332, 1998.
- [23] V. A. Harmandaris, V. G. Mavrantzas, and D. N. Theodorou. Atomistic molecular dynamics simulation of polydisperse linear polyethylene melts. *Macromolecules*, 31:7934–7943, 1998.
- [24] M. Dressler, B. J. Edwards, and H. C. Öttinger. Thermodynamics of flowing polymeric liquids. *Rheol. Acta*, 38:117–136, 1999.
- [25] F. Schwarzl and A. J. Staverman. Time-temperature dependence of linear viscoelastic behaviour. *J. Appl. Phys.*, 23:838–843, 1952.
- [26] J. D. Ferry. *Viscoelastic Properties of Polymers*. John Wiley and Sons, New York, third edition, 1980.
- [27] H. Markovitz. Superposition in rheology. *J. Polym. Sci.: Polym. Symp.*, 50:431–456, 1975.
- [28] L. W. Morland and E. H. Lee. Stress-analysis for linear viscoelastic materials with temperature variation. *Trans. Soc. Rheol.*, 4:233–263, 1960.
- [29] M. J. Crochet and P. M. Naghdi. A class of simple solids with fading memory. *Int. J. Eng. Sci.*, 7:1173–1198, 1969.
- [30] M. J. Crochet and P. M. Naghdi. A class of non-isothermal viscoelastic fluids. *Int. J. Eng. Sci.*, 10:775–800, 1972.
- [31] M. J. Crochet and P. M. Naghdi. On thermal effects in a special class of viscoelastic fluids. *Rheol. Acta*, 12:321–329, 1973.
- [32] M. J. Crochet and P. M. Naghdi. On a restricted non-isothermal theory of simple materials. *J. Méc.*, 13:97–114, 1974.
- [33] B. D. Coleman and W. Noll. The thermodynamics of elastic materials with heat conduction and viscosity. *Arch. Rat. Mech. Anal.*, 13:167–178, 1963.
- [34] B. D. Coleman. On thermodynamics, strain impulses, and viscoelasticity. *Arch. Rat. Mech. Anal.*, 17:231–254, 1964.
- [35] B. D. Coleman. Thermodynamics of materials with memory. *Arch. Rat. Mech. Anal.*, 17:1–40, 1964.

- [36] R. S. Rivlin. Review of The Non-Linear Field Theories of Mechanics. *J. Acoust. Soc. Amer.*, 40:1213, 1966.
- [37] R. S. Rivlin. Red herrings and sundry unidentified fish in nonlinear continuum mechanics. In M. F. Kanninen, W. F. Adler, A. R. Rosenfield, and R. I. Jaffee, editors, *Inelastic Behavior of Solids*, pages 117–134. McGraw-Hill, New York, 1970.
- [38] R. S. Rivlin. The thermomechanics of materials with fading memory. In J. F. Hutton, J. R. A. Pearson, and K. Walters, editors, *Theoretical Rheology*, chapter 6, pages 83–103. Applied Science Publishers Ltd., 1975.
- [39] J. G. Oldroyd. Rheological equations of state and thermodynamic principles. In J. F. Hutton, J. R. A. Pearson, and K. Walters, editors, *Theoretical Rheology*, chapter 7, pages 104–110. Applied Science Publishers Ltd., 1975.
- [40] L. C. Woods. *The Thermodynamics of Fluid Systems*. Oxford University Press, London, 1975.
- [41] B. H. Lavenda. *Thermodynamics of Irreversible Processes*. John Wiley and Sons, New York, 1978.
- [42] A. V. Tobolsky and R. D. Andrews. Systems manifesting superposed elastic and viscous behavior. *J. Chem. Phys.*, 13:3–27, 1945.
- [43] G. Astarita. Thermodynamics of dissipative materials with entropic elasticity. *Polym. Eng. Sci.*, 14:730–733, 1974.
- [44] G. Astarita and G. C. Sarti. Thermomechanics of compressible materials with entropic elasticity. In J. F. Hutton, J. R. A. Pearson, and K. Walters, editors, *Theoretical Rheology*, chapter 9, pages 123–137. Applied Science Publishers Ltd., 1975.
- [45] G. Astarita and G. C. Sarti. An approach to thermodynamics of polymer flow based on internal state variables. *Polym. Eng. Sci.*, 16:490–495, 1976.
- [46] G. Astarita and G. C. Sarti. The dissipative mechanism in flowing polymers: Theory and experiments. *J. Non-Newtonian Fluid Mech.*, 1:39–50, 1976.

- [47] G. Marrucci. The free energy constitutive equation for polymer solutions from the dumbbell model. *Trans. Soc. Rheol.*, 16:321–330, 1972.
- [48] R. B. Bird. Use of simple molecular models in the study of the mechanical behaviour of solutions of flexible macromolecules. *J. Non-Newtonian Fluid Mech.*, 5:1–12, 1979.
- [49] R. K. Gupta and A. B. Metzner. Modeling of nonisothermal polymer processes. *J. Rheol.*, 26:181–198, 1982.
- [50] X.-L. Luo and R. I. Tanner. A computer study of film blowing. *Polym. Eng. Sci.*, 25:620–629, 1985.
- [51] M. A. McClelland and B. A. Finlayson. Heat transfer effects in extrudate swell of elastic liquids. *J. Non-Newtonian Fluid Mech.*, 27:363–374, 1988.
- [52] J. M. Wiest. Time-temperature superposition in nonisothermal flow. *J. Non-Newtonian Fluid Mech.*, 27:127–131, 1988.
- [53] J. M. Wiest and N. Phan-Thien. Non-isothermal flow of polymer melts. *J. Non-Newtonian Fluid Mech.*, 27:333–347, 1988.
- [54] F. Sugeng, N. Phan-Thien, and R. I. Tanner. A study of non-isothermal non-Newtonian extrudate swell by a mixed boundary element and finite element method. *J. Rheol.*, 31:37–58, 1987.
- [55] R. I. Tanner. *Engineering Rheology*. Clarendon Press, Oxford, 1985.
- [56] R. G. Larson. *Constitutive Equation for Polymer Melts and Solutions*. Butterworths Series in Chemical Engineering, Boston, 1988.
- [57] D. A. Carey, C. J. Wust, and D. C. Bogue. Studies in nonisothermal rheology: Behaviour near the glass transition temperature and in the oriented glassy state. *J. Appl. Polym. Sci.*, 25:575–588, 1980.
- [58] H. Janeschitz-Kriegl. *Polymer Melt Rheology and Flow Birefringence*. Polymers / Properties and Applications. Springer, Berlin, 1993.

- [59] D. C. Venerus, S.-H. Zhu, and H.C. Öttinger. Stress and birefringence measurements during the uniaxial elongation of polystyrene melts. *J. Rheol.*, 43:795–813, 1999.
- [60] G. W. M. Peters, F. M. Schoonen, F. P. T. Baaijens, and H. E. H. Meijer. On the performance of enhanced constitutive models for polymer melts in a cross-slot flow. *J. Non-Newtonian Fluid Mech.*, 82:387–427, 1999.
- [61] M. Matsui and D. C. Bogue. Studies in non-isothermal rheology. *Trans. Soc. Rheol.*, 21:133–148, 1977.
- [62] T. Matsumoto and D. C. Bogue. Non-isothermal rheological response during elongational flow. *Trans. Soc. Rheol.*, 21:453–468, 1977.
- [63] J. R. A. Pearson and L. V. McIntire. Non-isothermal rheology of polymers and its significance in polymer processing. *J. Non-Newtonian Fluid Mech.*, 6:81–95, 1979.
- [64] P. Wapperom and M. A. Hulsen. Thermodynamics of viscoelastic fluids: The temperature equation. *J. Rheol.*, 42:999–1019, 1998.
- [65] J. F. Dijksman and G. D. C. Kuiken, editors. *Numerical Simulation of Non-Isothermal Flow of Viscoelastic Liquids*, Fluid Mechanics and its Applications, Kerkade, The Netherlands, 1993. IUTAM, Kluwer Academic Publishers.
- [66] I. Prigogine, N. Trappeniers, and V. Mathot. On the application of the cell method to r-mer liquids. *J. Chem. Phys.*, 21:559–560, 1953.
- [67] I. Prigogine. *The Molecular Theory of Solutions*. Interscience Publishers, Inc., New York, 1957.
- [68] A. Ciferri, C. A. J. Hoeve, and P. J. Flory. Stress-temperature coefficients of polymer networks and the conformational energy of polymer chains. *J. Am. Chem. Soc.*, 83:1015–1022, 1961.
- [69] P. J. Flory, C. A. J. Hoeve, and A. Ciferri. Influence of bond angle restrictions on polymer elasticity. *J. Polym. Sci.*, 34:337–347, 1959.

- [70] P. J. Flory, A. Ciferri, and C. A. J. Hoeve. The thermodynamic analysis of thermoelastic measurements on high elastic materials. *J. Polym. Sci.*, 45:235–236, 1960.
- [71] P. J. Flory. Molecular configuration in bulk polymers. *Rubber Chem. Tech.*, 48:513–525, 1975.
- [72] P. J. Flory. Theoretical predictions on the configurations of polymer chains in the amorphous state. *J. Macromol. Sci., Phys. Ed.*, B12:1–11, 1976.
- [73] P. J. Flory. Introductory lecture: Levels of order in amorphous polymers. *Faraday Discuss, R. Soc. Chem.*, 68:14–25, 1979.
- [74] P. J. Flory. Molecular structure, conformation and properties of macromolecules. *Pure Appl. Chem.*, 52:241–252, 1980.
- [75] P. J. Flory. Conformations of macromolecules in condensed phases. *Pure Appl. Chem.*, 56:305–312, 1984.
- [76] H. B. Callen. *Thermodynamics and an Introduction to Thermostatistics*. John Wiley and Sons, New York, second edition, 1985.
- [77] M. Grmela. Hamiltonian mechanics of complex fluids. *J. Phys. A*, 22:4375–4394, 1989.
- [78] D. W. van Krevelen. *Properties of Polymers*. Elsevier, Amsterdam, 1990.
- [79] W. Kuhn and F. Grün. Beziehungen zwischen elastischen Konstanten und Dehnungsdoppelbrechung hochelastischer Stoffe. *Kolloid Z.*, 101:248–271, 1942.
- [80] D. Y. Yoon and P. J. Flory. Moments and distribution functions for polymer chains of finite length. II. Polymethylene chains. *J. Chem. Phys.*, 61:5366–5380, 1974.
- [81] B. Wunderlich. Motion in polyethylene. I. Temperature and crystallinity dependence of the specific heat. *J. Chem. Phys.*, 37:1203–1207, 1962.
- [82] K. Loufakis and B. Wunderlich. Computation of heat capacity of liquid macromolecules based on statistical mechanical approximations. *J. Phys. Chem.*, 92:4205–4209, 1988.

- [83] A. Abe, R. L. Jernigan, and P. J. Flory. Conformational energies of n-alkanes and the random configuration of higher homologs including polymethylene. *J. Am. Chem. Soc.*, 88:631–639, 1966.
- [84] P. J. Flory. Moments of the end-to-end vector of a chain molecule, its persistence and distribution. *Proc. Nat. Acad. Sci.*, 70:1819–1823, 1973.
- [85] M. V. Volkenstein. *Configurational Statistics of Polymeric Chains*. Interscience, New York, 1963. Translated from the Russian ed., S. N. Timasheff and M. J. Timasheff.
- [86] U. W. Suter, E. Saiz, and P. J. Flory. Conformational characteristics of polyisobutylene. *Macromolecules*, 16:1317–1328, 1983.
- [87] T. G. Fox and P. J. Flory. Viscosity-molecular weight and viscosity-temperature relationships for polystyrene and polyisobutylene. *J. Am. Chem. Soc.*, 70:2348–2395, 1948.
- [88] A. K. Doolittle. Studies in Newtonian flow. II. The dependence of the viscosity on liquids of free-space. *J. Appl. Phys.*, 22:1471–1475, 1951.
- [89] T. Matsumoto and D. G. Bogue. Non-isothermal rheological response during elongational flow. *Trans. Soc. Rheol.*, 21:453–468, 1980.
- [90] H. Voigt and M. Kröger. Rheological crossover in polymer melts via non-equilibrium molecular dynamics. *Phys. Rev. Lett.*, ??:??–??, 2000.
- [91] H. Braun. A model for the thermorheological behaviour of viscoelastic fluids. *Rheol. Acta*, 30:523–529, 1991.
- [92] G. W. M. Peters. Thermorheological modeling of viscoelastic materials. In J. F. Dijksman and G. D. Kuiken, editors, *Numerical Simulation of Non-Isothermal Flow of Viscoelastic Liquids*, Dordrecht, Boston, London, November 1993. Kluwer Academic Publishers.
- [93] D. Jou, J. Casas-Vázquez, and G. Lebon. *Extended Irreversible Thermodynamics*. Springer, New York, second edition, 1996.

- [94] B. J. Edwards and A. N. Beris. Non-canonical Poisson bracket for nonlinear elasticity with extensions to viscoelasticity. *J. Phys. A*, 24:2461–2480, 1991.
- [95] B. J. Edwards and A. N. Beris. Unified view of transport phenomena based on the generalized bracket formulation. *Ind. Eng. Chem. Res.*, 30:873–881, 1991.
- [96] M. Grmela and H. C. Öttinger. Dynamics and thermodynamics of complex fluids: I. Development of a general formalism. *Phys. Rev. E*, 56:6620–6632, 1997.
- [97] B. J. Edwards. An analysis of single and double generator formalisms for complex fluids. I. The macroscopic description. *J. Non-Equilib. Thermodyn.*, 23:301–333, 1998.
- [98] B. J. Edwards, A. N. Beris, and H. C. Öttinger. An analysis of single and double generator thermodynamic formalisms for complex fluids: II. The microscopic description. *J. Non-Equilib. Thermodyn.*, 23:334–350, 1998.
- [99] R. J. J. Jongschaap. Microscopic modeling of the flow properties of polymers. *Rep. Prog. Phys.*, 53:1–55, 1990.
- [100] R. J. J. Jongschaap. Towards a unified formulation of microrheological models. *Springer Lecture Notes in Physics*, 381:215–247, 1991.
- [101] R. J. J. Jongschaap, K. H. de Haas, and C. A. J. Damen. A generic matrix representation of configuration tensor rheological models. *J. Rheol.*, 38:769–796, 1994.
- [102] B. J. Edwards, H. C. Öttinger, and R. J. J. Jongschaap. On the relationship between thermodynamic formalisms for complex fluids. *J. Non-Equilib. Thermodyn.*, 22:356–373, 1997.
- [103] R. F. Rodriguez, M. López de Haro, and O. Manero. A thermodynamic approach to non-linear viscoelasticity. *Rheol. Acta*, 27:217–223, 1988.
- [104] M. Grmela, D. Jou, and J. Casas Vázquez. Nonlinear and hamiltonian extended irreversible thermodynamics. *J. Chem. Phys.*, 108:7937–7945, 1998.

- [105] N. S. Kalospiros, B. J. Edwards, and A. N. Beris. Internal variables for relaxation phenomena in heat and mass transfer. *Int. J. Heat Mass Transw.*, 36:1191–1200, 1993.
- [106] D. D. Holm, J. E. Marsden, T. Ratui, and A. Weinstein. Nonlinear stability of fluid and plasma equilibria. *Phys. Rep.*, 123:1, 1985.
- [107] P. J. Morrison. Hamiltonian description of the ideal fluid. *Rev. Mod. Phys.*, 70:467–521, 1998.
- [108] B. J. Edwards and H. C. Öttinger. Time-structure invariance criteria for closure approximations. *Phys. Rev. E*, 56:4097–4103, 1997.
- [109] J. F. Milthorpe and R. I. Tanner. On the extrusion of viscoelastic fluids subject to viscous heating. *Int. J. Numer. Methods in Fluids*, 24:263–270, 1987.
- [110] R. Srinivasan and B. A. Finlayson. Corrections for the non-isothermal hole pressure problem. *J. Non-Newtonian Fluid Mech.*, 27:1–15, 1988.
- [111] H. Braun and C. Friedrich. Transient processes in couette flow of a Leonov fluid influenced by dissipation. *J. Non-Newtonian Fluid Mech.*, 33:39–51, 1989.
- [112] J. Stickforth. The rational mechanics and thermodynamics of polymeric fluids based upon the concept of a variable relaxed state. *Rheol. Acta*, 25:447–458, 1986.
- [113] H. Braun and C. Friedrich. Dissipative behaviour of viscoelastic fluids derived from rheological constitutive equations. *J. Non-Newtonian Fluid Mech.*, 38:81–91, 1990.
- [114] G. W. M. Peters and F. P. T. Baaijens. Modelling of non-isothermal viscoelastic flows. *J. Non-Newtonian Fluid Mech.*, 68:205–224, 1997.
- [115] M. Matsui and D. C. Bogue. Non-isothermal rheological response in melt spinning and idealized elongational flow. *Polym. Eng. Sci.*, 16:735–741, 1976.
- [116] E. Ben-Sabar and B. Caswell. Heat effects in die swell. *J. Rheol.*, 25:537–548, 1981.



- [117] A. Dutta and R. A. Mashelkar. Thermal conduction in polymeric liquids. In R. A. Mashelkar, A. S. Mujumdar, and R. Kanal, editors, *Transport Phenomena in Polymeric Systems*, volume 1, pages 285–338. Wiley Eastern Limited, New Delhi, 1987.
- [118] A. A. Cocci and J. J. P. Picot. Rate of strain effect on the thermal conductivity of a polymer liquid. *Polym. Eng. Sci.*, 13:337–341, 1973.
- [119] J. J. P. Picot, G. I. Goobie, and G. S. Mawhinney. Shear-induced anisotropy in thermal conductivity of a polyethylene melt. *Polym. Eng. Sci.*, 22:154–157, 1982.
- [120] A. I. Leonov. Nonequilibrium thermodynamics and rheology of viscoelastic polymer media. *Rheol. Acta*, 15:85–98, 1976.
- [121] B. J. Edwards and A. N. Beris. The dynamics of a thermotropic liquid crystal. *Eur. J. Mech. B*, 11:121–142, 1992.
- [122] B. H. van den Brule. The non-isothermal elastic dumbbell: A model for the thermal conductivity. *Rheol. Acta*, 29:416–422, 1990.
- [123] C. Truesdell. *Rational Thermodynamics*. Springer-Verlag, New York, second edition, 1984.
- [124] R. B. Bird, C. F. Curtiss, and K. J. Beers. Polymer contribution to the thermal conductivity and viscosity in a dilute solution (Fraenkel Dumbbell model). *Rheol. Acta*, 36:269–276, 1997.
- [125] M. Grmela. Hamiltonian dynamics of incompressible elastic fluids. *Phys. Lett. A*, 130:81–86, 1988.
- [126] F. R. Phelan, M. M. Malone, and H. H. Winter. A purely hyperbolic model for unsteady viscoelastic flow. *J. Non-Newtonian Fluid Mech.*, 32:197–224, 1989.
- [127] B. J. Edwards and A. N. Beris. Remarks concerning compressible viscoelastic fluid models. *J. Non-Newtonian Fluid Mech.*, 36:411–417, 1990.
- [128] A. N. Beris and B. J. Edwards. Poisson bracket formulation of incompressible flow equations in continuum mechanics. *J. Rheol.*, 34:55–78, 1990.

- [129] N. Phan-Thien. On the time-temperature superposition principle of dilute polymer liquids. *J. Rheol.*, 23:451–456, 1979.
- [130] H. Giesekus. A simple constitutive equation for polymer fluids based on the concept of deformation dependent tensorial mobility. *J. Non-Newtonian Fluid Mech.*, 11:69–109, 1982.
- [131] A. N. Beris and B. J. Edwards. Poisson bracket formulation of viscoelastic flow equations of differential type: A unified approach. *J. Rheol.*, 34:503–538, 1990.
- [132] B. J. Edwards, A. N. Beris, and M. Grmela. The dynamical behaviour of liquid crystals: A continuum description through the generalized brackets. *Mol. Cryst. Liq. Cryst.*, 201:51–86, 1991.
- [133] H. C. Öttinger. General projection operator formalism for the dynamics and thermodynamics of complex fluids. *Phys. Rev. E*, 57:1416–1420, 1998.
- [134] R. J. Gordon and W. R. Schowalter. Anisotropic fluid theory: A different approach to the dumbbell theory of dilute polymer solutions. *Trans. Soc. Rheol.*, 16:79–97, 1972.
- [135] M. W. Johnson and D. Segalman. A model for viscoelastic fluid behaviour which allows non-affine deformation. *J. Non-Newtonian Fluid Mech.*, 2:225–270, 1977.
- [136] N. Phan-Thien and R. I. Tanner. A new constitutive equation derived from network theory. *J. Non-Newtonian Fluid Mech.*, 2:353–365, 1977.
- [137] M. Doi and S. F. Edwards. Dynamics of concentrated polymer systems. Part 4. rheological properties. *J. Chem. Soc. Faraday Trans. II*, 75:38–54, 1979.
- [138] M. A. Hulsen. A sufficient condition for a positive definite configuration tensor in differential models. *J. Non-Newtonian Fluid Mech.*, 38:93–100, 1990.
- [139] J. R. Prakash and H. C. Öttinger. Viscometric functions for a dilute solution of polymers in a good solvent. *Macromolecules*, 29:2028–2043, 1999.

- [140] H. C. Öttinger. A thermodynamically admissible reptation model for fast flows of entangled polymers. *J. Rheol.*, 43:1461–1493, 1999.
- [141] N. J. Inkson, T. C. B. McLeish, O. G. Harlen, and D. J. Groves. Predicting low density polyethylene melt rheology in elongational and shear flows with "pom-pom" constitutive equations. *J. Rheol.*, 43:873–896, 1999.
- [142] R. B. Bird, R. C. Armstrong, and O. Hassager. *Dynamics of Polymeric Liquids, Vol. 1, Fluid Mechanics*. Wiley-Interscience, New York, second edition, 1987.
- [143] H. Hürlimann. A multidirectional shear rheometer for polymer melts. *Rheol. Acta*, 30:480–490, 1991.
- [144] J. Meissner. Experimental problems and recent results in polymer melt rheology. *Makromol. Chem. Macromol. Symp.*, 56:25–42, 1992.
- [145] J. Meissner and J. Hostettler. A new elongational rheometer for polymer melts and other highly viscoelastic liquids. *Rheol. Acta*, 33:1–21, 1994.
- [146] A. K. Doufas, I. S. Dairanieh, and A. J. McHugh. A continuum model for flow-induced crystallization of polymer melts. *J. Rheol.*, 43:88–109, 1999.
- [147] A. Souvaliotis and A. N. Beris. An extended White Metzner viscoelastic fluid model based on an internal structural parameter. *J. Rheol.*, 36:241–271, 1992.
- [148] M. R. Apelian, R. C. Armstrong, and R. A. Brown. Impact of the constitutive equation and singularity on the calculation of stick-slip flow: The modified upper convected Maxwell model (MUCM). *J. Non-Newtonian Fluid Mech.*, 27:299–321, 1988.
- [149] J. A. Deiber and W. R. Schowalter. Modeling the flow of viscoelastic fluids through porous media. *AIChE Journal*, 27:912–920, 1981.
- [150] E. J. Hinch. Mechanical models of dilute polymer solutions in strong flows. *Phys. Fluids*, 20:S22–S30, 1977.

- [151] J. M. Rallison and E. J. Hinch. Do we understand the physics of the constitutive equation? *J. Non-Newtonian Fluid Mech.*, 29:37–55, 1988.
- [152] R. K. Upadhyay and A. I. Isayev. Nonisothermal elongational flow of polymeric fluids according to the Leonov model. *J. Rheol.*, 28:581–599, 1984.
- [153] J. M. Wiest. Kinetic theories for nonisothermal flows: Differential constitutive equations. In J. F. Dijksman and G. D. Kuiken, editors, *Numerical Simulation of Non-Isothermal Flow of Viscoelastic Liquids*, Dodrecht, Boston, London, November 1993. Kluwer Academic Publishers.
- [154] A. J. Kovacs, R. A. Stratton, and J. D. Ferry. Dynamic mechanical properties of polyvinyl acetate in shear in the glass transition temperature range. *J. Chem. Phys.*, 67:152–161, 1963.
- [155] H. M. Laun. Description of the non-linear shear behaviour of a low density polyethylene melt by means of an experimentally determined strain dependent memory function. *Rheol. Acta*, 17:1–15, 1978.

# Index

- $A$  = coefficient, 14, 104  
 $A_0$  = activation energy, 86, 127  
 $a_1$  = elastic free energy, 39  
 $\mathbf{A}$  = symmetric part of  $\nabla\mathbf{v}$ , 25, 68, 106  
 $\mathbf{a}$  = persistence vector, 31  
 $a_i$  = coefficients, 73, 86  
 $\alpha_0$  = liquid strength, 12, 14  
 $\alpha_1$  = elastic strength, 20, 40, 124  
 $\alpha$  = thermal conductivity matrix, 73, 78, 86  
 anisotropic drag, 106, 110  
 $a, a(T)$  = degree of non-affine motion, 94, 103, 104, 110, 113  
 Arrhenius form, 62, 86, 128  
 $a_T$  = shift factor, 62  
 $\tilde{a}$  = coefficient, 104  
  
 $B$  = coefficient, 14, 71  
 $b$  = coefficient, 104  
 balance equations, 79  
     conformation tensor, 79, 101, 120  
     density, 79, 80, 120  
     entropy, 81  
     internal energy, 79, 80  
     momentum, 79, 80  
     temperature, 81, 83, 120  
 $\mathbf{b}$  = body force vector, 66, 80  
  
 $\beta$  = thermal expansion, 10  
 $\beta, \beta_\zeta$  = Giesekus parameter, 110, 126  
 bracket formalism, 102, 121  
  
 $c$  = specific heat capacity, 10, 67, 90, 121, 125  
 Cayley/Hamilton theorem, 73, 86, 90  
 $\mathbf{c}$  = conformation tensor, 9, 39, 74, 102, 120  
 $\check{c}$  = FOV/SG parameter, 12, 124  
 $c_{\text{conf}}$  = specific heat capacity, 21, 40, 125  
 chain  
     freely rotating, 30, 45  
     hindered rotations  
         independent, 30, 45  
         interdependent, 30, 45  
 characteristic ratio  
     temperature coefficient of, 35  
 $C_n$  = characteristic ratio, 34, 125  
 compressible process  
     non-isothermal, 138, 139  
         force density, 141  
         history, 139, 140  
         morphology, 141  
         thermodynamics, 142, 143  
     contour length, 35  
     Cox-Merz rule, 106, 109  
      $c_p$  = specific heat capacity, 11  
     critical cooling, 144, 146  
  
 $\Delta$  = coefficient, 14  
 $\delta$  = coefficient, 14  
 density variable formulation, 39  
  
 $E$  = total energy (generator), 76  
 $E_\sigma$  = energy barrier, 30  
 $E_v$  = energy barrier, 30  
 $E_\xi$  = energy barrier, 49  
 $\mathbf{E}_s$  = identity matrix, 22  
 Ellis-model, 106  
 $e_m$  = external field, 77  
 entropy density  
     Hookean spring, 41  
 $\epsilon$  = PTT parameter, 104, 110  
 $\epsilon$  = internal energy density, 40, 74  
 equation of Ferry, 127, 144  
 $E_{\zeta\eta}$  = energy of  $u_{\zeta\eta}$ , 21, 43  
  
 $F$  = functional, 76  
 $f$  = orientation factor, 122  
 $\mathbf{F}$  = deformation gradient, 102  
 $\mathbf{F}_i$  = generator matrix, 22  
 FENE-P model, 92  
     conformation tensor, 92  
     extra stress tensor, 92  
     force law, 55  
     Massieu function, 92  
 Feta models, 109  
 fiber spinning  
     isothermal, 134, 135  
     non-isothermal, 131  
         force density, 135, 136  
         history, 132  
     morphology, 134  
     relaxation time, 133  
     thermodynamics, 137, 138  
 force density, 122  
 FOV  
     compressibility, 16  
     equation of state, 14  
     heat capacity, 20, 124  
     Massieu function, 14  
     temperature coefficient of  $p$ , 16  
     thermal expansion, 16  
 functional derivative, 76  
  
 $\Gamma, \Gamma_0$  = coefficients, 14  
 $\gamma$  = temperature coefficient of  $p$ , 10  
  
 $\mathbf{G}_i$  = generator matrix, 44  
 GENERIC, 75, 102, 121  
     degeneracy, 76, 77, 79  
     generator, 76, 77  
     master equation, 75, 76  
     metric matrix, 76, 78, 93, 94  
     Poisson operator, 76, 77  
 Giesekus model, 111, 112  
     conformation tensor, 91  
     non-isothermal, 91, 145  
     relaxation matrix, 91  
  
 Helmholtz free energy, 39  
 $\eta$  = specific entropy, 65  
 $\eta$  = viscosity, 86  
 hexadecane  
     compressibility, 19  
     density, 15  
     isotherms, 28  
     temperature coefficient of  $p$ , 17

- thermal expansion, 18
- $I_i$  = invariants of  $\mathbf{c}$ , 90
- internal energy density  
Hookean spring, 41
- $\kappa$  = bulk viscosity, 86
- $\kappa$  = compressibility, 10
- $k_B$  = Boltzmann constant, 12
- $K(T)$  = spring constant, 20, 40, 70, 85, 110, 124
- $L$  = Poisson operator, 76
- $\mathbf{\Lambda}$  = relaxation matrix, 78, 102, 103, 121, 126
- $\lambda_r$  = relaxation time, 127
- Lennard-Jones potential, 55
- $\mathbf{l}_i$  = bond vector, 23, 44
- $M$  = metric matrix, 76
- Massieu function, 9, 75, 85, 121, 123  
elastic part, 10, 102, 123  
FENE-P spring, 92  
Hookean spring, 20, 85, 103, 124  
liquid part, 10, 123
- Maxwell model, 129, 131, 139  
conformation tensor, 87  
extra stress tensor, 87, 95  
internal energy, 87  
modified, 106  
non-isothermal, 87, 129, 131, 139  
relaxation matrix, 87  
temperature balance, 89
- MC, 110
- MD, 110
- molar gas constant, 30, 45, 127
- $\mu$  = stiffness parameter, 70
- $M_W$  = molecular weight, 12
- $n = \alpha_1 \rho$  = number density of dumbbells, 70
- $N_A$  = Avogadro number, 12
- $n$ -alkanes, 27  
characteristic ratio, 31  
persistence vector, 24  
second moment, 26  
spring constant, 34
- $\mathbf{n}$  = normal vector, 65
- NEMD, 55
- non-affine motion, 92, 113, 114
- $\nu$  = coefficient, 71
- Oldroyd-B model  
conformation tensor, 87  
extra stress tensor, 87  
internal energy, 87  
non-isothermal, 87, 144, 145  
relaxation matrix, 87  
temperature balance, 90
- $p$  = pressure, 10, 75, 85, 121
- $p^*$  = FOV parameter, 13
- PDMS, 53
- PE, 27, 45, 125  
characteristic ratio, 125  
compressibility, 19, 126  
density, 15  
heat capacity, 29, 126  
isotherms, 28  
pressure, 126  
temperature coefficient of  $p$ , 17, 126  
thermal expansion, 18, 126
- $\phi_i$  = torsional angle, 23, 44
- $\pi$  = SG parameter, 12
- PIB, 49, 129
- PS, 53
- $\psi$  = statistical weight, 30, 45

- $\Psi_1, \Psi_2$  = normal stress coefficients, 110
- PTT model  
conformation tensor, 94  
non-affine motion matrix, 94  
non-isothermal, 95  
relaxation matrix, 94
- PVA, 53, 129
- $Q$  = specific radiation energy, 65, 67, 80
- $\mathbf{Q}$  = viscous dissipation matrix, 78, 86, 121, 128
- $\mathbf{q}$  = heat flux vector, 65, 72
- quasi equilibrium, 74, 76
- $R$  = cooling rate, 120
- Rational Thermodynamics, 66, 80
- $\mathbf{R}$  = end-to-end vector, 20, 124
- $\mathbf{r}$  = position vector, 63
- relaxation time, 110  
conformation, 105, 107  
extra stress, 104, 108
- $R_G$  = radius of gyration, 113
- $\rho$  = density, 9, 39, 65, 74, 102, 120
- $\rho_0$  = SG parameter, 12
- $\rho^*$  = FOV parameter, 13
- $\boldsymbol{\rho}$  = second moment, 25
- $\rho_r$  = reference density, 127
- RIS, 21, 43, 111, 125
- Rouse model, 111
- $S$  = total entropy (generator), 76
- $s$  = entropy density, 40
- SG  
compressibility, 13  
equation of state, 12

- heat capacity, 13
- Massieu function, 12
- temperature coefficient of  $p$ , 13
- thermal expansion, 13
- shear thinning, 109
- $\sigma$  = statistical weight, 30, 45
- $\boldsymbol{\sigma}$  = extra stress tensor, 68, 79, 102, 103, 122
- $\boldsymbol{\sigma}^{(a)}$  = Gordon Schowalter derivative, 106
- $\boldsymbol{\sigma}^{(c)}, \widehat{\boldsymbol{\sigma}}^{(c)}$  = upper convected derivative, 88
- $\boldsymbol{\sigma}^e, \boldsymbol{\sigma}^v$  = elastic, viscous part of stress tensor, 69
- $\sigma_s$  = local entropy source term, 65, 81
- slip, *see* non-affine motion
- stress relaxation  
non-isothermal, 129, 130
- $T$  = temperature, 9, 39, 65, 74, 102, 120
- $t$  = time, 63
- $T^*$  = FOV parameter, 13
- $\mathbf{T}$  = total stress tensor, 66, 80
- $\mathbf{T}_i$  = transformation matrix, 23, 44
- temperature equation, 67–69
- Theory  
Purely Entropic Elasticity, 67, 129  
Simple Fluids with Fading Memory, 65
- $\theta_i$  = bond angle, 23, 44
- time-temperature superposition principle, 62
- $T_m$  = melting temperature, 127
- $T_r$  = reference temperature, 127
- Trouton viscosity, 146

$u$  = specific internal energy, 67  
 $\mathbf{U}_i$  = statistical matrix, 21, 43  
 $\mathbf{u} = \rho \mathbf{v}$  = momentum density,  
76  
 $v$  = statistical weight, 30, 45  
 $u_{\zeta\eta}$  = statistical weight, 21, 43  
  
 $\mathbf{v}$  = velocity, 66, 102  
viscosity  
    elongational, 122  
    shear, 109  
  
White Metzner model, 106  
WLF equation, 127, 132  
  
 $x$  = set of system variables, 74,  
76  
 $\mathbf{X}$  = non-affine motion matrix,  
93, 94, 102, 103  
 $\xi$  = pseudo time, 63  
 $\xi$  = statistical weight, 49  
  
 $Z$  = partition function, 22  
 $\mathbf{Z}$  = relaxation matrix, 69  
 $\mathbf{z}$  = orientational field, 75, 102,  
103, 121, 125  
 $\zeta$  = friction coefficient, 70, 111  
 $\zeta$  = mobility tensor, 91, 111  
Zimm model, 55

# Curriculum Vitae

## Personal Data

Name Marco Dressler  
Date of Birth January 8th, 1970  
Place of Birth Qierschied  
Citizen of Germany

## Education and Professional Experience

1976 – 1980 Primary School in Heusweiler, Germany  
1980 – 1989 Secondary School in Lebach, Germany  
1989 Matura Exam  
1989 – 1995 Undergraduate study in physics, Universität des Saarlandes, Saarbrücken, Germany  
1993 – 1995 Diploma Thesis on Rayleigh Bénard Convection in horizontal throughflow  
1995 – 1997 SNS Pisa, Italy  
Electrooptical properties of low dimensional semiconductor heterostructures (GaAs) in the group of F. G. Bassani (Condensed Matter Physics)  
1997 – 2000 ETH Zurich  
Doctoral Candidate, Department of Materials Science

# Acknowledgments

Many people have contributed, through their knowledge and friendship, to make the years at ETH such a fruitful period. I would like to express my thanks to: Prof. Dr. H. C. Öttinger for his confidence, enthusiasm, and guidance, which were all a continuous source of inspiration; Prof. Dr. U. W. Suter, my second advisor; Dr. Brian Edwards, for his friendship and for introducing me to non-equilibrium thermodynamics, thus helping me in the initial stages of this work; Dr. Thomas Schweizer for his friendship and his efforts in doing non-isothermal stress relaxation experiments for HDPE; Markus Herrchen, Dr. Markus Hütter, Dr. Martin Kröger, and all members of the Polymer Physics group for interesting and helpful discussions; ETH Zurich for financial support. I am grateful to my parents, to my brother, and to Dr. Anna La Barbera for their confidence and their support.

